Turun yliopisto
University of Turku

THE CHROMATOID BODY ENTOURAGE:

Molecular characterization of the Chromatoid body-associated cytoplasmic vesicles

Matteo Da Ros

TURUN YLIOPISTON JULKAISUJA – ANNALES UNIVERSITATIS TURKUENSIS
Sarja - ser. D osa - tom. 1206 | Medica - Odontologica | Turku 2015

University of Turku

Faculty of Medicine
Institute of Biomedicine
Department of Physiology
Turku Doctoral Programme of Molecular Medicine (TuDMM)
Turku Doctoral Programme of Biomedical Sciences (TuBS)

Supervised by

Noora Kotaja, PhD Docent Assistant Professor
Department of Physiology
Institute of Biomedicine
University of Turku
Turku, Finland

Jorma Toppari, MD PhD Professor
Departments of Physiology and Paediatrics
Institute of Biomedicine
University of Turku
Turku, Finland

Reviewed by

Timo Tuuri, PhD Docent
Research Programs Unit
Molecular Neurology and
Biomedicum Stem Cell Centre
University of Helsinki
Helsinki, Finland

Varpu Marjomäki, PhD Docent
Department of Biological and
Environmental Science
Nanoscience Center
University of Jyväskylä
Jyväskylä, Finland

Opponent

Ramesh S. Pillai, PhD
European Molecular Biology Laboratory
(EMBL)
Grenoble
France

The originality of this thesis has been checked in accordance with the University of Turku quality assurance system using the Turnitin OriginalityCheck service.

ISBN 978-951-29-6306-5 (PRINT)
ISBN 978-951-29-6307-2 (PDF)
ISSN 0355-9483
Painosalama Oy - Turku, Finland 2015

For my ancestors

Abstract

Matteo Da Ros

The Chromatoid body entourage: Molecular characterization of the Chromatoid body-associated cytoplasmic vesicles

University of Turku, Faculty of Medicine, Institute of Biomedicine, Department of Physiology, Turku Doctoral Programme of Molecular Medicine (TuDMM) and Turku Doctoral Programme of Biomedical Sciences (TuBS), Turku, Finland.

Turku, 2015.

Spermatogenesis is a unique process compared to cell differentiation in somatic tissues. Germ cells undergo a considerable number of metabolic and morphological changes during their differentiation: they initially proliferate by mitosis to increase in number; at some point they scramble their genetic material by meiosis, to create new genetic combinations that are the basis for evolution through natural selection and, finally, they change their shape and produce specialized structures characteristic of the mature sperm.

Germ cells display an astonishingly broad transcription of their genome compared to differentiated somatic cells. Moreover, the different RNAs need to be specifically regulated in space and time for sperm production to occur appropriately. Different proteins localized in specific subcellular compartments, along with regulatory small RNAs, have an essential role in the proper execution of the different steps of spermatogenesis. These ribonucleoprotein granules interact with cytoplasmic vesicles and organelles to accomplish their role during sperm development.

In this study, we characterized the most prominent ribonucleoprotein granule found in germ cells, the Chromatoid body (CB). For the first time we investigated the interaction of the CB with the cytoplasmic vesicles that surround it. These studies directed us to the description of Retromer proteins in germ cells and their involvement with the CB and the acrosome formation. Moreover, we discovered the interplay between the CB and the lysosome system in haploid round spermatids, and identified FYCO1, a new protein central to this interaction.

Our results suggest that the vesicular transport system participates in the CB-mediated RNA regulation during sperm development.

Keywords: spermatogenesis, Chromatoid body, small RNAs, Retromer, autophagy

Tiivistelmä

Matteo Da Ros

Kromatoidikappaleen ja solun vesikkeliliikenteen välinen toiminnallinen vuorovaikutus miesten sukusoluissa

Turun yliopisto, Lääketieteellinen tiedekunta, Biolääketieteen laitos, Fysiologian oppiaine, Molekyylilääketieteen tohtoriohjelma (TuDMM) ja Biolääketieteen tohtoriohjelma (TuBS), Turku, Suomi.

Turku, 2015.

Spermatogeneesi on ainutlaatuinen, tarkasti säädelty, kehitysprosessi, joka pitää sisällään suuren määrän vain sukusoluille ominaisia mekanismeja sekä metabolisia ja morfologisia muutoksia. Ensin solut jakautuvat mitoottisesti kasvattaakseen määräänsä. Meioosissa ne sekoittavat geneettisen materiaalinsa luoden uusia yhdistelmiä, jotka luonnonvalinnan kautta mahdollistavat evoluution. Lopulta ne käyvät läpi morfologisen muodonmuutoksen, jonka seurauksena syntyy siittiölle tyypillinen rakenne.

Sukusolut ilmentävät genomiaan aktiivisesti ja niiden RNA transkriptomi on poikkeuksellisen monimuotoinen verrattuna erilaistuneisiin somaattisiin soluihin. Näin ollen RNA-säätely on erittäin tärkeässä asemassa siittiön muodostuksen aikana, ja säätelyyn osallistuu laaja kirjo mekanismeja. Tärkeässä osassa ovat niin sanotut RNA-kappaleet (RNA granules, tai ribonucleoprotein granules), jotka keräävät RNA:ta sitovien proteiinien avulla säädeltävät RNA-molekyylit samaan rakenteeseen ja mahdollistavat tehokkaan säätelyn. RNA-kappaleiden tiedetään myös vuorovaikuttavan soluliman vesikkelien kanssa, mikä tarjoaa aivan uuden tason RNA-säätelylle.

Tämän väitöskirjan kolmessa osatyössä olemme selvittäneet sukusolujen merkittävimmän RNA-kappaleen, kromatoidikappaleen (Chromatoid body, CB), toimintaa. Erityisesti keskityimme tutkimaan tätä rakennetta ympäröivien vesikkelien luonnetta molekyylitasolla. Näytimme, että osa vesikkeleistä on ns. retromer-vesikkeleitä, jotka näyttävät osallistuvan akrosomin muodostumiseen siittiönkehityksen aikana. Paljastimme myös CB:n ja lysosomaalisen järjestelmän yhteyden, ja näytimme, että CB:n ympäristössä tapahtuu autofagosytoosia. FYCO1 proteiinilla osoitettiin olevan tärkeä rooli CB:n ja vesikkeliliikenteen sekä CB:n rakenteen ylläpidon säätelyssä. Tulostemme perusteella solun vesikkeliliikenne osallistuu tärkeällä tavalla CB-välitteiseen RNA:n säätelyyn spermatogeneesin aikana.

Table of Contents

Abstract 4
Tiivistelmä 5
Table of Contents 6
Abbreviations 8
List of original publications 9
1 Introduction 10
2 Review of the literature 12
2.1 Spermatogenesis 12
2.2 RNA regulation 14
2.2.1 From DNA to RNA 14
2.2.2 Translational regulation 16
2.2.3 New players in gene regulation 16
2.2.3.1 Long non-coding RNAs (lncRNAs) 17
2.2.3.2 Small non-coding RNAs (sncRNAs) 18
2.2.3.2.1 miRNAs 18
2.2.3.2.2 siRNAs 19
2.2.3.2.3 piRNAs 20
2.3 Ribonucleoprotein granules 21
2.3.1 Germ granules 23
2.3.2 The Chromatoid body (CB) 24
2.4 The endomembrane system 27
2.4.1 The exocytic system 27
2.4.2 The endocytic system 28
2.5 The Retromer 29
2.5.1 The membrane-targeting homo/hetero-dimer 29
2.5.2 The cargo-recognition heterotrimer 30
2.5.3 Retromer assembly and function 31
2.5.4 The Retromer and associated diseases 32
2.6 Autophagy 33
2.6.1 Macroautophagy 34
2.6.2 Microautophagy 36
2.6.3 Chaperone-mediated autophagy 37
2.6.4 RNautophagy/DNautophagy 37
2.7 The acrosome - a male germ cell specific vesicle 37
2.8 Small RNAs and cytoplasmic vesicles 40
3 Aims of the present study 42
4 Materials and methods 43
Ethics statement 43
Antibodies and lectins 43
Electron microscopy and tomography 43
Chromatoid body isolation 44
Northern blot 44
Western blotting 44
RT-qPCR 45
Preparation of germ cells and tissues for immunostaining 45
***In situ* hybridization** 46
Immunofluorescence and imaging 46

Seminiferous tubule cultures **46**
Isolation of germ cells and cytoplasmic vesicle fractionation **47**
Immunoprecipitation **48**
Mass spectrometry **48**
Generation of Fyco1 knockout mice **49**
Histology, morphological analysis (sperm) **49**

5 Results **50**
5.1 Chromatoid body isolation and preliminary analysis (I) **50**
5.1.1 Isolation of the CB 50
5.1.2 Protein components of the CB 52
5.1.3 RNA content of the CB 52
5.1.4 Accumulation of PIWI-interacting RNAs in the CB 52
5.2 Retromer functions in haploid male germ cells (II) **53**
5.2.1 VPS26A and VPS35 expression in the male germ line 53
5.2.2 Cytoplasmic surroundings of the CB 54
5.2.3 The CB relationship with Retromer vesicles 55
5.2.4 Relationship between different organelles in the cytoplasm of haploid round spermatids 55
5.2.5 Retromer vesicles interact with the lysosome pathway 56
5.2.6 Differences in Retromer vesicle formation in mouse models with disrupted Chromatoid bodies 56
5.3 FYCO1 – A bridge between the CB and lysosomes (III) **57**
5.3.1 A novel CB component – FYCO1 57
5.3.2 FYCO1 interaction partners 58
5.3.3 Testicular phenotype of FYCO1 knockout mice 58
5.3.4 FYCO1 is required for the integrity of the CB 59
5.3.5 The CB and autophagocytosis 59
5.3.6 Recruitment of lysosomes to the CB is supported by FYCO1 60

6 Discussion **62**
6.1 Isolation of the CB and identification of its components **62**
6.2 New factors in CB-vesicles interplay **64**
6.2.1 CB components and the acrosome 64
6.2.2 Retromer proteins in mouse models with disrupted CBs 66
6.2.3 The CB and lysosomes 67
6.2.4 FYCO1-cKO: CB broken but functional? 67
6.2.5 CB dynamics 68
6.3 The meaning of the CB-vesicle interaction **69**

7 Summary and conclusions **72**

8 Acknowledgements **73**

9 References **75**

ORIGINAL COMMUNICATIONS **89**

Abbreviations

AAL	Aleuria aurantia lectin
ALS	amyotrophic lateral sclerosis
APP	β-amyloid precursor protein
ATG	autophagy protein
CB	Chromatoid body
CMA	chaperone-mediated autophagy
DMSO	Dimethyl sulfoxide
dsRNA	double stranded RNA
Endo-siRNA	endogenous small interfering RNA
ESCRT	Endosomal Sorting Complex Required for Transport
EU	5'-ethynyluridine
FFPE	Formalin-fixed, paraffin-embedded
HPA	Helix pomatia agglutinin
IAM	inner acrosomal membrane
IMC	inter-mitochondrial cement
LIR	LC3-interacting region
lncRNA	long non-coding RNA
miRNA	microRNA
MPR	mannose-6-phosphate receptor
mRNA	messenger RNA
MTA	5'-methylthioadenosine
mTOR	mammalian target of Rapamycin
MVB	multivesicular body
ncRNA	non-coding RNA
OAM	outer acrosomal membrane
PAG	proacrosomal granule
PE	phosphatidylethanolamine
PGC	primordial germ cell
PI3	phosphatidylinositol-3
piRNA	PIWI-interacting RNA
PTM	post-translational modification
PNA	peanut agglutinin
RISC	RNA-induced silencing complex
RNA pol	RNA polymerase
RNAi	RNA interference
RNP	ribonucleoprotein
sDMR	symmetrical di-methylated arginine
siRNA	small interfering RNA
sncRNA	short non-coding RNA
TDRD	Tudor domain-containing protein
TGN	Trans-Golgi network
UBA	ubiquitin-associated binding domain
UTR	untranslated region

List of original publications

This thesis is based on the following original publications, which are referred to in the text by Roman numerals I-III:

I. *Accumulation of piRNAs in the Chromatoid bodies purified by a novel isolation protocol.* Meikar O, **Da Ros M**, Liljenbäck H, Toppari J, Kotaja N. Exp Cell Res. 2010 May 15;316(9):1567-75. doi: 10.1016/j.yexcr.2010.02.023. Epub 2010 Feb 26. PMID: 20219458

II. *Retromer vesicles interact with RNA granules in haploid male germ cells.* **Da Ros M**, Hirvonen N, Olotu O, Toppari J, Kotaja N. Mol Cell Endocrinol. 2015 Feb 5;401:73-83. doi: 10.1016/j.mce.2014.11.026. Epub 2014 Dec 5. PMID: 25486514

III. *FYCO1 and autophagy control the integrity of the haploid male germ cell-specific RNA granules.* **Da Ros M**, Lehtiniemi T, Olotu O, Vihinen H, Jokitalo E, Toppari J, Kotaja N 2015 (submitted for publication)

The original publications have been reproduced with the permission of the copyright holders.

1 Introduction

The survival of a species depends upon the successful transmission of its genetic material from one generation to the next, and therefore on the production of functional gametes. In recent years, several reports have cautioned on the decline in the sperm quality of the human species. On consideration on the importance of this process for the survival of our species with those scientific reports on declining male fertility, it is surprising that still so little is known about how sperm actually is produced. Whilst true, the overall physiological process is well known, yet the cellular and molecular mechanisms that control it have begun only recently to be revealed.

In contrast to other fields of research, studies of male fertility are limited by the challenges posed to reproduce the process *in vitro*. As such, few research groups have reported the successful production of functional sperm *in vitro* from germ line stem cells. Unfortunately, other research groups have not yet reproduced those results and much important molecular characterization has yet to be completed. Even though these techniques are far from standardised procedures in research laboratories with, therefore, their application still unforeseeable in humans, they raise many questions, both scientific but also ethical. One important question related to the quality of such sperm produced in artificial conditions. As such, the precise molecular mechanisms involved in the production of fertile sperm needs to be first understood, before any evaluation can be made of the quality of sperm produced in the laboratory.

Compartmentalization and segregation of specific processes in discrete areas inside the cell increase the efficiency and minimize interference from other reactions. Different protein complexes, with the help of non-coding RNAs, execute post-transcriptional control of mRNA in the cytoplasm. Often, the product of one protein complex represents the substrate for another: close contact between them in a working chain further increments the efficiency of the whole process. When different complexes unite, granules are formed. This mechanism is quite well exploited in the germ line, with the formation of different cytoplasmic granules – termed germ granules – at different steps of sperm development. Due to its size, the Chromatoid body (CB) represents an outstanding germ granule, with its single presence in the cytoplasm of haploid round spermatids, and its central role in spermiogenesis. Several components of the CB are essential for the correct production of sperm and its composition indicates that it is involved in many different gene regulatory processes. After more than 100 years of studies on the CB, this study demonstrates the development of a robust protocol for the reproducible isolation of intact CBs.

Some processes require a specific environment that cannot be compatible with other processes. Inside the cell, such an environmental isolation is achieved by seclusion processes in compartments, surrounded by a membrane, such as the endoplasmic reticulum, the Golgi complex and lysosomes. The role of these compartments – also termed intracellular organelles – has been widely studied at both the cellular and molecular level, and at present, even though much

information remains absent, there is a relatively good comprehension of their function and molecular composition – particularly in somatic cells. Male germ cells show peculiar characteristics that render them very different from somatic cells. Their morphological changes in the process of spermiogenesis require extensive remodelling, inclusive of compaction of the nucleus and reorganization of mitochondria, creation of new organelles, such as the acrosome and the flagellum, and the elimination of some others. All these processes require a specific set of proteins and RNAs to be activated at specific time points, and in specific locations inside the cell, and then degraded, along with the degradation of whole cellular components. Autophagocytosis is the mechanism of choice when bulk degradation and cellular remodelling is required. Despite that already much is known on autophagy in somatic cells, studies in the germ line have been remarkably limited. In consideration of the importance of the lysosome pathway for the homeostasis of the cell, and in the development of an organism, it is reasonable to predict similar, if not even more important, roles in the production of fertile sperm, too.

Recent studies have linked the lysosome and secretory pathways with the regulatory action of small RNAs and the degradation of ribonucleoprotein (RNP) granules. Redundant observations, by electron microscopy, also indicated the presence of small vesicles and multivesicular bodies (MVBs) which surround the CB. A few studies also indicate that these vesicles and membranous organelles are positive for markers of lysosomes. In this present study, the nature and molecular composition of these vesicles along with their interactions with the CB, have begun to be uncovered.

2 Review of the literature

2.1 Spermatogenesis

Spermatogenesis is the process of the male gamete formation, the *spermatozoon*. The *spermatozoon*, in uniting with its female counterpart, the *ovum*, gives rise to a new embryo and thereby to a new individual life, leading to the propagation of the species.

Spermatogenesis stands out as an unusual process when compared to the differentiation of other tissues in the body. Following a massive proliferation by mitosis, germ cells scramble up their genome during meiosis; each cell so produced has a distinct combination of genes. This genetic variability provides the material upon which evolution, through natural selection, can occur. The morphology of the differentiated cell, the *spermatozoon*, is completely different from the standard concept of a cell. In several groups of animals, the *spermatozoon* is the only cell whose action occurs externally to the body that produced it: it is to be delivered inside the female genital tract, where it will pursue its function to locate and fertilize the *ovum*.

Spermatogenesis begins early in the embryo with the determination of the primordial germ cells (PGC). These are the first cells whose destiny is determined during development. After birth, the primordial germ cells differentiate into spermatogonia[1], the cell type that will undertake the maintenance of spermatogenesis through the adult life of the organism.

A complete wave of spermatogenesis spans about 35 days in *Mus musculus* but 64 days in *Homo sapiens*[2,3], and this process occurs inside the seminiferous tubules in the testis. There are two somatic cell types that form the tubules: peritubular myoid cells delineate the wall of the tubule (basal lamina), they are rich in actin and perform the peristaltic contractions that push the mature sperm out of the tubules into the epididymis[1,2]; Sertoli cells extend from the basal compartment to the lumen of the tubule and are responsible for the nurture of the differentiating germ cells. The plasma membrane of Sertoli cells invaginates to form pockets in which differentiating germ cells are embedded. Sertoli cells have a central role in spermatogenesis since they provide structural support and molecular signals to regulate all the different stages of spermatogenesis[4–6]. The majority of cells in the seminiferous epithelium are germ cells, *viz*: spermatogonia, spermatocytes and spermatids. Tight junctions between adjacent Sertoli cells divide the seminiferous epithelium into the basal compartment and the luminal compartment to form the so termed blood-testis barrier[1,7]. Sperm formation commences from spermatogonia, located in the basal compartment. The next cell type toward the lumen is the spermatocyte, which is present on the opposite side of the blood-testis barrier. Close to the lumen, there are round and elongated spermatids. When the process approaches its completion, the cells are next to the lumen, where the mature sperm is released[1,2] (**Figure 1**).

An historical hand-drawn detailed representation of the rat spermatogenesis, from Leblond and Clermont[8], is represented in **Figure 2**.

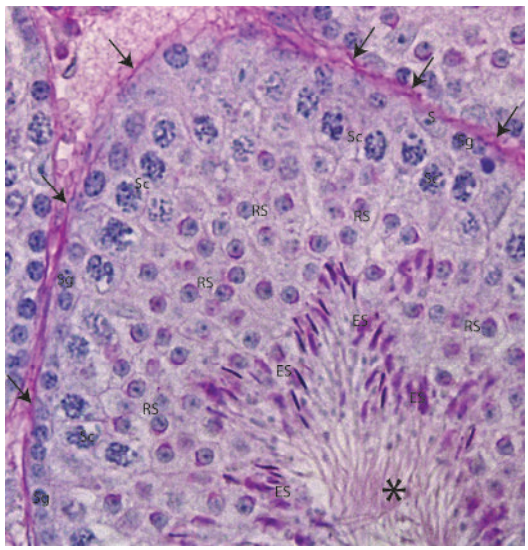

Figure 1 Cross section of a mouse seminiferous tubule. Spermatogenesis proceeds from the basal lamina (arrows) towards the lumen (asterisk). Testis was fixed with PFA and stained with periodic acid-Schiff. S, Sertoli cell; Sg, spermatogonia; Sc, spermatocyte; RS, round spermatid; ES, elongating spermatid.

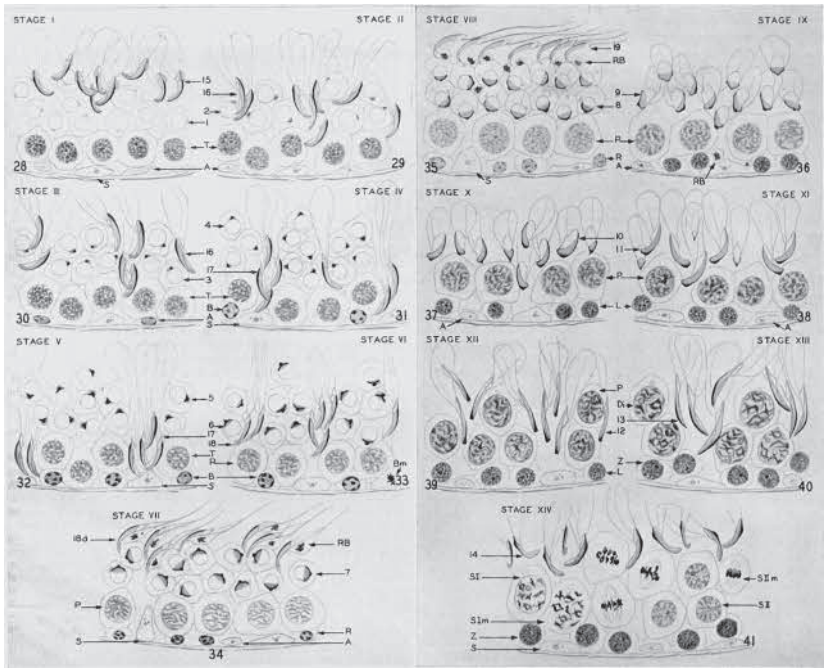

Figure 2 Dynamic drawings of Stage I-VII (left panel) and Stage VIII-XIV (right panel) of the cycle of the seminiferous epithelium in the rat. Numbers 1-19 refer to spermatids at different stages of spermatogenesis. Letters:: A, type A spermatogonia; B, type B spermatogonia; Bm, mitosis of spermatogonia; R, preleptotene spermatocyte; L, leptotene stage; Z, zygotene stage; T, transition form or early pachytene; P, pachytene; Di, diplotene and diakinesis; SI, primary spermatocyte; SIm, primary spermatocyte metaphase; SII, secondary spermatocyte; SIIm, secondary spermatocyte metaphase; S, Sertoli element; RB, residual body. (Modified from: DEFINITION OF THE STAGES OF THE CYCLE OF THE SEMINIFEROUS EPITHELIUM IN THE RAT, C. P. Leblond, Y. Clermont, Annals of the New York Academy of Sciences. Copyright © 2006 John Wiley and Sons).

Spermatogenesis can be divided into three major phases, *viz*: 1) mitotic phase, 2) meiotic phase and 3) spermiogenesis.

During the mitotic phase, spermatogonia divide by mitosis. The daughter cells can take two alternative paths: either continue to be spermatogonial stem cells, to maintain the pool of spermatogonia in the testis, or alternatively commit to differentiate into mature sperm. Committed cells undergo a series of mitotic divisions, which considerable increases their number. At the completion of this clonal expansion, a new cell type is formed: the spermatocyte.

The spermatocyte is the cell type that undergoes the meiotic divisions. Meiosis is divided into meiosis I, during which the ploidy is reduced from diploid to haploid, and meiosis II, which segregates sister chromatids. The prophase of meiosis I is divided into different steps, *viz*: preleptotene, leptotene, zygotene, pachytene and diplotene. During the succession of these steps, the synaptonemal complex forms to bring together sister chromosomes, and crossing over occurs to shuffle the genetic content of the cell. Following first doubling its genome and then undergoing two meiotic divisions, each spermatocyte gives rise to four haploid cells: the round spermatids.

Round spermatids divide no furtherer. Instead, they undergo a series of morphological and metabolic changes that will end in the formation of the mature male gamete: the *spermatozoon*. This process is referred to as spermiogenesis.

This differentiation process, which leads to the production of mature sperm, constantly continues within the testis. On the observation of mouse seminiferous tubules through light microscopy, a longitudinal pattern can be discerned, derived by the presence, at each section along the tubules, of specific germ cell combinations at different points of spermatogenesis[1]. The seminiferous tubules of mice and rats can therefore be divided into stages (12 in the mouse and 14 in the rat, **Figure 2**) that recur in an orderly pattern along the whole tubules. A cross-section of each stage shows a distinct group of differentiating germ cells, representative of that stage[1]. This property thus allows for the precise and detailed study of the different germ cell types in the testis[9–11].

2.2 RNA regulation

The journey of gene expression from gene activation to the action of the final product it encodes goes through a number of different steps, each of which represents a likely target for regulation.

2.2.1From DNA to RNA

At the chromatin level, the active or inactive status of a gene represents the first step of gene regulation. The chromatin can be present in two different states: euchromatin, open and accessible to transcription factors, or heterochromatin, compacted and therefore out of reach for the transcription machinery[12].

DNA methylation is a chemical modification of the DNA nucleotides, most commonly of cytosine, associated with reversible but stable gene inactivation[13]. In particular, DNA methylation is mostly found in CpG repeated sequences, termed CpG islands, common in the promoter of many genes[14]. The methylation of CpG islands triggers a cascade of events that culminate in the eventual inactivation of the adjacent gene[14].

Histones are highly basic proteins that are associated together and with DNA in control of the structure of chromatin, and can be post-transcriptionally modified in different ways (i.e. phosphorylation, acetylation, methylation, ubiquitination and sumoylation); all these different modifications have a specific purpose, triggering compaction or loosening of chromatin and binding different sets of proteins, to guide gene expression or inactivation. All these different histone modifications, each with its own specific purpose, represent the so termed histone code[15]. CpG islands can bring to the DNA proteins involved in repressive histone modifications. Dependent on their specific post-translational modifications, histones themselves can marshal to the DNA proteins involved in the activation or inactivation of gene expression[14].

Along with chromatin organization, the other significantly regulated process that controls gene expression is the initiation of gene transcription. In eukaryotic cells, gene transcription is undertaken by three different RNA polymerases (RNA pol): RNA pol II produces messenger RNAs (mRNAs), while RNA pol I and III produce structural and regulatory RNAs, such as ribosomal RNAs, transfer RNAs and small RNAs[12]. Transcription factors, which are able to recognize specific sequences of DNA, are responsible for the recruitment of the RNA pol II to the promoter site of the genes that are required to be transcribed. Transcription factors, RNA pol II and other factors involved in the regulation of gene transcription, bind together to form the RNA pol II complex, responsible for the transcription of a gene into RNA[12,16].

Eukaryotic genes are characterized by the presence in their DNA sequence of two different parts: protein-coding regions called exons, and non-coding regions called introns. Exons and introns alternate with one another in the gene sequence. RNA pol II initially transcribes the whole gene sequence into RNA, termed pre-mRNA[12]. Already when the transcription is under progress, specific protein complexes recognize the boundaries between exons and introns. These complexes remove the introns from the RNA sequence and link the exons together to form the mature mRNA. This process is called splicing[12]. Splicing itself can be regulated: some exons can be skipped and so not included in the final sequence. In this way, one single gene can produce different forms of a protein, called isoforms, which can perform separate roles in the cell[12]. This property of eukaryotic genes allows an increase in the complexity of the genome, but without considerable increase in its size.

Other modifications that the RNA undertakes during its transcription, are the binding of a "cap" at the 5'-end and the adding of a polyA tail at the 3'-end[12]. At the completion of transcription, the mRNA will be formed by the 5'-cap, the 5'-untranslated region (UTR), the protein coding sequence, the 3'-UTR and the

polyA-tail[12]. The UTRs do not code for protein, but are important for the sorting of the mRNA to specific locations inside the cell and for the regulation of its translation into protein.

The mRNA can also be a subject to nucleotide modifications that will alter the final RNA sequence and possibly the translational regulation or coded protein. These modifications are referred to as RNA editing[17,18].

Inside the nucleus, the mRNA is readily bound by different proteins that regulate its movement to the cytoplasm through the nuclear pores. These proteins also perform a preliminary assessment on the correct processing of the mRNA and, if any problem is detected, drive it to degradation[19].

Once in the cytoplasm, dependent on the set of proteins bound to it, the mRNA is directed to a specific cytoplasmic location, where the protein it encodes is required[20–22]. Besides the decision on where the mRNA is to be transported, the proteins bound to it also regulate its translation.

2.2.2 Translational regulation

Translation of an mRNA into protein requires a very precise quantitative and qualitative regulation. A certain protein is usually required in a specific location inside the cell and in a specific quantity. mRNA translation is required to occur where and when needed.

In eukaryotes, specific proteins bind to the 5'-cap to form the ribosome recruitment complex, which will direct the ribosome onto the mRNA. The ribosome will then scan the mRNA until it locates the translation start codon, where the ribosome will then start synthesis of a new protein. Other proteins bind the polyA tail and connect it to the cap. In this way, the end of the mRNA is close to the beginning, a structure that is presumed to increase the translation efficiency[12]. Different pathways can control the ability of these proteins to interact with each other and support protein synthesis[23].

Regulatory proteins, which bind to the 5'-UTR or the 3'-UTR, can inhibit translation by interference with the recruitment of the ribosome or translation initiation factors. These proteins can also direct the mRNA for degradation. Usually mRNA degradation commences with the shortening of the polyA tail and degradation by 3'-5' exonucleases. This then leads to the elimination of the 5'-cap by a specific decapping enzyme, DCP1A, which exposes the mRNA to degradation by 5'-3' exonucleases[12].

2.2.3 New players in gene regulation

The Human Genome Project opened new horizons to comprehend human biology. Arguably, one of the most important – and unexpected – discoveries was the very limited number of protein coding genes present in it. When considering the difference in complexity between humans and other animals, such as the fruit fly

and the roundworm, it had been expected that the human genome would code for comparably far more genes than such lower organisms. Thus, to discover that only 3% out of the 3 billion bases that form the human genome code for proteins, was rather surprising[24–26]. At the time, scientists were not able to account for a purpose for the reminder, and thus referred to it as "junk-DNA". Although, the Human Genome Project boosted the development of new techniques for the study of the genome itself and of other cellular properties. As a consequence of this enormous effort to understand our biology, new technologies for DNA and RNA sequencing arose, and allowed for a new comprehension of gene regulation. While the Human Genome Project originally spanned approximately 15 years, cost 3 billion US-dollars and involved the collaborative effort of hundreds of research groups around the world, nowadays it is feasible for virtually any research group to sequence the entire genome of an organism in few days. These technologies and the unanswered questions posed by the so called "junk-DNA" drove the realisation that this DNA is not "junk" at all, but most significantly, rather accounts for most of the actual differences between a roundworm and a human[27–29].

Indeed, recent findings suggest that 70-90% of the genome is transcribed into RNA[30], and part of what was once called "junk-DNA", codes for genes that are not translated into proteins, but that the RNA itself mediates their effects.

RNAs that do not code for proteins are called non-coding RNAs (ncRNAs). Only a few ncRNAs have been known for a long time, such as ribosomal RNAs and transfer RNAs, which are both involved in protein synthesis. ncRNAs are involved in the regulation of likely all biological pathways, from the control of epigenetic DNA modifications, to mRNA stability and protein translation[27,31].

In the literature, dependent on their length, ncRNAs are divided into two major classes, *viz*: long non-coding RNAs (lncRNAs) are more than 200 nucleotides long, while all the others are considered small non-coding RNAs (sncRNAs).

2.2.3.1 Long non-coding RNAs (lncRNAs)

lncRNas are mostly transcribed by RNA pol II with similar characteristics to mRNA, such as 5'-cap and polyA. These represent the largest family of non-protein-coding transcripts in mammals (70-90% of the genome)[32]. However, in only a few cases are the functions of lncRNAs understood: in most cases, they remain unknown. In general, it is assumed that lncRNAs harbour sequences recognized by specific proteins and function as a scaffold for multiprotein complexes[33–35]. Moreover, they can mediate the interaction between lncRNA-bound proteins and DNA sequences complementary to the lncRNA[35]. Some lncRNA can even function as molecular decoys: they associate with DNA-binding proteins for the purpose to isolate them from their target DNA[36].

One of the best characterized lncRNA is Xist, which is expressed from one of the X-chromosomes in female mammals and directs chromatin remodelling that will eventually cause X-chromosome inactivation[37]. X-chromosomes without Xist fail to inactivate. When Xist is artificially expressed in an autosomal chromosome it directs the complete inactivation of such chromosome[37].

2.2.3.2 Small non-coding RNAs (sncRNAs)

Small non-coding RNAs act as negative regulators of gene transcription and translation, by driving their target RNA to degradation or translational repression[38,39]. The best-characterized sncRNAs are microRNAs (miRNAs), small interfering RNAs (siRNAs) and PIWI-interacting RNAs (piRNAs), which recognize a complementary sequence in the target RNA and drive a protein complex involved in RNA repression to it. Dependent on the sncRNA and the set of proteins it interacts with, the target RNA can be repressed and stored for later reactivation or, alternatively, it can be completely degraded (**Figure 3**).

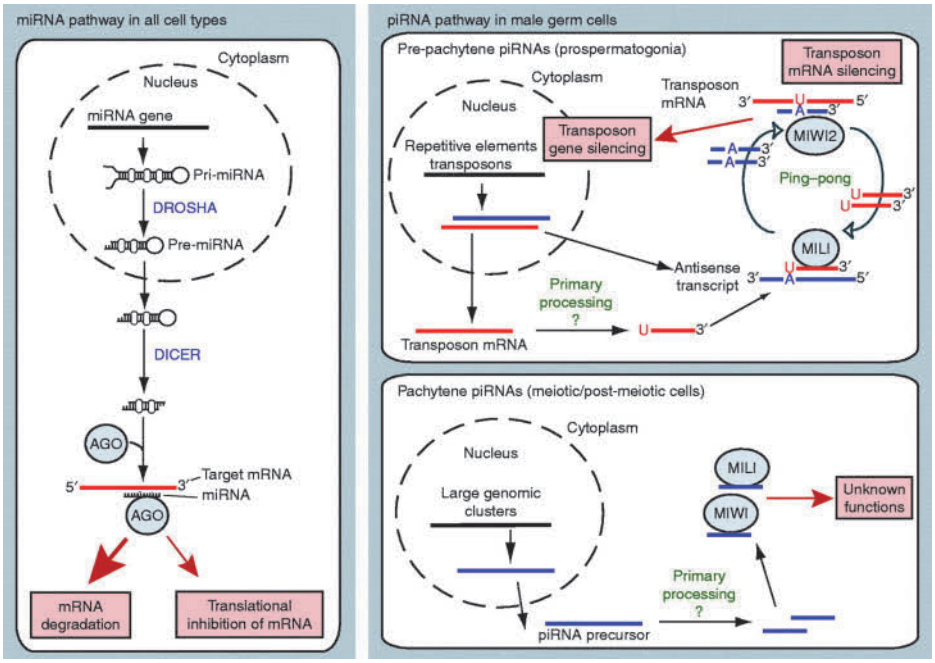

Figure 3 Biosynthesis and function of miRNAs and piRNAs. miRNAs are produced from long imperfect hairpin loops and are cut successively by DROSHA and DICER into mature miRNA. miRNAs are bound by AGO proteins and form the RNA-induced silencing complex (RISC) to control the stability or translation of their target protein-coding mRNAs. Based on the sequence characteristics of MILI- and MIWI2-bound pre-pachytene piRNAs in fetal prospermatogonia, their production is explained by the so-called ping–pong mechanism where piRNAs from the opposite strands promote each other's synthesis in a feed-forward way. Pre-pachytene piRNAs silence transposon expression post-transcriptionally and are also involved in the transcriptional silencing of transposable elements through methylation-dependent mechanisms. The ping–pong model requires an initial set of small RNAs to start the cycle. In the mouse, these primary piRNAs are cut off from transposon mRNAs by an, as yet, unknown mechanism. The MIWI and MILI-bound pachytene piRNAs in late meiotic cells and round spermatids are thought to derive from long single-stranded piRNA precursors, which are processed by an unknown mechanism. Pachytene piRNAs are produced in vast quantities but their functions are not yet characterized (Meikar *at al.* 2011[40], Copyright © 2011, BioScientifica Ltd).

2.2.3.2.1 miRNAs

miRNAs are 22 nucleotide-long RNAs that are involved in the repression of specific mRNAs[41–44]. Their biogenesis commences with the transcription of a 70 nucleotide-long RNA with self-complementary sequences[45,46]; this pri-miRNA folds to form a hairpin of about 22 base-pairs (stem) with a loop on one side and

free overhangs at the other. This pri-miRNA is recognized inside the nucleus by an endonuclease termed DROSHA and the free overhangs are eliminated, with the formation of the pre-miRNA[45,47]. The pre-miRNA is transported to the cytoplasm[48] where it is further processed by the endonuclease DICER, which then eliminates the loop[49–51]. One of the two strands that form the stem, called the guiding strand, is then bound by a member of the Argonaute protein family. Other factors join the protein loaded with the guiding miRNA to form the RNA-induced silencing complex (RISC). RISC can recognize those mRNAs that have a complementary sequence to the guiding miRNA in their 3'-UTR[52–56] (**Figure 3**). Most miRNAs do not show full complementarity with the 3'-UTR sequence they bind in the target mRNA[57]. Dependent on the level of complementarity, the miRNA-RISC complex can simply repress transcription of the mRNA (partial complementarity), or cause the complete degradation of the target mRNA (perfect complementarity)[57–59]. Arising from the partial complementarity with the target mRNA, one single miRNA can regulate multiple mRNAs. Moreover, the 3'-UTR of an mRNA can contain target sites for more than one miRNA. This complexity allows for a very sophisticated network of control miRNAs and controlled mRNAs, which can be differentially tuned in different tissues.

From its central role in miRNA biogenesis and to the fact that there is only one *DICER* gene in mammals, it is unsurprising that DICER can affect many different pathways, including spermatogenesis. DICER is essential for embryogenesis; in fact, DICER deletion in the mouse impairs development of the embryo to the extent it becomes embryonically lethal[60]. Different mouse knockout models for DICER in the male germ line have shown its importance in the development of the male gamete[61–65].

2.2.3.2.2 siRNAs

siRNAs are short, 22 nucleotide-long[66], RNAs that derive from the processing by DICER of a long double stranded RNA (dsRNA)[49]. The guiding strand is then bound by the RISC complex, exactly as occurs with miRNAs, and it drives the RISC complex to the target RNA[67,68]. siRNAs, contrary to miRNAs, show perfect complementarity with the target RNA and cause its degradation. Indeed, miRNAs and siRNAs share many different mechanisms, including the process of their precursors by DICER and gene silencing mediated by RISC[50,51,69,70].

The discovery of siRNAs and their mechanism of function came from experiments where dsRNAs were used in *C. elegans* to repress gene expression: this mechanism is now termed RNA interference (RNAi)[71,72]. The molecular mechanism involved in RNAi is connected with cellular defence against exogenous RNAs, especially those that represent the genome of retroviruses[73–76]. Subsequently, it was found that different organisms express dsRNAs that are processed into endogenous siRNAs (endo-siRNAs)[77–82]. Endo-siRNAs have also been described in the murine germ line[83].

2.2.3.2.3 piRNAs

piRNAs represent a quite different group of sncRNAs when compared with miRNAs and siRNAs. While more than one thousand miRNAs have been detected and their sequence is well conserved between species, tens of thousands of different piRNAs have been reported that do not show any evolutionary conservation. These are expressed specifically in germ cells and bind to PIWI proteins, a subgroup of the Argonaute protein family[84–90]. piRNAs are 26-30 nucleotide-long, dependent on which PIWI protein they are bound to[91–93]. Their mapping to the genome showed that they derive from clusters dispersed in different chromosomes[94]. The production pathway of piRNAs is yet not fully understood, but it is known that it does not require DICER[93,95,96]. The biogenesis of piRNAs involves two different steps, commencing with transcription by RNA pol II of a long, polycistronic, RNA from a piRNA cluster inside the nucleus[97–100]. This transcript is then processed to produce primary piRNAs. Primary piRNAs are loaded to their specific PIWI protein in the cytoplasm. Here a second step, termed ping-pong amplification, uses the primary piRNAs to process complementary RNAs (a complementary target RNA or an antisense transcript from the piRNA cluster) into 26-30 nucleotide-long secondary piRNAs[101,102]. Secondary piRNAs are then used to produce, by a similar process, more primary piRNAs. Notably, all the factors involved in the biogenesis of piRNAs remain as yet unknown[96–98,101–103] (**Figure 3**).

Of interest is that some factors involved in the ping-pong amplification process are associated with the cytoplasmic surface of mitochondria[104–106]. This may explain why most of the proteins associated with the piRNA pathway are localized in specific germ granules, termed *nuage* in *D. melanogater*[97], and inter mitochondrial cement in mammals[107–110], which surround the mitochondria. Mutants for these mitochondria-associated proteins of the piRNA pathway show severely reduced levels of piRNAs and emphasise the conservation of this pathway throughout evolution, from insects to mammals[105–108,111,112].

During male germ cell development there are two major resettings of epigenetic marks. The first takes place in the embryonic germ cells, when DNA-methylation is almost completely erased: embryonic marks are deleted and germ cell ones are established. At this stage, paternal imprinting is established[113,114]. During this process, transposon activity is notably increased, with the risk of genomic instability.

In *D. melanogaster*, piRNAs have been shown to repress the expression of transposable elements during primordial germ cell development[94,96,97]: in this stage, the genome becomes almost completely demethylated. Arising from the loss of CpG island-methylation in their regulatory sequences, transposable elements become active and start "jumping around" the genome uncontrolled, to undermine genome stability and germ cell development. However, piRNA repression mechanisms retain these transposable elements under control[94,96,97]. This genome-protection role of piRNAs has also been reported in other species.

In the mouse there are three different Piwi proteins, *viz*: MIWI (PIWIL1), MILI (PIWIL2) and MIWI2 (PIWIL4), all essential for male fertility[115–117], and are expressed at different stages of male germ cell development. MILI and MIWI2 mutants show impairment of spermatogenesis during spermatocyte meiosis, while MIWI mutants are affected at the round spermatid stage[115–117]. Each binds a specific subset of piRNAs[86,87,118]. piRNAs in mice can be divided into two major groups, dependent on the time of their expression. Pre-pachytene piRNAs are expressed in the embryo and newborn mice; they are enriched in repeated sequences and bind to MILI and MIWI2. Pachytene piRNAs are expressed throughout adulthood, are depleted of repeated sequences and are bound by MILI and MIWI[118,119]. Recently, a modulator of the pachytene piRNAs expression has been described. A-MYB (MYBL1) causes the transcription of long precursors of the pachytene piRNAs and also of piRNA effector proteins[119].

Pre-pachytene piRNAs appear to be specialized in the silencing of transposable elements during primordial germ cell differentiation. They silence transposon activity by directly targeting transposon RNA and causing its degradation and also by directly suppressing its transcription[106,115,120–124].

Recent studies suggest that MIWI-bound pachytene piRNAs are involved in the bulk degradation of mRNAs in meiotic and post-meiotic stages of sperm development[125–128].

Notably, piRNAs can mediate gene silencing by causing repressive histone modifications and DNA-methylation. These epigenetic marks can be passed on to the next generation: piRNAs are therefore able to cause transgenerational epigenetic gene regulation[129–132].

2.3 Ribonucleoprotein granules

Following the dogma of molecular biology, the messenger RNA has the task to bring the genetic information coding for proteins from the DNA in the nucleus to the site of protein production in the cytoplasm. The mRNA itself cannot accomplish this task alone, though. It requires the aid of several proteins at different steps. The mRNA harbours different regulatory sequences that attract specific proteins and these gather other proteins involved in the mRNA regulation, to form a RNP complex. Different RNPs involved in related functions or addressed to the same subcellular location, can be associated together forming larger RNP granules. Dependent on the cell type, intracellular localization, function and molecular composition, these granules are referred to with specific names, *viz*: P-bodies[133–138], GW-bodies[139–142], stress granules[133,134,138,143] and germ granules[144].

The different RNP granules have several features in common: all have mRNAs repressed from translation, but those mRNAs are capable of being re-activated upon specific conditions[145–148]; further, they share a number of protein components[149] and frequently, different granules interact with one another exchanging material[150–152].

Proteins involved in the assembly of the granules often present self-interacting domains, such as prion-like domains, which favour their clustering together; examples are TIA-1[151,153], TDP-43[154] and FUS[155] in stress granules. Another important strategy to control RNP granule assembly is by post-translational modification (PTM) of proteins, such as methylation[156–160], phosphorylation[161], acetylation[162] and ubiquitination[162]. PTMs are used to regulate proteins in all possible pathways inside the cell and can switch either on or off, the ability of a protein to interact with one another.

The cytoskeleton is also involved in RNP granule function, probably to unite the different components to aid in their subcellular localization. The blocking of microtubule polymerization has been shown to interfere with the assembly of stress granules; alternatively P-bodies have also been shown to increase in size[163]. Alteration of microtubule-dependent protein transport appears to have granule-specific effects, to aid unite their components in some cases, or rather their dissociation in others[163].

The recent field of lncRNAs has also opened new ways for the assembly of RNP granules. A single lncRNA can harbour different protein recognition sequences and therefore can bring together different proteins that will assemble yet other proteins with the formation of an RNP granule. A lncRNA can also operate as a link between proteins bound to it and mRNAs having complementary sequences with it. One so characterized lncRNA is NEAT1: involved in the formation of nuclear RNP granules called paraspeckles[164], but for which the function remains, to date, unknown. lncRNAs have been reported in the germ granule called the Chromatoid body[165], discussed further in **2.3.2**.

P-bodies are generally formed upon the action of small RNAs in mRNA repression. The active RISC complex targets specific mRNAs for repression or degradation by miRNAs and siRNAs, respectively. Upon recognition of the target mRNA a series of events causes the shortening of the polyA tail, triggered by CPEB[166] and the elimination of the 5'-cap by DCP1A[161,167], which is also considered a marker of P-bodies. Despite reports that some mRNAs can enter and successively exit these granules, P-body disassembly is considered to occur upon degradation of their mRNAs[168].

Different kinds of cellular stress induce the formation of stress granules: general translation is inhibited and only the mRNAs required to fight the stress and re-establish cell homeostasis are translated. Once the stress has passed, stress granules are disassembled and the repressed mRNA contained in them can be translated again[169].

Another mechanism involved in the clearance of RNP granules is autophagy. Mutants which affect the autophagy pathway, both in yeast and mammals, accumulate P-bodies and stress granules[170–172].

The membrane surface of cytoplasmic organelles can function as a dock for the assembly and localization of RNP granules. As described in **2.8**, GW182-containing-bodies (GW-bodies) function is coupled with their localization on MVB.

Mitochondria provide the surface for the assembly and localization of the germ granule termed intermitochondrial cement (IMC) in mouse spermatocytes. Specifically, phosphatidic acid (PA) present on the surface of mitochondria, seeds the formation of IMC[107,108]. Spermatids depleted of MITOPLD, the enzyme responsible for the formation of PA, do not have any IMC[107,108].

2.3.1Germ granules

Germ granules have been observed since early studies on germ cell development as far as the late 19th century[173–175]. When observed by electron microscopy they appear as highly electron dense fibrous material in the cytoplasm of germ cells, usually associated with either mitochondria or the nuclear envelope[176,177]. Early molecular studies directed to characterize the composition of these germ granules proved that they are formed both of proteins[178,179] and RNA[178,180–182], so verified recently[165,183,184] (I).

Germ granules have been described in different organisms, from the fruit fly, to the roundworm, to mammals. Initially germ granules were referred to with the general term *nuage* (from the French "cloud", prompted from their appearance under the microscope)[185]. Subsequently they were given different names depending on their morphology, cellular localization and the animal itself, *viz*: polar granules in *Drosophila melanogaster*, P-granules in *Caenorhabditis elegans*, intermitochondrial cement in *Xenopus laevis* and mouse, Chromatoid body in mouse and rat (reviewed in[144,186,187]).

In lower organisms, like the fly, the worm and the frog, germ granules appear early during embryogenesis and transport maternal mRNAs necessary for the specification of the germ line[188]. Instead of reliance upon maternal derived factors, germ cell determination in mammals depends upon intercellular signalling from somatic cells which surround the embryo[189]. Germ granules in mammals appear at later stages during gamete differentiation and therefore are expected to, at least partly, differ in their function from those in lower organisms. Nonetheless, they share key components, indicating that similar molecular machineries may be so used too.

Germ granules in different organisms vary in their function and properties, but they share some common components highly conserved during evolution. All germ granules include RNA helicases[127,165,190–192], Tudor domain containing proteins[127,156,165,193–196] and PIWI family members[191]. Germ line specific RNAs and non-coding RNAs, such as piRNAs, are also found in all germ granules[165].

RNA helicases use ATP to unwind double-stranded RNA structures and allow the remodelling of the RNA and its interaction with proteins[197,198]. Numerous animal models have shown the importance of RNA helicases for the determination of germ cells and fertility[190,199–201].

Tudor domain-containing proteins (TDRDs) are common among germ granules. The Tudor domain is able to specifically bind symmetrically di-methylated arginine (sDMR)[157–159,202,203]. sDMR is formed by the enzyme PRMT5[202,204], which

recognises arginines flanked by glycine or alanine ([A/G]R[A/G]); this sequence motif is often found in repeats[157]. Several proteins found in germ granules, such as PIWI proteins, have PRMT5 recognition motives in their amino acid sequence and indeed present sDMRs *in vivo*[205]. The blocking of the action of PRMT5 with 5'-methylthioadenosine (MTA) has been shown to disrupt the interaction between TDRDs and PIWI proteins[156,202,205,206]. One TDRD protein usually harbours several Tudor domains and therefore can bind many proteins that have sDMRs; they therefore represent a convenient scaffold for the formation of germ granules[203,207].

PIWI proteins bind 26-30 nucleotide-long RNAs termed PIWI-interacting RNAs and are necessary to provide genomic stability during embryogenesis and gamete formation[88,90,93,103,115,208,209]. piRNAs can recognize complementary RNAs derived from the activation of retrotransposons and guide their degradation before the genome becomes compromised[88,90,93,103,115,208,209]. This property of piRNAs as protectors of the genome has been conserved throughout evolution (see **2.2.3.2.3**).

Germ granules have been conjectured to contain a variety of mRNAs which undergo translational repression. During spermatogenesis, many mRNAs are expressed in early stages (differentiating spermatogonia and spermatocytes) and stored for later translation. This mechanism is necessary since in later stages, when compaction of the chromatin commences in elongating spermatids, transcription becomes no longer possible. The evidence for this transcriptional regulation comes from studies of transcriptome profiling of different germ cell types: mRNAs coding for proteins expressed in late stages (round and elongating spermatids) were identified already in early germ cell types (differentiating spermatogonia and spermatocytes)[210–213]. Since the germ granules are rich in PIWI proteins it is not surprising that piRNAs are concentrated in them[165]; miRNAs and lncRNAs have also been found in them (reviewed by Gao & Arkov[187]).

2.3.2 The Chromatoid body (CB)

Due to its central role in this study, the Chromatoid body deserves special consideration.

The CB was first described more than a century ago by von Brunn[214] and Benda[174] as a "particle/body" present in the cytoplasm of haploid round spermatids and by the techniques available of that time appeared like chromatin. Yet, despite its long awareness of, the comprehension of its composition and function proceeded remarkably slowly until only recent times[165].

A prominent germ granule called intermitochondrial cement appears during spermatogenesis in mammals in the cytoplasm of spermatocytes. By electron microscopy, IMC appears as a cloud of dark material that surrounds mitochondrial clusters. In late spermatocytes and during meiosis, small dense germ granules, about 0.5 μm in diameter, appear. In newly formed haploid round spermatids these granules assemble into one single body per cell, about 1 μm in diameter, adjacent to the nuclear envelope: this is the Chromatoid body (reviewed by Meikar *et al.*[40]).

The CB appears as a round granule in the cytoplasm of haploid round spermatids and is visible by phase contrast microscopy in living cells (**Figure 4A**). Due to the high concentration of proteins, the CB is also very electron dense in standard EM preparations (**Figure 4B,C**). Moreover, by use of antibodies against components of the CB, it becomes possible to visualize it by indirect immuno-fluorescence microscopy (**Figure 4D**).

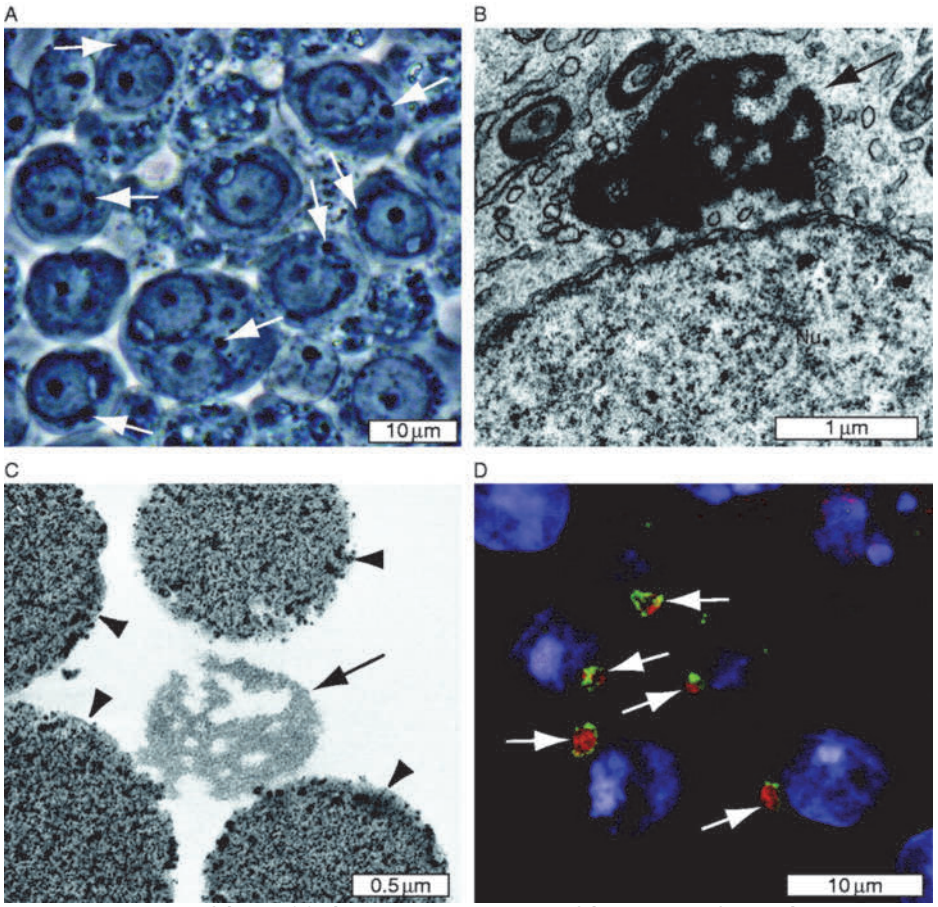

Figure 4 Appearance of the CB. (A) Phase contrast microscopy of the stage-specific squash preparation. A piece of mouse seminiferous tubule representing stage IV-V of the seminiferous epithelial cycle was squashed between a microscope glass slide and a glass cover slip and visualised by phase contrast microscopy. The CB is visible as a cytoplasmic dark granule close to the nuclear envelope (arrows). (B) Electron microscopy visualisation of the CB in the cytoplasm of round spermatid. Lobular structure and irregular network of the dense strands of varying thickness characteristic to the CB (arrow) are clearly visible; Nu, nucleus. (C) Electron microscopy of the isolated CB. The immunoprecipitated CB (arrow) is attached to the paramagnetic beads (arrowheads). (D) Immunofluorescence of mouse testis section stained with antibodies against two different CB proteins (red and green) (arrows) and visualised by confocal laser scanning microscopy. The red signal shows the well-characterised CB marker DDX4 (MVH) and green signal detects the novel CB component FYCO1 (III). Nuclei are stained blue with DAPI ([40], Copyright © 2011, BioScientifica Ltd).

The CB is a dynamic granule located close to the nuclear envelope in round spermatids; when the spermatids commence elongation, the CB reduces in size and moves to the back of the cell, towards the base of the flagellum, and dissociates into two smaller parts, a globular body that is discarded with the rest of the

cytoplasm in the residual body, and a ring which interacts with the base of the flagellum and functions to shape the mitochondrial sheath in the mid-piece[191,215]. Recently Shag *at al.* have described two protein components of the late CB which are eventually involved in the ring formation: TSSK1 and TSSK2 are testis-specific protein kinases important for male fertility[215]. These are transcribed after meiosis and concentrate in the CB at the commencement of spermatid elongation. Subsequently they are located in the ring structure and function in the mitochondria sheath formation[215]. Simultaneous depletion of TSSK1 and TSSK2 resulted in male infertility as a result of the production of defective sperm. Molecular analysis revealed that the ring structure had not been formed and the mitochondria were not adequately placed in the mid-piece[215].

Early studies investigating the composition of the CB concluded that it contains RNA of which some was mRNA[182,216,217]. Until recently, the majority of the CB components had been discovered only incidentally: researches investigating a specific protein in the testis noted its accumulation into one large granule in haploid round spermatids, and confirmed was the CB with report of such[183,191,216,218]. Several of these proteins are involved in post-transcriptional RNA regulation[116,183,219]. The main limitation on the study of CB composition was the absence of a CB isolation method that could enable biochemical characterization of the CB. Our group eventually developed a protocol to achieve this (I), so that the full composition of the CB at the protein and RNA level is now available[165].

The most abundant proteins present in the CB are involved in RNA binding, such as MVH/DDX4, GRTH/DDX25 and HuR, and in post-transcriptional regulation, such as MIWI[165]. piRNAs are also particularly concentrated in the CB[165].

Altogether, the timing of the CB appearance with its composition correlate well with the hypothesis that the CB is involved in the degradation of meiotic and haploid transcripts, and in the regulation and storage of mRNAs required for post-meiotic sperm development[40], until the time when they are required.

Experiments culturing seminiferous tubules with the uridine analogue 5'-ethynyl uridine (EU), showed that the newly transcribed RNAs are concentrated in the CB before their dispersal into the cytoplasm[165]. As such, it has been proposed that the CB could function like a quality control centre for RNAs[40,165,220]. In support of this hypothesis, is the presence in the CB of proteins involved in splicing and in the non-sense mediated decay pathway[165].

The creation of mouse models in which components of the CB were depleted showed the importance of this RNA-protein granule in spermatogenesis. All these models have a common characteristic: they all resulted in specific male infertility. Dependent on which protein was knocked-out, spermatogenesis became impaired at a specific stage. For instance, depletion of MVH/DDX4, which is already expressed in the primordial germ cells in the embryo, resulted in the failure of male germ cell differentiation before the pachytene stage of meiosis[201]. In those mouse models in which spermatogenesis continued to the post-meiotic phase before impairment, the CB morphology was severely compromised[116,156].

2.4 The endomembrane system

To consider the importance of the endomembrane system in the present study (especially in II and III), such intricate network present in all eukaryotic cells, should be briefly introduced: the endomembrane system is defined as "a collection of membranous structures involved in transport within the cell" (www.uniprot.org). Its main components consist of: nuclear envelope, endoplasmic reticulum, Golgi apparatus, cytoplasmic vesicles and plasma membrane (**Figure 5**). Mitochondria and plastids are not included, because of their different evolutionary origin. Several reviews are available in the literature which describe different aspects of the endomembrane system[221–224]; for this study consideration, it is limited to a basic description of the different components.

On commencement of eukaryotic development, the cytoplasm became divided by different membranes to form intra-cytoplasmic compartments, which were physically isolated from each other. This compartmentalization of major biochemical processes allowed more accurate control and sophistication. One major example is the isolation of the genomic material, the DNA, from the cytoplasm by the nuclear envelope. The nucleus allowed the separation of gene transcription from protein synthesis and energy metabolism, to increase specialization and protection of the genome from harmful agents.

The different compartments that form the endomembrane system are mainly involved in the synthesis, targeting, regulation and degradation of surface proteins, along with the uptake and digestion of material from the cellular environment. The endomembrane system can be functionally divided into exocytic, which involves the transportation of material on the surface of the cell, and endocytic, which consists of the internalization of molecules.

2.4.1 The exocytic system

The exocytic system commences at the endoplasmic reticulum, inside of which, nascent proteins are imported[225]. Following folding, quality control and post-translational modifications in the ER, mature proteins are packed inside transport vesicles and directed to the Golgi apparatus. Proteins pass through the different stacks that form the Golgi apparatus, where they acquire more PTMs. After being processed in the Golgi, different proteins are sorted into separate pathways dependent on their final destination. Proteins directed to the cell surface are packed inside exocytic vesicles, which will fuse with the plasma membrane, to release their contents into the extracellular space. Integral membrane proteins present in the vesicle membrane will become surface proteins (**Figure 5**). Other proteins, such as hydrolases, are instead sorted into vesicles directed to endosomes or MVBs, which shall eventually fuse with lysosomes. Retrograde transport targets molecules from the different cytoplasmic vesicles to the Golgi apparatus for their recycling and reuse (**Figure 5**).

2.4.2 The endocytic system

The endocytic pathway is divided into different groups, dependent on the size and type of material internalized: endocytosis is primarily referred to in the case of objects lesser than 500 nm in size, while phagocytosis is specified for larger cargo. The intake of extracellular material occurs by invagination or protrusion of the plasma membrane around it. This membrane reorganization is mediated by different classes of proteins, the main ones being clathrin and caveolin. The endocytosed cargo is delivered to early endosomes and, following maturation through late endosomes and MVBs, is finally degraded by fusion with lysosomes (**Figure 5**).

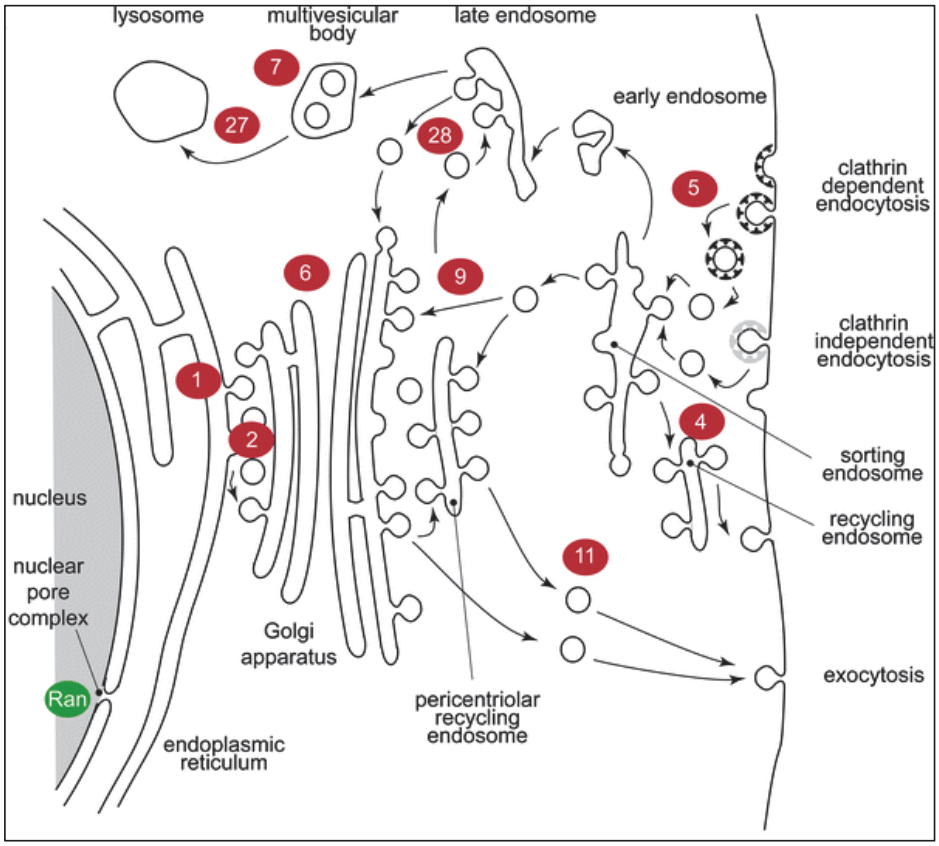

Figure 5 General features of the eukaryotic endomembrane system. Organelles and transport routes for major conserved pathways are shown. Rab proteins, which are main regulators and markers of the different pathways, are shown in red cycles along with the number of the specific Rab member. The related GTPase Ran is also shown (green cycle) at the nuclear pore complex. Transport routes are indicated by arrows. The figure is highly schematic. Endocytic coats are shown as black and grey 'T's. (Cellular and Molecular Life Sciences, 67, 2010, 20;3449-3465, Rab protein evolution and the history of the eukaryotic endomembrane system, Andrew Brighouse, Figure 1A; with kind permission from Springer Science and Business Media)

2.5 The Retromer

Different proteins are required inside the cell in specialized organelles. The compartmentalization of different activities increases their efficiency and minimises interference from other, unrelated, processes. Proteins must therefore be properly sorted and directed to their specific compartment. One example is provided by the lysosomal hydrolases: these are required for the degradation of different molecules in the lysosome. In order to reach the lysosome, hydrolases are first moved into the endoplasmic reticulum during their translation, and then transported to the Golgi apparatus, where they acquire post-translation modifications, such as glycosylation. A specific glycosylation: the attachment of mannose-6-phosphate represents the signal that targets hydrolases to the lysosome. Proteins that present the mannose-6-phosphate tag are recognised in the trans-Golgi-network (TGN) by the mannose-6-phosphate receptor (MPR) and are included in vesicles directed to late-endosomes. The low pH causes the release of the proteins from the MPR into the lumen of the late-endosome. The MPR is then included into vesicles budding from the late-endosome and directed to the TGN. In this way, MPRs are recycled and can be re-used to sort enzymes to the lysosomal pathway.

Different cargo receptors, such as the MPR, are involved in the sorting of proteins from the TGN to their final destination. These cargo receptors are then recycled back to the TGN for further re-use. This recycling involves specialized proteins that recognize the cytoplasmic domain of the cargo receptors and drive them into budding vesicles that are then directed to the TGN. The protein complex known as the Retromer undertakes this recycling process.

The Retromer is formed by two smaller complexes, *viz*: the cargo-recognition VPS26-VPS29-VPS35 heterotrimer, and a membrane targeting heterodimer or homeodimer of SNX1 and/or SNX2[226,227].

2.5.1 The membrane-targeting homo/hetero-dimer

Sorting nexins SNX1 and SNX2 were initially characterized as orthologues of the yeast Vps5p, a protein involved in the assembly of the yeast Retromer onto the surface of retrograde transport vesicles[228,229]. SNX1 and SNX2 show a 63% identity at the amino acid level; they also possess an unstructured N-terminal domain followed by a PX domain which binds phosphatidylinositol 3-phosphate[230–232] and a BAR domain which mediates dimerization and binding to highly curved membranes[231,233,234](**Figure 6**). SNX dimers bind the VPS26-29-35 complex to drive it to the vesicle membranes[228].

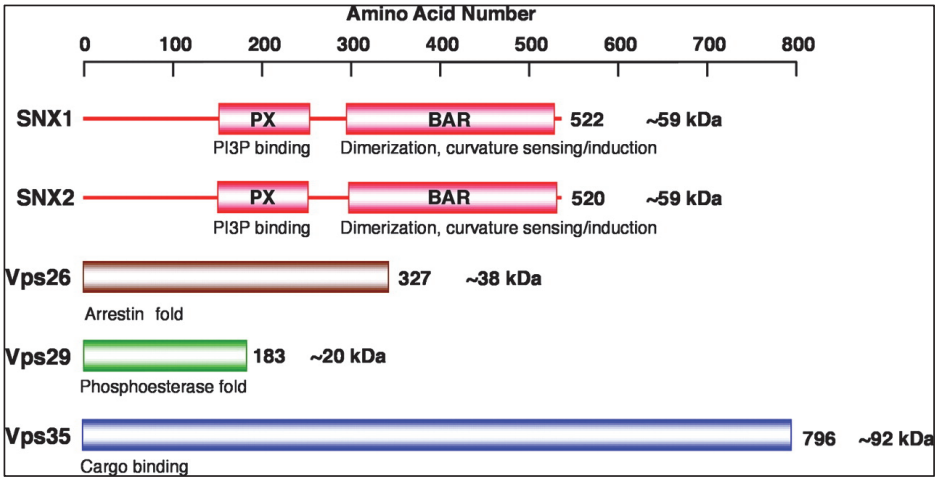

Figure 6 Schematic representation of mammalian Retromer subunits. The number of amino acids and molecular mass of each protein are indicated. The scheme also indicates the features of the different subunits or their domains (Reprinted from Rojas *et al.*[227]).

2.5.2 The cargo-recognition heterotrimer

VPS35 (92 KDa in size) is the largest component of the cargo-recognition complex and represents its central structural component and it links together VPS26 (38 KDa) and VPS29 (20 KDa). The C-terminal lobe of VPS26 interacts with the N-terminal part of VPS35[226]. On the opposite side, the C-terminus of VPS35 interacts with the metal-binding domain of VPS29[226] (**Figure 7**). The VPS35 protein, because of its size and secondary structure composed of 32 alpha-helices, is not a rigid molecule, but can marginally bend in its centre[226], which property allows the whole complex to adapt to the curved shape of the budding vesicle.

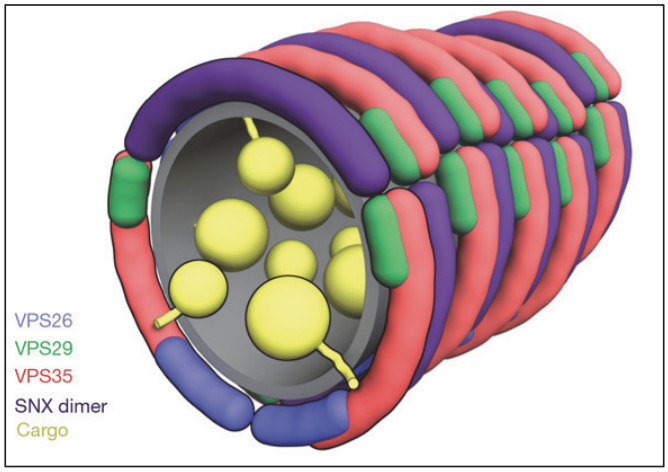

Figure 7 Schematic rendering of a speculative model for the Retromer coat on a tubular vesicle, with the SNX dimer in purple (Modified from Hierro *et al.*[226]. Reprinted by permission from Macmillan Publishers Ltd: Nature, Functional architecture of the Retromer cargo-recognition complex, Aitor Hierro, Adriana L. Rojas, Raul Rojas, Namita Murthy, Gregory Effantin et al., copyright © 2007).

Different studies have attempted to identify the specific role of each subunit in the Retromer complex. VPS35 has been shown to interact with the cytosolic tail of the mannose-6-phosphate receptor[235]. VPS29 presents a phosphodiesterase domain which is able to dephosphorylate a specific serine in the cytosolic tail of the MPR, when combined with VPS26 and VPS35[236].

Notably, in mammals there are two paralogues of VPS26, *viz*: VPS26A and VPS26B[237]. These show a 69% identity and an 82% similarity with one another. VPS26B was reported as a Retromer component because of its interaction with VPS35, even though it is primarily localized near the plasma membrane[237,238]. These two paralogues are expected to differ in the specificity for the cargo recognition[237,238]. It has also been conjectured that the Retromer may be involved in the sorting of proteins along the endocytic pathway, to extend its function beyond the recycling of receptors in the endosome-to-Golgi pathway[237,238].

2.5.3 Retromer assembly and function

The cargo-recognition hetero-trimer assembles independently of the membrane-targeting hetero/homo-dimer[227], and *vice versa*[227]. By use of the yeast two-hybrid system, Rojas and colleagues showed that SNX1 and SNX2 can interact with one another and also with both VPS29 and VPS35, but not with VPS26[227]. Retromer proteins co-localize in the cytoplasm of mammalian cells in distinct *foci*, which correspond to early endosomes[227,230,232–235,239–242]. Silencing experiments by said Rojas and colleagues shed some light on the mechanism of the Retromer assembly on the endosomal membrane. Notably, silencing of either SNX1 or SNX2 had no effect on the Retromer localization on endosomes[227], which prove that the membrane-targeting subcomplex can function either as a homo-dimer or, alternatively, as a heterodimer. Conversely, the silencing of SNX1 and SNX2 simultaneously, impaired the assembly and recruitment of the cargo-recognition complex[227]. Silencing of one of the cargo-recognition subunits did not affect the recruitment of the membrane-recognition subcomplex to endosomes[227]. The small GTPase RAB7A is required for the recruitment of the cargo-selective subcomplex[243,244].

The correct function of the Retromer complex is important for the correct sorting of proteins along the synthetic pathway. Depletion of VPS26 or VPS35 results in the erroneous degradation of the MPR protein in lysosomes[235,241]. Similar effects were observed also when SNX1 and SNX2 were both depleted in the same cell[227]. These experiments showed that SNX1 and SNX2 play redundant roles in targeting the assembly of Retromer subcomplexes to the endosome[227].

These observations, along with the importance of the Retromer in cell physiology itself, are supported by the phenotype from different mouse models. Knock-out mice for SNX1 or SNX2 were viable, but mice lacking both proteins did not survive beyond midgestation[245,246]. Further, a similarly lethal phenotype was observed in the VPS26/Hβ58 knock-out mouse model[247,248].

Different target proteins, which need to be recycled back to the TGN, are recognized by different subunits of the Retromer. VPS35 specifically recognizes

the conserved sorting motif [FW]L[MV][249] in the MPR, while VPS26 can bind to the integral membrane receptor WLS[250] and has also been shown to bind a hydrophobic motif (FTAFANSHY) in the cytoplasmic tail of SorL1/SorLA[251]. Finally, SNX proteins can also be involved in target protein recognition[252–254].

As reviewed in McGough *et al.*, the current model for the function of the Retromer involves the recognition of the cargo receptors on the endosome by the different subunits of the Retromer[255]. The clustering of the Retromer subunits aids the concentration of the cargo proteins into a localized membrane domain. The SNX1/2 subcomplex is then conjectured to be the major player involved in the curvature of the membrane[233] and the formation of the tubular bud that, by excision from the endosome, will then form the elongated vesicle coated by the Retromer complex[226]. The actin cytoskeleton, along with the mediation of the WASH complex, provides the scaffold and the motor force required for the elongation and budding of the Retromer-coated transport vesicle[256–258]. VPS35 specifically binds with a member of the WASH complex, FAM21[256], to recruit it into the endosome-associated Retromer. Once formed, the Retromer-coated vesicle is transported along microtubules, specifically toward the minus-end, to the TGN to recycle the cargo proteins[259,260].

Recent studies on the function of the Retromer in different model organisms have unveiled detailed mechanisms of action and identified several cargoes recognized by the Retromer[235,241,251,261–264]. These studies have shown that the two subcomplexes which form the Retromer can also function independently to recycle specific proteins[252,265]. Further, the mechanisms by which the Retromer drives the budding of the transport vesicles begins to become clear[256–258,266]: e.g., recruitment of the WASH complex by VPS35 is necessary to recycle the Retromer cargo to the TGN[256–258,266]. Subsequently, some of these accessory proteins have themselves been associated with other cellular activities, such as the internalization of membrane receptors and their recycling to the plasma membrane[267,268]. Thus, these studies conclude that the Retromer is indeed involved in a diverse group of cellular activities.

2.5.4 The Retromer and associated diseases

In recent years, proteins that form the Retromer have been associated with different neurodegenerative diseases.

The Retromer is involved in the correct localization and recycling of SorL1/SorLA[269,270]; SorL1/SorLA is involved in the processing of β-amyloid precursor protein (APP)[251,264]. Problems in the Retromer functions can lead to an increased amyloidogenic processing of APP[271–274].

Of note, a rare mutation in VPS35 has also been associated with a hereditary form of Parkinson's disease[275–277].

2.6 Autophagy

Autophagy is the cellular process that delivers cytoplasmic material to the lysosome for degradation. The main role of autophagy is the degradation of cytoplasmic molecules and organelles for the recycling of their components by the cell.

The molecular machinery involved in this degradation process began to be discovered through genetic studies in yeast[278–281]. The core proteins involved in autophagy are conserved between yeast and mammals[282]. However, the precise mechanism of autophagosome formation and processing has increased in complexity throughout evolution. In yeast, autophagosomes are formed from the same perivacuolar preautosomal structure, while in mammals different organelles can contribute to the formation of autophagosomes[283–286].

At any given time, basal levels of autophagy are predicted to be present in the cell. Conversely, autophagy is rapidly induced by different stimuli, such as nutrient starvation or aggregation of misfolded proteins inside the cell. It is evident that the cell has sensory mechanisms to react to each specific situation. When activated, these mechanisms induce autophagocytosis. Different conditions, such as the level of nutrients, growth factors and/or stress, can influence the activity of the mammalian target of Rapamycin (mTOR), a negative regulator of autophagocytosis[287,288]. In the presence of nutrients and growth factors, mTOR is active and inhibits the initiation of autophagy[289]. Autophagy serves as a dynamic recycling system to provide a source of building blocks and energy for cellular renovation and homeostasis. When the quantity of nutrients is low, or when there is a reduction in the level of growth factors, mTOR is inhibited which triggers the onset of autophagy. The release of recycled molecules, such as amino acids, arising from the increase in autophagy then reactivates mTOR, which in turn restores the cellular lysosomal population[290].

The term autophagy is generally used for all those pathways in which cytoplasmic material is directed to the lysosome in animal cells and to the vacuole in plants and yeast cells. At present autophagy is divided into 3 major classes, *viz*: macroautophagy, microautophagy and chaperone-mediated autophagy (CMA) (**Figure 8**).

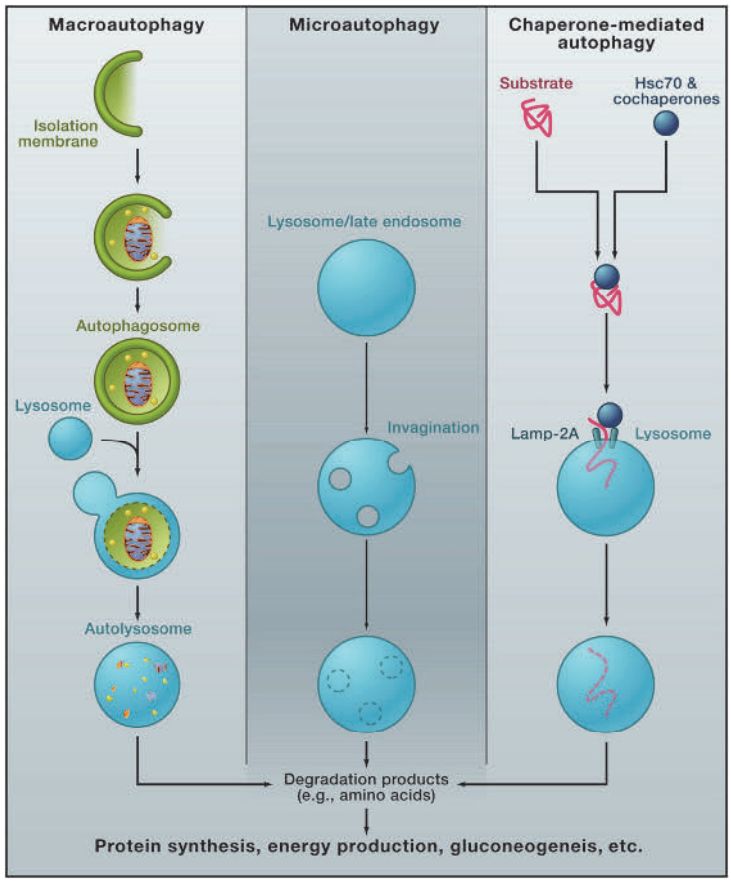

Figure 8 Different Types of Autophagy. Macroautophagy: a portion of cytoplasm, including organelles, is enclosed by an isolation membrane (also called phagophore) to form an autophagosome. The outer membrane of the autophagosome fuses with the lysosome, and the internal material is degraded in the autolysosome. Microautophagy: small pieces of the cytoplasm are directly engulfed by inward invagination of the lysosomal or late endosomal membrane. Chaperone-mediated autophagy: substrate proteins containing a KFERQ-like pentapeptide sequence are first recognized by cytosolic Hsc70 and co-chaperones. They are translocated into the lysosomal lumen after binding with lysosomal Lamp-2A. After all three types of autophagy, the resultant degradation products can be used for different purposes, such as new protein synthesis, energy production, and gluconeogenesis (Reprinted from Cell, 147/4, Noboru Mizushima and Masaaki Komatsu, Autophagy: Renovation of Cells and Tissues, 14, Copyright © 2011, with permission from Elsevier).

2.6.1Macroautophagy

The material to be degraded is first surrounded by a membrane (lipid bilayer) termed a phagophore, with formation of an autophagosome. Dependent on the material to be degraded, the autophagosome can fuse with endosomes, to form an amphisome. Autophagosomes and amphisomes eventually fuse with the lysosome (autolysosome or autophagolysosome) (**Figure 8**).

Phagophore membranes are derived from different cytoplasmic organelles, such as the ER[291–293], the Golgi complex[294,295], mitochondria[284] and the plasma membrane[285].

Macroautophagy can be induced in mammalian cell cultures by depletion of amino acids in the culture medium. As a result, proteins not essential for cell survival are degraded and their amino acids reused. Once the quantity of amino acids in the cell reverts to normal levels, the serine/threonine kinase mTOR is reactivated and inhibits macroautophagy[290].

Knockout mice for macroautophagy proteins (ATGs)[296–298] die immediately after birth since they cannot survive the neonatal starvation period, which demonstrates the physiological importance of macroautophagy under starvation.

Macroautophagy in starvation condition can be considered to have three major roles, *viz*:

1. To produce amino acids for new protein synthesis as an early reaction to starvation[299,300];
2. Later in the reaction to starvation, amino acids provided by the autophagy degradation can be used for energy production via the tricarboxylic acid (TCA) cycle[301];
3. Alongside provision of substrates for the TCA cycle, autophagy degrades lipids to provide a source of energy for the organism[302].d

It is probable that the role of macroautophagy, along with the metabolites it provides, can vary between tissues.

To date, many authors have extensively reviewed the molecular mechanism that ATG core proteins, which are involved in the autophagosome formation, perform[282,303–305]. In brief, in nutrient rich conditions, the mammalian target of Rapamycin complex 1 (mTORC1) suppresses the activity of the ULK1 (Atg1 homologue) complex. Under conditions which cause autophagocytosis, mTORC1 is inactivated and ULK1 complex translocates to the ER where it interacts with the phosphatidylinositol 3(PI3)-kinase complex, activated by it. Beclin 1, another regulator of autophagocytosis, is normally bound with Bcl-2 on the ER. When autophagocytosis is induced, Beclin1 dissociates from Bcl-2 and joins the PI3-kinase complex to contribute to its activation. Concurrently, Atg12-Atg15-Atg16L1 complex directs the conversion of LC3 (Atg8 homologue) to the membrane bound form LC3-PE. LC3-PE is itself involved in recognition of macroautophagy targets.

Initially considered as a bulky degradation pathway with little or no specificity, it has been recently shown that dedicated factors account for the selective degradation of cellular components by macroautophagy. For example, the receptor p62/SQSTM1 presents a self-oligomerization PB1 domain, an LC3-interacting (LIR) motif and an ubiquitin-associated (UBA) binding domain. p62/SQSTM1 (and its orthologue in *C. elegans*[306]) can recognise ubiquitinated proteins marked for degradation, to cluster them together in a granule called sequestosome. p62/SQSTM1 can then recruit phagophore membranes by interaction with LC3-PE, and cause autophagocytosis of the sequestosome[307–309].

The impairment of macroautophagy in adults leads to the accumulation of protein aggregates (also called inclusion bodies) inside the cell cytoplasm. These aggregates are positive for p62/SQSTM1 and ubiquitin[309]. Of interest, these aggregates disappear if loss of p62/SQSTM1 is induced[309]. Inclusion bodies are often identified in neurodegenerative diseases, including Alzheimer's disease[310], Parkinson's disease[310] and amyotrophic lateral sclerosis (ALS)[310,311]. One notable association is that of macroautophagy with aging. Many strategies directed at the increase of an organism's lifespan, including calories restriction[312,313] and mTOR suppression[314] are connected with the induction of macroautophagy.

2.6.2 Microautophagy

In microautophagy, the lysosome itself envelops the material to be degraded by inward invaginations of the lysosomal membrane. At the commencement of a microautophagic event, the lysosome membrane invaginates and elongates into a characteristic tubular shape called an "autophagic tube"[315]. The membrane bends at the neck of the tube and forms a constriction, which enables distinguishing between autophagic tubes and ordinary invagination. This dramatic invagination is facilitated by the segregation of transmembrane proteins away from the invaginating membrane[315]. This is an active process that requires ATP, as demonstrated by *in vitro* reconstruction experiments[316]. After fission from the autophagic tube, the vesicles freely move inside the lumen of the lysosome and are eventually degraded[317]. The nutrients are then recycled into the cytoplasm[318] (**Figure 8**).

Microautophagy can be either non-selective, acquiring unspecified material from the cytoplasm, or selective. Selective microautophagy is referred to by use of different terms, based on the target organelle. As reviewed by Li *et al*[319], micropexophagy specifically envelops peroxisomes[320], with piecemeal microautophagy of the nucleus involved in the degradation of parts of the nucleus in yeast[321], and micromitophagy degrades mitochondria[322].

An important function associated with microautophagy, is the control of the whole lysosomal membrane surface: macroautophagy, through fuse of autophagosomes and amphisomes with the lysosome, provides an extensive quantity of additional membrane for the lysosome, increasing its size. Thus microautophagy, by removal of the membrane from the lysosome, aids to maintain its size within physiological limits.

The core proteins, which control degradation of cytoplasmic components by the lysosome, are shared between macro- and microautophagy and the two systems are conjectured to work synergistically together to maintain the homeostasis of the cell.

The main difference between macro- and microautophagy may only be the availability of specific factors on a local level in the cytoplasm. For instance, the availability of cytoskeleton-interacting proteins (required for the recruitment of a phagophore membrane with the formation of the autophagosome) would favour macroautophagy. Conversely, factors involved in lipid/membrane protein

segregation (required for the formation of autophagic tubes) would trigger microautophagy. This model would then explain the large number of common factors involved in both mechanisms.

It is significant to consider that the classification of different mechanisms and structures is a strategy used to describe and attempt to comprehend what is actually observed in the cell. Nevertheless, this is only an artificial categorization. From the cell's perspective, such classification may prove irrelevant, since the cell's imperative is merely its survival along with that of the entire organism.

2.6.3Chaperone-mediated autophagy

Contrarily to macro- and microautophagy, CMA involves no membrane reorganization. Rather, proteins to be degraded are directly transferred inside the lysosome one by one, through the lysosomal membrane[323,324]. HSC70 (heat shock cognate 70) and other cofactors[324,325] bind a specific sequence, termed CMA-targeting motif, in the target protein and direct it to the lysosomal membrane[323]. Besides the deliverance of target proteins to the lysosomal membrane, HSC70 is further involved in the unfolding of the proteins, to aid the translocation process[325]. Approximately 30% of cytosolic proteins are predicted to possess the CMA-targeting motif in their sequence[326]. Once upon the surface of the lysosome, LAMP2A recognizes the unfolded protein and thus directs it to inside the lumen of the lysosome[327,328] (**Figure 8**).

2.6.4RNautophagy/DNautophagy

ON search for interaction proteins for LAMP2C - one of three isoforms of LAMP2, the receptor for CMA - Fujiwara and colleagues noted that the cytosolic tail of LAMP2C bound exclusively RNA-binding proteins[329]. Further studies have shown that LAMP2C directly binds RNA and participates in the active (ATP-dependent) transfer of RNA inside the lysosome for its degradation[329]. The authors termed this process RNautophagy[329]. Subsequently, they further characterized a similar mechanism, involving LAMP2C, for the degradation of DNA, termed DNautophagy[330–332].

2.7 The acrosome - a male germ cell specific vesicle

The acrosome is a sperm specific structure that covers the head of the sperm and is involved in the process of fertilization. Notably, the acrosome contains enzymes and proteins which are necessary for the fertilization of the egg[333–335].

Acrosome formation is generally divided into four phases, *viz*: Golgi, Cap, Acrosome and Maturation (**Figure 9**). Some proteins directed to the acrosome are already synthetized in pachytene spermatocytes[336–338]. During meiosis, these proteins are packed into small vesicles (proacrosomal granules, PAGs) by the Golgi apparatus and retained close by. After meiosis, when formation the acrosome has been commenced (Golgi phase), PAGs move from the Golgi to the surface of the nucleus and cluster together to eventually fuse to form the

acrosomal granule[339]. The migration of the PAGs from the Golgi to the nuclear membrane and their fusion is dependent on the microtubule system[340,341]. During the cap phase, more vesicles fuse with the acrosomal granule to form the acrosomal vesicle. The acrosomal vesicle continues to grow and flatten over the nuclear envelope to cover up to two-thirds of the nuclear surface[1,342]. This growth is enabled through the fusion of new cytoplasmic vesicles with the acrosome. When spermatid elongation commences, in the acrosome phase, the acrosome-nucleus complex migrates towards the cell surface to contact the plasma membrane[1]. During this process, the acrosome-nucleus complex rotates so that the acrosome faces the basal membrane of the seminiferous tubule (**Figure 9**). At the conclusion of this maturation phase two different domains of the acrosome membrane are specified, *viz*: the inner acrosomal membrane (IAM), which lies on the top of the nuclear membrane, and the outer acrosomal membrane (OAM), which contacts the plasma membrane[1]. These two domains are functionally and molecularly different. During the acrosome reaction, the OAM fuses with the plasma membrane to release the acrosomal content, while the IAM persists throughout the fertilization process[343,344].

The origin of acrosomal granules remains uncertain, but two different theories propose the source of the acrosomal material. The first theory explains the origin of acrosomal granules from the Golgi apparatus. As, in round spermatids, the Golgi apparatus is indeed oriented with the trans-Golgi network towards the growing acrosome, rather than towards the plasma membrane, as is in the case of somatic cells. The second theory includes the endocytic pathway as a source for the acrosomal material[345–347]. For a few of the acrosomal granules might originate from endosomes, so that a portion of the acrosomal material is of extracellular origin, possibly provided by Sertoli cells. Evidence for this theory comes from studies which show that molecules added to the culture medium were internalized by testicular germ cells and eventually localized in the acrosome[347]. Other such evidence includes the localization of proteins in the acrosome which are characteristic of the endocytic pathway[346,348–351]. Among these proteins, several are involved in the trafficking of endosomal vesicles. For example, proteins that form the ESCRT complex (Endosomal Sorting Complex Required for Transport) are detected in the acrosome. The ESCRT complex is required for the identification of endosomal vesicles[352] and sorting to their final destination[346,353,354].

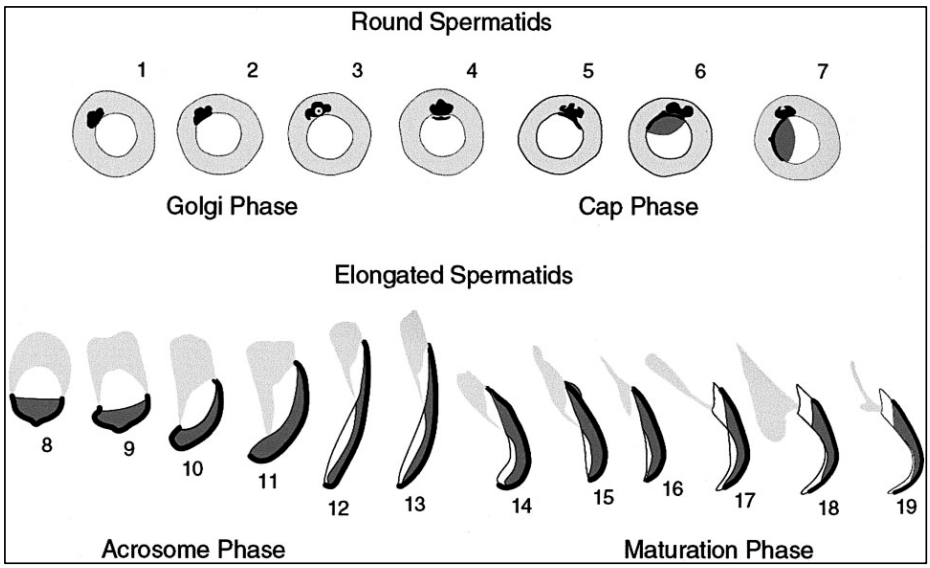

Figure 9 Diagram illustrating 19 stages of the transformation of round spermatids into spermatozoa (spermiogenesis) in the rat. The acrosome is gradually formed during four phases, as indicated in the figure. These phases are as follows: Golgi phase, stages 1–3; cap phase, stages 4–7; acrosome phase, stages 8–14; and maturation phase, stages 15–19. The stages vary from species to species: rat and rabbit, 19 stages; mouse, 16 stages; and man, 6 stages (Reprinted from Archives of Biochemistry and Biophysics, 379/2, Aida Abou-Haila and Daulat R.P. Tulsiani, Mammalian Sperm Acrosome: Formation, Contents, and Function, 10, Copyright © 2000, with permission from Elsevier).

Of note, the two theories are not necessarily mutually exclusive and there are ways in which their differences can actually conflate: for instance, the acrosome could be considered as a highly specialized lysosome[333,339,345,355]. Lysosomal enzymes are provided by vesicle transport from the TGN and has likewise been shown for hydrolytic enzymes present in the acrosome. In the standard endocytic pathway, endosomes eventually fuse with lysosomes to degrade their content. Germ line development is strictly dependent on signals and material provided by Sertoli cells, which continuously communicate and also possibly exchange material with round spermatids. It is likely that Sertoli cells may provide some of the acrosomal material, and the endocytic pathway would then likely be the path of choice for its delivery to the acrosome.

Rab5 is a protein involved in the formation of early endosomes from the plasma membrane[356,357]. Rab7 is involved in the heterotypic docking and fusion of late endosomes and lysosomes and also in the homotypic fusion between lysosomes[356,357]. Rab5 and Rab7 are both detected in the acrosome in round and elongating permatids[358,359].

Acrosome formation likely represents the main objective for vesicular transport in the developing spermatid. This is evidenced by the concentration of vesicle fusion proteins, such as COP and SNARE proteins, on the surface of the acrosome during its formation and maturation[358].

2.8 Small RNAs and cytoplasmic vesicles

Up until recent times both small RNA related studies and autophagy studies had been conducted separately. Of late, these two fields of gene regulation have now come together. It has long been observed that post-transcriptional control by small RNAs occurs in discrete granules that unite the machinery involved in target-mRNA recognition and repression. Dependent on the cell type and specific gene regulation involved, these RNP granules are termed P-bodies, GW-bodies, stress granules and germ granules (these further divided in P-granules, polar granules, *nuage*, inter-mitochondrial cement, pi-bodies and piP-bodies, Chromatoid body). These granules are not delimited by a lipid bi-layer and are considered to freely reside in the cytoplasm. Recent studies suggest that these granules and the cytoplasmic membrane system closely work together[142,171,360,361]. Different RNP granules have been observed to localize near vesicular structures inside the cell[362,363], but a mechanistic analysis has been absent.

The connection between the RNA-regulatory machinery and lipid membrane surfaces may actually be a conserved mechanism. As comparison, in bacteria, which notoriously lack any intracellular membrane system, RNA degradation is isolated from RNA transcription and translation processes by association of the RNA degradosome with the bacterial membrane[364].

AGO2 and TNRC6 are components of the RISC complex: AGO2 bears the guiding miRNA/siRNA strand to recognise the target mRNA, while TNRC6 (also known as GW182) disassembles the interaction between the polyA-binding complex and the cap-binding complex from the target mRNA, to trigger its repression[140,142]. Once the repression of the target mRNA has occurred, the RISC complex then must disassemble in order to initiate another round of repression. The active RISC complex coincides with the so-termed GW-bodies (due to the presence of GW182/TNRC6) and is often associated with the membrane of MVBs[141,142]. Internalization of TNRC6 into the MVB is necessary for the correct function of the silencing complex. Indeed, mutants of TNRC6 that cannot disassemble from the RISC complex, block the repression of reporter genes by siRNAs[142]. The same effect is obtained by the blockage of the ESCRT complex, involved in the internalization of proteins, such as TNRC6, into MVBs[142]. Another protein complex involved in the endosome/lysosome pathway and which regulates the action of RISC, is BLOC-3. This is involved in membrane trafficking and fusion between late endosomes and lysosomes[141]. Depletion of proteins which form BLOC-3, increases the loading rate of RISC with miRNAs and siRNAs[141]. ESCRT and BLOC-3 complexes therefore seem to have opposite effects on the regulation of RISC activity. These opposing actions are conjectured to be required for the fine tuning of the repression/degradation activity by small RNAs in the cell[141,142]. Notably, these studies underline the cooperative interaction between both the intracellular membrane system and small RNA pathways (**Figure 10**).

The loading of miRNA from Dicer to AGO2 is dependent on their interaction with the autophagy apparatus. Gibbings *at al.* showed that Dicer and AGO2 not loaded with miRNAs are constantly degraded by selective autophagy through recognition

by the autophagy target receptor NDP52[171]. Unloaded Dicer and AGO2 are presumed to compete for the binding of co-effectors and target molecules, and therefore require degradation to institute the correct function of the small RNA pathways. The authors further conjecture that such degradation may be required for the turnover of RISC complexes[171].

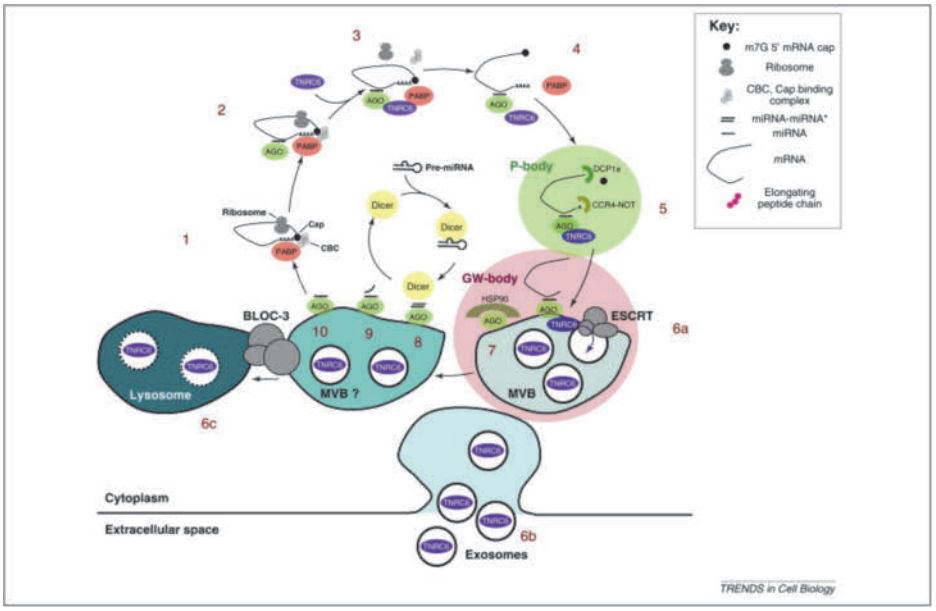

Figure 10 Model of action and turnover of RNA silencing complexes. (1) A mRNA with a 3' polyA tail and a 5' m^7G Cap. PABP binds the Cap-Binding Complex (CBC) composed of translation initiation factors (eIF4E, eIF4F and eIF4G), as well as the polyA-tail thereby circularizing the mRNA. In this form, mRNA can be translated by ribosomes. (2) Recognition of a mRNA by a miRNA bound to AGO. (3) TNRC6 binds to both AGO and PABP. TNRC6 binding to PABP prevents PABP binding to the CBC, presumably favoring the release of CBC from mRNA. Upon CBC release, new translation initiation cannot any longer occur, and ribosomes are eventually released from the repressed mRNA. (4) Repressed mRNA is no longer circularized by PABP linking the 5'-cap and polyA tail. PABP is presumably released at this stage from repressed mRNA, since PABP is not enriched in P-bodies. (5) P-bodies are enriched in mRNA decapping and deadenylation complexes (DCP1A and CCR4-NOT, respectively). Cap and polyA tail are removed from repressed mRNA. (6a) P-bodies are often adjacent to GW-bodies, themselves often adjacent to, or co-localized with, MVB. TNRC6 is removed from the complex of AGO and repressed mRNA, and sorted into intraluminal vesicles (ILVs) of MVB. This process appears to be affected by ESCRT that sorts proteins into ILV. (6b) TNRC6 in ILV may be released into the extracellular space in exosomes upon MVB fusion with the plasma membrane, or be eventually degraded upon MVB trafficking to lysosomes (6c). (7) AGO is released from miRNA and repressed mRNA. Hsp90 stabilizes empty AGO, which is presumably retained on the membrane. (8) DICER cleaves hairpin pre-miRNA into double-stranded complexes containing miRNA and miRNA* strands. AGO binds Dicer and acquires the miRNA-miRNA* complex. (9) AGO disassociates from DICER and the miRNA* strand disassociates from AGO. (10) AGO bound to miRNA is prepared to bind target mRNA (1, 2) (Reprinted from Trends in Cell Biology, 20/8, Derrick Gibbings and Olivier Voinnet, Control of RNA silencing and localization by endolysosomes, 11, Copyright © 2010, with permission from Elsevier).

3 Aims of the present study

The Chromatoid body is a ribonucleoprotein granule found exclusively in haploid round spermatids. To date, only a few proteins have been characterized as CB components, but even this limited knowledge was still enough to confirm the central role of the CB in the differentiation of male germ cell into mature and functional sperm. As such, the general aim of this particular study has been to characterize the role of the Chromatoid body in haploid germ cell-specific RNA regulation. In particular, the elucidation of the intriguing association of the CB with the vesicular transport system, was sought. Despite that this close association of the CB with small vesicles and multivesicular bodies has now been known for some time, the molecular nature of these vesicles still remained unclear.

As such, the specific aims identified in this present study included:

- To develop a protocol for the isolation of the intact CB from haploid round spermatids
- To characterize the CB-cytoplasmic vesicle interaction and the possible involvement of the CB in the acrosome biogenesis
- To characterize the CB and its possible interaction with the MVB/lysosome pathway

4 Materials and methods

Ethics statement

All mice (C57BL/6 and FVB strains) were handled in accordance with the institutional animal care policies of the University of Turku. Mice were maintained under controlled environment at the Central Animal Laboratory of the University of Turku and sacrificed by CO_2 inhalation and cervical dislocation. The Laboratory Animal Care and Use Committee of the University of Turku approved these studies.

Antibodies and lectins

Primary antibodies used in this study were: alpha actin (sc-32251) and DDX25 (sc-51271) from Santa Cruz Biotechnology (Heidelberg, Germany); alpha tubulin (MS-581-P1) from Thermo Fisher Scientific (Watham, MA, USA); DDX4/MVH (ab13840), EEA1 (ab2900), VPS26A (ab23892), VPS35 (ab10099), LAMP1 (ab25245) from Abcam (Cambridge, UK); MIWI/PIWIL1 (G82) from Cell Signalling Technology (Danvers, MA, USA); FYCO1 (H00079443-A01) form Abnova (Taipei City, Taiwan); FYCO1 (HPA035526 and SAB1400697) from Sigma-Aldrich (St. Louis, MO, USA). Anti-MARCH11 rabbit polyclonal antibody was a gift from Dr. Nobuhiro Nakamura (Tokyo Institute of Technology, Tokyo, Japan). Rabbit polyclonal antibody against TSKS was a kind gift from Prof. J.A. Grootegoed, Department of Reproduction and Development, Erasmus MC - University Medical Center Rotterdam. For glycoprotein labelling, we used the following lectins: rhodamine labelled peanut agglutinin (PNA, RL-1072) and biotinylated Aleuria aurantia lectin (AAL, B-1395) from Vector Laboratories (Burlingame, CA, USA); Alexa Fluor 488 conjugated Helix pomatia agglutinin (HPA, L11271) from Life Technologies (Carlsbad, CA, USA). Secondary antibodies conjugated with Alexa Fluor 488, 546, 594 and 647 made in donkey and streptavidin conjugated with Alexa Fluor 488 or 647 were purchased from Life Technologies (Carlsbad, CA, USA). ECL anti-mouse IgG HRP-linked whole antibody made in sheep (NA931) and ECL anti-rabbit IgG HRP-linked made in donkey (NA934) were purchased from GE Healthcare Life Sciences (Little Chalfont, UK).

Electron microscopy and tomography

Testis samples were fixed in 5% glutaraldehyde in 0.1 M collidine solution and treated with a potassium ferrocyanide-osmium fixative. The samples were embedded in epoxy resin (Glycidether 100; Merck, Kenilworth, NJ, USA), sectioned, stained with 5% uranyl acetate and 5% lead citrate, and visualized on a JEOL 1400 Plus transmission electron microscope (JEOL Ltd., Tokyo, Japan). Electron tomography samples were prepared following the same protocol, but staining with uranyl acetate and lead citrate was done on the block before sectioning. Serial semithick 250 nm sections were prepared and picked on single slot grids. Colloidal gold particles of 10 nm in diameter were placed below the sections to serve as fiducial markers for alignment of the tomograms. Dual axis tilt series were acquired using SerialEM software (http://bio3b.colorado.edu/serialEM) running on a Tecnai FEG 20 microscope (FEI, Hillsboro,

OR, USA) operating at 200 kV. Images from three consecutive sections were recorded at 1 degree intervals at 11.5k magnification. Recorded images were 1988 x 1878 x 210 pixels at 16 bits, pixels size 1.94 nm in the xy plane. IMOD software (http://bio3d.colorado.edu/imod) was used to create 3D reconstructions from the tilt series. The images were segmented using Microscopy Image Browser, developed by Electron Microscopy Unit, Institute of Biotechnology, University of Helsinki. 3D rendering of the segmented structures was performed with BioimageXD version 1[365].

Chromatoid body isolation

CB immunoprecipitation was performed as described previously [366]. Briefly, germ cells were released from four testes of adult C57BL/6 mice and fixed in 0.1% paraformaldehyde (PFA) in PBS (Electron Microscopy Sciences, Hatfield, PA, USA). After fixation cells were lysed by sonication (UCD-200; Diagenode, Liege, Belgium) in 1.5 mL of RIPA buffer [50 mM Tris-HCl pH 7.5, 1% NP-40, 0.5% w/v sodium deoxycholate, 0.05% w/v sodium dodecyl sulphate, 1 mM EDTA, 150 mM NaCl, 1X complete protease inhibition cocktail (Roche, Basel, Switzerland), 0.2 mM PMSF and 1 mM DTT] and the CB-enriched pellet fraction was separated by centrifugation at 500 × *g* for 10 min. The CBs were immunoprecipitated using Dynabead Protein G (Thermo Fisher Scientific, Watham, MA, USA) coupled to either anti-MVH antibody or rabbit IgG (NC-100-P; Thermo Fisher Scientific, Watham, MA, USA) at 4°C overnight.

Northern blot

Extracted RNA was separated by 15% denaturing polyacrylamide urea MOPS-NaOH gel, transferred onto nylon membrane and cross-linked with 1-ethyl-3-(3-dimethylaminopropyl)-carbodiimide (Sigma-Aldrich, St. Louis, MO, USA)[367]. The membrane was hybridized using EasyHyb (Roche, Basel, Switzerland) solution following the protocol suggested by the manufacturer. piRNA-030365 (NCBI ID: DQ715868)[89] signal was detected with γ[32P] ATP-labeled LNA (locked nucleic acid) probe (Exiqon, Vedbaek, Denmark): 5′-aataAagCtaTctGagCacCtgTgtgatgtt-3′ (capital letters stand for LNA and small letters for DNA nucleotides).

Western blotting

Tissue samples were homogenized in RIPA lysis buffer containing 1 mM DTT, 0.2 mM PMSF and 1X protease inhibitor cocktail (Roche, Basel, Switzerland), and the lysates were cleared by centrifugation at 14000 × *g* for 5 min. Samples diluted in Laemmli buffer were incubated 5 min at 70°C before loading them on the gel. Samples were run at 120 V and then transferred to a PVDF membrane (RPN303F; GE Healthcare Life Sciences, Little Chalfont, UK) with wet-blotting system (BioRad, Hercules, CA, USA) at 100 V for 1 hour at 4°C. After blotting the PVDF membrane was incubated in 100% methanol for 15 seconds and air-dried for 30 min at 37°C or at room temperature overnight. The membrane was then incubated with primary antibody diluted in 5% skimmed-milk, 0.1% Triton X-100 in phosphate buffered saline (PBS) (blocking solution) for 1 hour at room temperature, washed 3 × 5 min with 0.1% Triton X-100 PBS (PBST), incubated with secondary antibody

diluted 1:1000 in blocking solution, washed 5 × 5 min in PBST, incubated 1 min with Western Lightning ECL Pro (NEL121001EA; Perkin Elmer, Waltham, MA, USA). The chemioluminescence signal was recorded using LAS4000 (Fujifilm, Tokyo, Japan) as 16 bit .TIFF files. Band intensity was measured using ImageJ software. The band intensities from actin and tubulin were used for normalization. The results represent the mean of biological duplicates.

RT-qPCR

RNA was isolated from FVB mouse testis at different time points postpartum with TRIsure (BIO-38033; Bioline, London, UK) following the manufacturer's instructions. RNA was re-suspended in milliQ water to a final concentration of 1 µg/µL. Before cDNA synthesis, 1 µg of RNA per sample was treated with DNase I (AMPD1; Sigma-Aldrich, St. Louis, MO, USA). cDNA was synthesized with DyNAmo cDNA Synthesis Kit (F-470; Thermo Fisher Scientific, Watham, MA, USA) following the manufacturer's instructions using 1 µg of RNA as a template. The reverse transcription reaction was then re-suspended 1:20 in milliQ water for qPCR. qPCR was performed with the DyNAmo HS SYBR Green qPCR kit (F-410; Thermo Fisher Scientific, Watham, MA, USA) following the manufacturer's instructions in a 5 µL final reaction volume. Hprt1, Ppia and Rpl13a were used as reference genes. The geometric mean of the Ct values from the three reference genes was used as a normalization factor for the calculation of the delta-Ct for each gene of interest at each time point. The delta-delta-Ct value was calculated using the 1-week time point as reference. Three biological replicates were analysed. All RT-qPCR reactions and analysis were performed following MIQE guidelines[368].

Preparation of germ cells and tissues for immunostaining

Squash slides of stage specific sections of mouse seminiferous tubules were prepared as described earlier [11]. Briefly, testes from FVB or C57BL/6 adult mice were de-capsulated and sections representing specific stages of the seminiferous epithelium were isolated based on the light absorption pattern with the help of a stereomicroscope. The sections of the seminiferous tubules were then transferred to a glass slide with the use of a pipette and a glass coverslip deposited on top of the tubule section to allow the germ cells to spread outside of the tubule section. Once the germ cells formed a monolayer, the glass slide was snap-frozen in liquid nitrogen and, after removal of the coverslip, fixed in 100% ice-cold acetone for 10 min and air-dried overnight at room temperature. Slides were post-fixed in 4% paraformaldehyde in PBS for 10 min, washed 5 min in PBS, incubated 5 min in 0.2% Triton X-100 in PBS and washed 3 × 5 min in PBS before starting with IF staining.

For paraffin embedding, testes collected from FVB or C57BL/6 adult mice were fixed in 4% paraformaldehyde in PBS overnight at room temperature. Testes were washed in milliQ water for 2 h with repeated changes of fresh milliQ water, incubated 2 × 30 min in 50% ethanol and 2 × 30 min in 70% ethanol before embedding in paraffin. Paraffin-embedded testis sections were deparaffinised by incubation 3 × 5 min in xylene, 2 × 10 min in 100% ethanol, 2 × 10 min in 96% ethanol, 2 × 10 min in 70% ethanol and then washed in milliQ water 2 × 2 min. Antigen retrieval was performed by incubation in sodium citrate solution (10 mM

sodium citrate, 0.05% Tween 20, pH 6.0) or in Tris-EDTA solution (10 mM Tris base, 1 mM EDTA Solution, 0.05% Tween 20, pH 9.0) for 20 min, at 1 atmosphere at 120°C. After cooling down to room temperature for at least 2 hours slides were washed 4 × 3 min in milliQ water and 5 min in PBS before starting with IF staining.

In situ hybridization

Stage-specific squash preparations were fixed in 4% PFA. After acetylation with 0.25% acetic anhydride in 0.1 M triethanolamine (pH 8.0) for 5 min, sections were prehybridized in hybridization buffer without a probe [50% formamide (Sigma-Aldrich, St. Louis, MO, USA), 5% SSC buffer (Sigma-Aldrich, St. Louis, MO, USA), 250 µg/ml yeast RNA (Thermo Fisher Scientific, Watham, MA, USA), 1X Denhardt's solution (Sigma-Aldrich, St. Louis, MO, USA) in diethylpyrocarbonate (DEPC; Sigma-Aldrich, St. Louis, MO, USA)-treated water]. Hybridization was done in the same buffer containing 2.5 µM of 5′ DIG-labeled LNA probe (Exiqon, Vedbaek, Denmark): 5′-GccAtcActCcaAtaTttGgt-3′ (capital letters stand for LNA and small letters for DNA nucleotides) against piRNA-038309 (NCBI ID: DQ727400) or scrambled probe (Exiqon, Vedbaek, Denmark) at 37 °C for 18 h. Sections were washed three times in 0.1X SSC and once in 1X SSC, and signal was detected by Fluorescent Antibody Enhancer Set for DIG Detection (Roche, Basel, Switzerland).

Immunofluorescence and imaging

Slides were incubated with 10% normal donkey serum and 3% bovine serum albumin in PBST (blocking solution) for 1 hour. Primary antibody was diluted in blocking solution and incubation was performed for 1 hour at room temperature or overnight at 4°C. Slides were washed 3 × 5 min with PBST. Secondary antibody was diluted 1:1000 in blocking solution and incubation performed for 1 h at RT. Slides were washed 3 × 5 min in PBST, incubated 5 min in DAPI (D9542, 5 mg/mL stock; Sigma-Aldrich, St. Louis, MO, USA) diluted 1:20000 in PBS, washed 5 min in PBS and mounted with Vectashield HardSet Mounting Medium (H-1400; Vector Laboratories, Burlingame, CA, USA) or ProLong Diamond Antifade Mountant (P36970; Life Technologies, Carlsbad, CA, USA). Widefield fluorescence images were acquired with Zeiss Axio Imager M1 microscope equipped with AxioCam MRc camera using 40X/0.75 DIC Plan-NeoFluar objective (Carl Zeiss AG, Oberkochen, Germany). Widefield images were acquired and processed for publication with Zen 2011 software (Carl Zeiss AG, Oberkochen, Germany). Confocal images were acquired using either a Zeiss 510 META or a Zeiss 780 laser scanning confocal microscope with 40X/1.2 Water or 100X/1.4 Oil DIC objectives (Carl Zeiss AG, Oberkochen, Germany). Resolution in the 3 dimensions was set at optimal with Zen 2 software (Carl Zeiss AG, Oberkochen, Germany). Confocal images were analysed and modified for publication (background subtraction, contrast and brightness adjustment) with BioimageXD version 1.0[365]. All IF figures represent confocal images unless otherwise stated in the figure legends.

Seminiferous tubule cultures

Brefeldin A (B7651; Sigma-Aldrich, St. Louis, MO, USA) and U18666A (U3633; Sigma-Aldrich, St. Louis, MO, USA) were diluted to 10 mg/mL in DMSO and water,

respectively. Rapamycin (sc-3504; Santa Cruz Biotechnology, Heidelberg, Germany) and Nocodazol (M1404; Sigma-Aldrich, St. Louis, MO, USA) were diluted in DMSO to 10 mg/mL; Bafilomycin A1 (sc-201550; Santa Cruz Biotechnology, Heidelberg, Germany) was diluted 0.1 mg/mL in DMSO. Sections of the seminiferous tubules representing stage II-V of the seminiferous epithelial cycle were dissected as described above and cultured in 50 µL final volume of DMEM with drug or vehicle alone diluted 1:100 for 6 hours in a humidified incubator at 34°C, 5% CO_2. After incubation, squash slides were prepared, and samples were labelled for IF as described above.

Isolation of germ cells and cytoplasmic vesicle fractionation

Testes from 2 C57Bl/6J adult mice were collected in PBS, transferred in 8 mL 1X KREBS buffer (25 mM $NaHCO_3$, 1.2 mM KH_2PO_4, 120 mM NaCl, 1.2 mM $MgSO_4 \cdot 7H_2O$, 11.10 mM dextrose, 1.3 mM $CaCl_2 \cdot 2H_2O$, 4.8 mM KCl)[369], tunica albuginea was removed and seminiferous tubules were minced with scissors. The solution containing the seminiferous tubule fragments was divided into two tubes containing 25 mL collagenase solution [1X KREBS buffer with 22.5 mg Collagenase Type I (Worthington Biochemical Corporation, Lakewood, NJ, USA)] each pre-warmed at 34°C. Cells in collagenase solution were incubated at 34°C for 10 min with gentle shaking on a hula mixer. Cell suspensions were centrifuged 2 min, 500 × *g* at RT, supernatant was discarded and each pellet (composed of germ cells and seminiferous tubule fragments) was resuspended in 25 mL trypsin solution [1X KREBS buffer with 15 mg trypsin (Worthington Biochemical Corporation, Lakewood, NJ, USA) and 5 µg DNase I (DN25; Sigma-Aldrich, St. Louis, MO, USA)] pre-warmed at 34°C. Cell suspensions in trypsin solution were incubated at 34°C for 10 min with gentle shaking on a hula mixer. Cell suspensions were mixed 10 times with a wide bore pipette. 5 µg DNase I were added to each cell suspension and again incubated at 34°C for 10 min with gentle shaking on a hula mixer. After 2 min, 500 × *g* centrifugation at RT, the cell pellets were resuspended in 25 mL 1X KREBS buffer containing 5 µg DNase I and filtered through 100 µm filter. Cell suspensions were pooled together and centrifuged 2 min, 500 × *g* at RT. Cell pellet was resuspended in 5 mL ice-cold 1X KREBS buffer with 1 µg DNase I. Cell suspension was loaded on the top of an ice-cold discontinuous BSA density gradient (1-2-3-4-5-6% BSA in 1X KREBS, 5 mL each) in a 50 mL tube. Cells were allowed to sediment for 1.5 h at 4°C. 1 mL fractions were collected starting from the top of the gradient, centrifuged 5 min at 500 × *g*, washed twice with ice-cold 1X KREBS buffer and stored on ice. 5 µL of each fraction were diluted in 10 µL fixing solution (4% PFA, 0.05% Triton X-100) with DAPI (D9542, diluted 1:20000 from 5 mg/mL stock solution; Sigma-Aldrich, St. Louis, MO, USA). Each fraction was analysed by fluorescence microscopy for the enrichment in round spermatids. Fractions enriched in round spermatids were pooled together, centrifuged 5 min at 500 × *g* and resuspended in vesicle isolation solution [0.25 M sucrose, 10 mM HEPES pH 7.2, 1X complete protease inhibitor cocktail (04693116001; Roche, Basel, Switzerland)]. Cells were disrupted by nitrogen cavitation (500 p.s.i 5 min at RT; Parr Instruments, Moline, IL, USA). Cell lysate was centrifuged 5 min, 2000 × *g* at 4°C. Supernatant was centrifuged 5 min, 17000 × *g* at 4°C. Pellet representing enriched cytoplasmic vesicles was used for immunoprecipitation with rabbit anti-FYCO1 or control antibody as described below.

Immunoprecipitation

4 testes from adult mice were collected in PBS. Seminiferous tubules were released from the tunica albuginea, quickly minced with scissors and incubated 60-90 min at RT in 50 mL of collagenase solution (0.5 mg/mL Collagenase Type I, 0.1% glucose in PBS) on a hula mixer to release the germ cells from the seminiferous tubules. Cells suspension was centrifuged 5 min, 500 × *g* at 4°C. Pellet was resuspended in ice-cold 50 mL 0.1% glucose in PBS, filtered through 100 µm filter to eliminate pieces of seminiferous tubules and centrifuged again. Cells were lysed by sonication (6 × 30 sec with 30 sec pause, medium power; UCD-200; Diagenode, Liege, Belgium) on-ice in 1 mL isotonic non-denaturing lysis buffer [150 mM NaCl, 5 mM EDTA, 50 mM Tris-HCl pH 8.0, 1% Triton X-100, 1X complete mini mix (Roche, Basel, Switzerland), 0.2 mM PMSF and 1 mM DTT] followed by 30 min incubation on-ice. Samples was centrifuged 10 min, 500 × *g* at 4°C to eliminate cellular debris and intact Chromatoid bodies. FYCO1 complexes were immunoprecipitated using Dynabead Protein G (Thermo Fisher Scientific, Watham, MA, USA) coupled to either rabbit anti-FYCO1 antibody (Sigma-Aldrich, St. Louis, MO, USA) or rabbit IgG (NC-100-P; Thermo Fisher Scientific, Watham, MA, USA) at 4°C overnight.

Mass spectrometry

To remove Triton X-100, beads were washed 2 × 1 mL 25 mM NH_4HCO_3 buffer and 2 × 200 µL 6 M urea / 25 mM NH_4HCO3 buffer. Samples were loaded on a Criterion XT Bis-Tris precast 12% SDS-PAGE gel (BioRad, Hercules, CA, USA) and ran with constant 200 V for 9 min. MOPS buffer was used as a running buffer. Three pieces from the upper part of SDS-PAGE gel were cut and samples were in-gel digested at the Turku Proteomics Facility according to the standard protocol. Digested peptides were dissolved in 1% formic acid (ctrl 11 µL and all the rest 15 µL); 5 µL of each sample was submitted to LC-ESI-MS/MS analysis. The LC-ESI-MS/MS analyses were performed on a nanoflow HPLC system (Easy-nLCII; Thermo Fisher Scientific, Bremen, Germany) coupled to the LTQ Orbitrap Velos Pro mass spectrometer (Thermo Fisher Scientific, Bremen, Germany) equipped with a nano-electrospray ionization source. Peptides were first loaded on a trapping column and subsequently separated inline on a 15 cm C18 column (75 µm × 15 cm, Magic 5 µm 200 Å C18, Michrom BioResources Inc., Sacramento, CA, USA). The mobile phase consisted of water/acetonitrile [98:2 (v/v)] with 0.2% formic acid (solvent A) and acetonitrile/water [95:5 (v/v)] with 0.2% formic acid (solvent B). A linear 30 min gradient from 5% to 35% B was used to elute peptides. MS data was acquired automatically by using Thermo Xcalibur 3.0 software (Thermo Fisher Scientific, Bremen, Germany). An information dependent acquisition method consisted of an Orbitrap MS survey scan of mass range 300-2000 m/z. The data files were searched for protein identification using Proteome Discoverer 1.4 software (Thermo Fisher Scientific, Bremen, Germany) connected to an in-house Mascot server running the Mascot 2.4.1 software (Matrix Science, Boston, MA, USA). Data was searched against the SwissProt database (release 2014_08). The following search parameters were used. Type of search: MS/MS Ion Search, Taxonomy: *Mus musculus*, Enzyme: Trypsin, Fixed modifications: Carbamidomethyl (C), Variable modifications: Oxidation (M), Mass values:

Monoisotopic, Peptide Mass Tolerance: ± 5 ppm, Fragment, Mass Tolerance: ± 0.5 Da, Max Missed Cleavages: 1, Instrument type: ESI-TRAP. Results from ProteomeDiscoverer were exported and saved as Excel files. Only proteins assigned at least with two peptides were accepted.

Generation of Fyco1 knockout mice

Mice were housed at the Animal Facility of the University of Turku, Finland, under controlled environmental conditions, and was followed by local laws and regulations [Finnish Act on the Protection of Animals Used for Scientific or Educational Purposes (497/2013), Government Decree on the Protection of Animals Used for Scientific or Educational Purposes (564/2013)] The genetic background of all the mice used in this study was mixed background with C57Bl/6J and SV129. The construct for the generation of the FYCO1 conditional knockout (MGI:107277) was purchased from the International Mouse Phenotyping Consortium, and validity of construct was confirmed by restriction enzyme digestion and by sequencing. G4 embryonic stem cells (ES, derived from mouse 129S6/C57BL/6Ncr mice) were cultured on neomycin-resistant primary embryonic fibroblast feeder layers, and 10^6 cells were electroporated with 30 µg of linearized targeting construct. After electroporation, the cells were plated on 100-mm culture dishes and exposed to G418 (300 µg/ml; Sigma-Aldrich, St. Louis, MO, USA). Colonies were picked up after 7-9 days selection, and grown on 96-well plate. In order to delete *Neo* cassette in the targeted ES cells, targeted ES cells were re-electroporated with plasmid pCAGGS-*Cre*. After electroporation, the cells were plated on 100-mm culture dishes and colonies were picked up after 3-5 days growth, and grown on 96-well plate. Targeted ES clones and ES clones with Neo deletion were detected by LR-PCR and PCR, and right PCR products were further confirmed by sequencing. The right-targeted ES clones with *Neo* deletion were used for blastocyst injection and for creation of chimera. Male chimera were bred with wild type female to determine the germ line transmission. *Ngn3Cre* line was from Korhonen *et al.*[63]. To achieve selective inactivation of FYCO1 in germ cells, transgenic *Ngn3Cre* mice were mated with mice with homozygous FYCO1 floxed alleles, $FYCO1^{fx/fx}$ in order to generate $FYCO1^{fx/wt}$;$Ngn3Cre^{+}$ and $FYCO1^{fx/wt}$;$Ngn3Cre^{-}$ mice. These animals were then inter-crossed to produce $FYCO1^{fx/fx}$; $Ngn3Cre^{+}$, and $FYCO1^{fx/fx}$ and $FYCO1^{fx/wt}$;$Ngn3Cre^{-}$ littermates. Cre-mediated recombination was detected and confirmed by PCR with different primer pairs.

Histology, morphological analysis (sperm)

For histological analyses, tissues were collected and directly fixed in 4% PFA or in Bouin's fixative (4 to 20 hours at room temperature). Tissues were then dehydrated in a series of ethanol washes and embedded in paraffin. Paraffin embedded tissues were cut and stained with hematoxylin and eosin (HE) or periodic acid-Schiff (PAS) according to standard protocols.

Epididymal sperm was released in PBS from cauda epididymis and spread on glass slides, air dried and stained with hematoxylin for morphological analysis.

5 Results

5.1 Chromatoid body isolation and preliminary analysis (I)

The CB was first described over a century ago by von Brunn and Benda[174,214], but its actual study has been hampered by failure of its isolation to date. In 1998, Figueroa and Burzio[370] reported the isolation of CBs from 60 rat testes, but with a very poor yield and low purity in the final sample. Thus, when considering the presumed importance of the CB arising from the mouse models for the few known CB components[116,156,193–195,371], it is essential in the field of male fertility to precisely describe what the CB is composed of and its role in sperm differentiation. As such, a reliable and robust protocol for the isolation of pure CBs from mice with high efficiency was developed. With this protocol, 2-4 mouse testes are sufficient to isolate CBs for subsequent studies, both at the protein and RNA level.

5.1.1 Isolation of the CB

The CB isolation protocol (**Figure 11**) developed during this study took advantage of the size of the CB compared to other cellular structures, and of the antigenic qualities of one core component of the CB, the mouse VASA homolog protein, MVH/DDX4[191]. MVH/DDX4 has long been associated with the CB and has developed over the years into use as a CB marker. Moreover, it proved to be a highly effective antigen for antibody production, since both homemade and commercial anti-MVH antibodies show high specificity and avidity for the endogenous protein. Germ cells were initially released from the seminiferous tubules by a gentle digestion with collagenase. The size of the CB can be a challenge for its isolation, since the more liable components can detach from it during the isolation process; in order to isolate the CB in its intact form, CB components were cross-linked together through a mild treatment with the cross-linking agent paraformaldehyde. After such cross-link, the cells were lysed by sonication in lysis buffer. CBs were precipitated by selective centrifugation at 500 × *g* in order to concentrate the CBs in solution and eliminate the cytosolic, non-CB associated, MVH/DDX4. The resulting pellet, containing the CBs, but not the cytosolic MVH/DDX4 antigen, was then resuspended in the lysis buffer. By taking advantage of MVH/DDX4 antigenic properties, MVH specific antibodies were used to pull down the CB by immunoprecipitation. As a control for the specificity of the CB immunoprecipitation, a parallel IP using serum from non-immunized animals or a non-specific antibody was used.

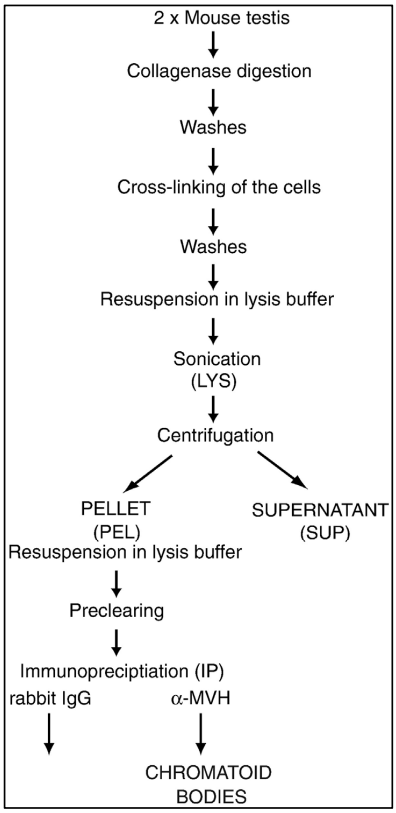

Figure 11 Schematic presentation of the CB isolation protocol. Germ cells were released by collagenase digestion from two mouse testes. Cells were washed and cross-linked with 0.1% PFA. After termination of the cross-linking reaction and washes, cells were resuspended in the lysis buffer and sonicated. Lysates were centrifuged for 10 min at 500 × *g*. The pellet fraction was resuspended in the lysis buffer, and immunoprecipitation performed with anti-MVH antibody and Protein G-coupled Dynabeads (Reprinted from Experimental Cell Research, 316/9, Meikar *et al.*, Accumulation of piRNAs in the Chromatoid bodies purified by a novel isolation protocol, 1567-1575, Copyright © 2010, with permission from Elsevier).

This protocol included several strategies to monitor the success of the whole process. Test samples from different steps along the protocol were analysed by western-blot and silver staining to estimate the efficiency of the CB isolation. WB with the anti-MVH antibody showed how the final sample was enriched by this CB component, while the control IP was free of it (I, Fig.2G).

Drying-down slides from the different test samples were analysed by immunofluorescence microscopy to assess the purity of the isolated CB: particles positive for MVH and of the expected size (0.5-1 μm), were visible in the pellet and CB fractions (I, Fig.2A,C), but not in the supernatant and control-IP (I, Fig.2B,D). Finally, electron microscopy of the isolated CB samples proved their purity and absence of other cellular structures (I, Fig.2E). EM analysis also showed the absence of CBs in the control sample (I, Fig.2F).

5.1.2 Protein components of the CB

Silver staining analysis of the isolated CB showed clear bands representative of the main proteins that form the CB (I, Fig.3A). Mass-spectrometric analysis of these bands identified MVH/DDX4 (Mouse Vasa Homolog/DEAD-box helicase 4), MIWI/PIWIL1 (Mouse PIWI/PIWI-like protein 1), TDRD6 (Tudor domain containing protein 6), TDRD7 (Tudor domain containing protein 7), GRTH/DDX25 (Gonadotropin Regulated Testicular RNA Helicase/ DEAD-box helicase 25) and PABPC3 (PolyA-binding protein, Cytoplasmic 3). The presence of MIWI, PABP and DDX25 proteins in the isolated CB was also confirmed by western-blot analysis (I, Fig3B-D). Previous studies had identified these proteins in the CB by immunofluorescence[116,183,193,371,372]. The presence of these proteins in the final samples can be considered as proof of the integrity and purity of the CBs obtained thought this isolation protocol.

5.1.3 RNA content of the CB

It has long been known that mRNAs and microRNAs are present in the CB[216]. RNA was purified from the isolated CBs and the presence of mRNA by RT-PCR was confirmed.

GRTH is a RNA helicase and several of its target mRNAs have been described[190,371]. Primers were used for some of the haploid germ cell-specific GRTH target mRNAs, *viz*: transition protein 2 (Tp2), protamine 2 (Prm2) and outer dense fibre protein 1 (Odf1)[371]. The Ets-related molecule (ERM) is a Sertoli cell specific protein[373], while CD9 is a surface marker for spermatogonia[374]. While all these mRNAs were detected in the lysate and supernatant samples, only the GRTH-specific mRNAs were present in the CB-enriched pellet sample, and in the isolated CB. Neither ERM nor CD9 mRNAs were detected in the CB-associated RNA (I, Fig.4).

5.1.4 Accumulation of PIWI-interacting RNAs in the CB

During the development of the CB isolation protocol, it was of interest to study the possible CB-RNA interaction. RNA from the pellet and supernatant fraction was isolated, separated by polyacrylamide gel electrophoresis and visualized by SYBR Gold. Long RNAs (> 100 nts) were present in both fractions, and particularly in the supernatant. One prominent 30 nucleotide-long RNA band was visible, predominantly in the CB-enriched pellet fraction (I, Fig.5A). Analysis of the RNA extracted from the purified CB showed that this 30 nucleotide-long RNA band was present exclusively in the CB sample (I, Fig.5B).

MIWI and MILI, also known as PIWIL1 and PIWIL2 (PIWI-like protein 1 and 2), belong to the PIWI subfamily of the Argonaute/PIWI protein family, which bind a specific class of 26-30 nucleotide-long RNAs called piRNAs (PIWI-interacting RNAs). Both MIWI and MILI localize to the CB. It was hypothesised that the small RNA band enriched in the CB extracts corresponds to piRNAs. Northern-blot analysis was performed by use of probes against specific piRNAs and their

presence confirmed in the 30 nucleotide-long RNA band from CB extracts (I, Fig.5C), but not in the control IP.

Squash preparations of seminiferous tubule sections were used to study the cellular localization of piRNAs by fluorescence *in situ* hybridization. Besides a diffused signal in the cytoplasm, piRNAs showed to be highly concentrated in one single granule near the nucleus of haploid round spermatids; phase contrast microscopy revealed this granule to be the CB (I, Fig.5D). Independent experiments demonstrated that piRNAs were concentrated in the CB of haploid round spermatids.

5.2 Retromer functions in haploid male germ cells (II)

A comprehensive list of proteins which form the CB has recently been published by our group[165]. For the follow on study, it was of interest to characterize the interaction between the CB and the numerous vesicles that surround it and are clearly visible by EM. In the list of CB components, two proteins stood out: VPS26A and VPS35, which are main components of the Retromer protein complex.

5.2.1VPS26A and VPS35 expression in the male germ line

Due to the paucity of information on VPS26A and VPS35 proteins in the testis, it was decided to first characterize their expression and cellular localization during spermatogenesis. The first wave of spermatogenesis occurs immediately after birth during the first 5 weeks in male mouse: in the seminiferous tubules of 1 week-old testis, only Sertoli cells and spermatogonia are found. After two weeks spermatocytes are present; by week three, round spermatids become present and by the fourth week elongating spermatids can be detected. RT-qPCR and western-blot analysis were performed to detect the VPS26A and VPS35 mRNA and protein, respectively, during the first wave of spermatogenesis (II, Fig.1A). Both techniques showed that both VPS26A and VPS35 expression increased during the first wave of spermatogenesis, to reach a stable level in the adult. This data indicated that these proteins were expressed at all the different stages of spermatogenesis and especially in round spermatids.

Stage-specific squash preparations of mouse seminiferous tubules were used for indirect immunofluorescence detection of VPS26A and VPS35 inside germ cells. VPS35 was concentrated in cytoplasmic granules, predominantly in spermatocytes and round spermatids (II, Fig.1B), which granules were dispersed throughout the cytoplasm. Using high-resolution confocal microscopy, VPS26A and VPS35 were shown to co-localize on circular structures that resembled vesicles, in the cytoplasm of haploid round spermatids (II, Fig.1C).

5.2.2 Cytoplasmic surroundings of the CB

EM images of the CB in the cytoplasm of haploid round spermatids showed the presence of small vesicular-like structures all around it. These assumed vesicles had a morphology similar to those vesicles provided by the Golgi apparatus for the assembly of the acrosome. These were notably different from the stacks of the endoplasmic reticulum (II, Fig.2A). To enable a better comprehension of the structure of these vesicles, electron tomography (ET) of the CB in haploid round spermatids was performed. From the ET image stack, manual segmentation was performed of the different cytoplasmic organelles, *viz*: the CB, MVBs, ER, nuclear membrane, Golgi complex, mitochondria and cytoplasmic vesicles (II, Fig.2B). 3D rendering of the segmented structures clarified the spatial disposition of all the different organelles, relative to the CB (II, Fig.2C). The CB was positioned close to the nuclear membrane and nuclear pores appeared concentrated in the area directly facing the CB. The small vesicle-like structures that surround the CB in the EM pictures were – as predicted – discrete cytoplasmic vesicles. Of note, some of these vesicles were positioned inside hollows of the CB itself. The ER was also in very close proximity to the CB, and in this particular case, a tubule of the ER network was observed to pass directly through the CB (**Figure 12**).

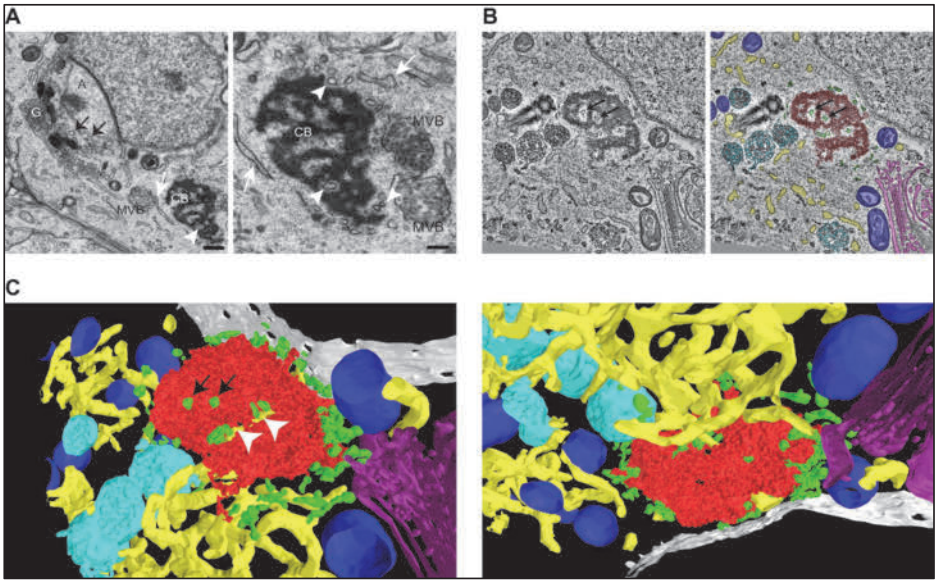

Figure 12 Cytoplasmic surroundings of the CB. A) EM analysis to visualize membrane structures and vesicles (arrowheads) that surrounded the CB or were engulfed by it. MVBs were always found close to the CB. The CB was often observed close to the Golgi complex (G) and developing acrosome (A). Scale bars: 500 nm (left panel) and 200 nm (right panel). The vesicles that surrounded the CB resembled those provided by the Golgi for the development of the acrosome (left panel, black arrows) and were clearly different from the cross-sections of the endoplasmic reticulum (white arrows). B) A representative section of electron tomography of the cytoplasm of a haploid round spermatid (stages II–V). Different organelles were segmented for 3D rendering and differentially coloured. C) Representative snapshots of 3D rendering of the segmented structures in B). The CB (red) was found close to the nuclear membrane (white). Holes visible in the nuclear membrane represent nuclear pores. The CB was surrounded by small cytoplasmic vesicles (green); some of these vesicles were localized inside cavities of the CB (black and white arrows). MVBs (cyan), mitochondria (blue) and the Golgi complex (purple) were found close to the CB. A tubular segment of the ER (yellow) passing through the CB is indicated with white arrowheads (Reprinted from Molecular and Cellular Endocrinology, 401, Da Ros *et al.*, RETROMER VESICLES INTERACT WITH RNA GRANULES IN HAPLOID MALE GERM CELLS, 73-83. Copyright © 2015, with permission from Elsevier).

5.2.3 The CB relationship with Retromer vesicles

As aforementioned, in the list of CB protein components were the Retromer associated proteins VPS26A and VPS35. Their presence in the CB was validated by immunoblotting with antibodies against VPS26A and VPS35 in CB extracts (II, Fig.3A). To comprehend their relationship to the CB inside the cell, indirect immunofluorescence of spermatids co-stained for VPS35 and two different CB markers: MVH/DDX4[191] and MIWI/PIWIL1[375], was performed. Laser scanning confocal microscopy of these samples revealed that VPS35 to not be a core protein of the CB. The VPS35 signal did not overlap with MVH or MIWI, but rather was adjacent to it (II, Fig3B). In some cases, it appeared to be located inside pockets of the MIWI-stained CB (II, Fig.3B zoom-in). This very close localization may explain why Retromer proteins co-precipitated with the CB. From the same images, it also became possible to distinguish other cytoplasmic structures positive for VPS35 that were not associated with the CB. These structures appeared to be smaller than those found adjacent to the CB.

5.2.4 Relationship between different organelles in the cytoplasm of haploid round spermatids

In somatic cells, the Retromer is involved in the recycling of cargo receptors from endosomes/MVBs to the Golgi complex. Since it appeared that no prior investigation into Retromer proteins in male germ cells had been undertaken, the relationship between VPS35 and the endosome/MVB system in haploid round spermatids was studied. VPS35 was co-stained along with the E3 ubiquitin ligase MARCH11, a membrane protein located in MVBs[376,377]. Some of the VPS35 positive structures showed co-localization with MARCH11 (II, Fig.4A). VPS35 positive vesicles also showed cargo marked by *Aleuria aurantia* lectin (AAL) (II, Fig.4B). AAL marks proteins present in the MVBs, which supports the results obtained with MARCH11. VPS35 was therefore associated with MVBs in haploid round spermatids. VPS35 also showed co-localization with EEA1 (Early Endosome Antigen 1) (II, Fig.4C). These results indicate the likelihood that Retromer associated proteins in haploid round spermatids are involved in similar processes as are in somatic cells.

The acrosome can be considered as a gigantic organelle formed by the fusion of smaller vesicles, termed acrosomal granules. Two theories have been advanced to explain the source of acrosomal granules. In the standard model, they originate from the Golgi; although in a more recent model, some of these vesicles originate from endosomes. Co-staining of VPS35 was performed with PNA (peanut agglutinin) and HPA (*Helix pomatia* agglutinin), two lectins which recognize material usually present in the acrosome and in the Golgi, respectively[378]. HPA-positive Golgi was often associated with the PNA-positive acrosome in haploid round spermatids (II, Fig4D). Additionally to this, PNA also stained small granules in the cytoplasm. Of note, these granules were often surrounded by VPS35-positive signal (II, Fig.4D). As such, a likely interpretation is that VPS35-positive vesicles transport PNA-marked acrosomal material. In fact, these vesicles were sometimes located very close to the acrosome (II, Fig.4D zoom-in).

5.2.5 Retromer vesicles interact with the lysosome pathway

These previous results indicated interaction of the Retromer proteins with the endosomal system. As such to better elucidate the mechanism of these interactions, pieces of seminiferous tubules in culture were treated with Brefeldin A, a drug that disrupts the Golgi apparatus, which became no longer visible after this treatment (II, Fig.5A). If the role of VPS35 was somehow connected to the transport of vesicles to the Golgi apparatus, either a decrease of these vesicles due to inhibition of their formation would be expected, or their accumulation in discrete regions inside the cell, following the disappearance of their target organelle. Contrarily, VPS35-positive vesicles appeared unaffected by the Brefeldin A treatment (II, Fig5A). As such, Retromer proteins may therefore possess Golgi independent roles in haploid round spermatids. This data shown above, suggests that Retromer-positive vesicles may be involved in the transport of acrosomal cargo between the acrosome and the endosome/MVBs system. Pieces of seminiferous tubules in culture were treated with U18666A, a molecule that disrupts the flow of cholesterol along the endosome/lysosome pathway and, as a cytological effect, blocks the interaction between different compartments of the MVB-lysosome system[379–381]. Incubation with U18666A resulted in the complete disappearance of the VPS35-positive vesicles (II, Fig.5B). Further, MARCH11 signal did not show any difference compared to the control, to indicate that MVBs remain present in the cell (II, Fig.5B). Conversely, EEA1 particles were no longer visible following the U18666A treatment (II, Fig.5B). These results indicate that the formation of endosomes and VPS35-positive vesicles depends on the correct functionality of the endosome-lysosome pathway. Of note, EM analysis of the U18666A treated samples did not reveal any noticeable difference in the morphology of the CB (II, Supplementary Fig.S1).

5.2.6 Differences in Retromer vesicle formation in mouse models with disrupted Chromatoid bodies

The Tudor domain containing proteins 6 and 7 are core components of the CB (I), which are considered to be scaffold proteins involved in tethering together the different components of the CB[156,194]. The cellular localization of VPS35 in the testis of TDRD6 and TDRD7 knockout mice was studied and, even though the CB structure is completely compromised in these mouse models[156,193,194], VPS35-positive vesicles appeared still unaffected (II, Fig6.A,B).

Another interesting mouse model for the study to of the role of the CB is the MIWI knockout. MIWI is involved in the piRNA pathway, likely the main molecular pathway present in the CB (I). MIWI-KO mice present the arrest of spermatogenesis at the haploid round spermatid stage, and the CB morphology becomes severely compromised[116,183]. Of note, VPS35-positive vesicles were disrupted in late round spermatids, which are present at stages VI-VIII of the seminiferous epithelial cycle (I, Fig.6C).

The depletion of MIWI, a main regulator of gene expression by the piRNA pathway, is expected to have a wide downstream effect on different cellular processes that regulate spermiogenesis. Indeed, it was found that the acrosome was also affected: it would appear that the acrosomal granules did not correctly fuse together to form the acrosomal vesicle (II, Fig.6D). PNA staining of control testis showed the classical flat morphology of the acrosome on the top of the nuclear membrane in stage VII-VIII seminiferous tubule sections. Contrarily, MIWI-KO tissue showed only small, scattered PNA-positive granules (II, Fig.6D). As such, abnormality in the VPS35-positive vesicles could be an indirect effect arising from the more general defects in the endomembrane system in MIWI-KO round spermatids. Conversely, this along with other independent data provided by this study, indicate a correlation between the CB and the endosome-dependent acrosome formation, with VPS26A-VPS35 positive vesicles as players in this process.

5.3 FYCO1 – A bridge between the CB and lysosomes (III)

It has long been observed that small cytoplasmic vesicles surround the CB. In a similar area in the cell, Haraguchi *et al.* showed the presence of the lysosomal marker LAMP1, which indicates that the CB is associated with lysosomal activity. Following the successful isolation of the CB (I) and the accurate description of its composition[165], further comprehension of the CB-cytoplasmic vesicles conundrum was achieved.

5.3.1A novel CB component – FYCO1

With the objective to unveil a molecular connection between the CB and the vesicular system that surrounds it, a search among the proteins that form the CB was conducted, for likely candidates involved in vesicular pathways. FYCO1 (FYVE and coiled-coil domain containing 1), a protein known to be involved in the microtubule-dependent transport of autophagy vesicles, proved to be one of the most abundant proteins identified by the mass-spectrometry analysis of the CB-IP[165]. The MS analysis was first validated by western-blot detection of FYCO1 in CB-IP samples (III, Fig.1A). Since FYCO1 had never been reported before in the testis, its expression was characterized during postnatal development (III, Fig.1C). FYCO1 expression increased during the first wave of spermatogenesis, to indicate its expression in all the germ cell types. Its expression was elevated 4 weeks post-partum and in the adult, this means that its expression was particularly concentrated in haploid spermatids (III, Fig.1C).

Western-blot analysis of different tissue lysates revealed that FYCO1 is a ubiquitous protein expressed in all the adult tissues analysed (III, Fig.1B).

To clarify the cellular localization of FYCO1 indirect immuno-fluorescence of FFPE testis sections was performed: FYCO1 was clearly expressed in spermatocytes and it localised into discrete granules around their cytoplasm (III, Fig.2). In round spermatids, it localised in one large granule adjacent to the nucleus, to resemble the CB, and in smaller granules dispersed in the cytoplasm (III, Fig.2). In elongated

spermatids, FYCO1 was concentrated in one middle-sized granule located near the basis of the flagellum (III, Fig.2). To confirm the FYCO1 localisation in the CB in haploid spermatids, co-staining was undertaken by IF of squash preparations of seminiferous tubule sections that represented stages II-V of the seminiferous epithelial cycle. Laser scanning confocal microscopy of round spermatids confirmed the presence of FYCO1 in the CB marked by DDX4, MIWI and DDX25 (III, Fig.3A). FYCO1 also co-localised with the late CB marker TSKS in the cytoplasm of elongating spermatids (III, Fig.3A). FYCO1 already co-localized with CB components in spermatocytes in smaller cytoplasmic granules that, subsequent to meiosis, then unite to form the CB (III, Fig.3B). Closer analysis of FYCO1 in the CB revealed that FYCO1 was not positioned in the centre of the CB, but rather on its periphery (III, Fig.3C). Moreover, FYCO1 also co-localised with CB components in non-CB-associated small cytoplasmic granules in round spermatids (III, Fig.3C). These data indicate that FYCO1 interacts with the CB during the entire lifetime of the CB itself.

5.3.2 FYCO1 interaction partners

FYCO1-IP from mouse testis was performed to identify the FYCO1 interactome by MS. In the list of the proteins that co-precipitated with FYCO1, different CB components, such as the early CB markers DDX4 and TDRD1 were identified together with MIWI, TDRD7 and DDX25, and the late CB markers TSSK1 and TSSK2 (III, Supplementary Table 1). The association of FYCO1 with different CB components was thereby confirmed. Of interest, in MIWI-KO and TDRD6-KO testis, in which the CB morphology is compromised[116,194], FYCO1 remains localized in the fragments of the CB stained by DDX25 (III, Supplementary Figure 1). Therefore, MIWI and TDRD6 are not required for the recruitment of FYCO1 to the CB.

In support of the known role of FYCO1 as a microtubule-dependent vesicle transport protein, different kinesin proteins were also identified among the FYCO1 partners, such as kinesin heavy chain isoform KIF5C, kinesin-like proteins KIFC2, KIFC3, KIF3A, KIF3B and kinesin light chain 3 (KLC3) (III, Supplementary Table1). The interaction of FYCO1 with kinesins in the testis indicated that FYCO1 retains, in the germ line, its function in the microtubule-dependent transport system[382,383]. Of interest, different proteins involved in the ubiquitination pathway were found, such as E3 ubiquitin protein ligases HERC2, TRIM36 and UBR4, which support the role of FYCO1 in degradation processes (III, supplemental Table1).

5.3.3 Testicular phenotype of FYCO1 knockout mice

To better comprehend the role of FYCO1 during spermatogenesis, a germ line specific FYCO1-cKO mouse was generated by the crossing of mice with two loxP sites flanking FYCO1 exon 6 (*FYCO1$^{fx/fx}$*), and a transgenic mouse which expressed the Cre recombinase under the control of the *Ngn3* promoter (*Ngn3Cre^{+}*). The depletion of exon 6 in the germ line of *FYCO1$^{fx/fx}$; Ngn3Cre^{+}* mice (referred to as FYCO1 cKO in this study) causes a frame shift, with the generation of a premature stop codon. The resulting mRNA is therefore degraded through the non-sense

mediated decay pathway. FYCO1 depletion was verified by WB and IF (III, Fig.4A,B). Histological analysis of the testis and epididymis failed to show any defect in the germ cell differentiation or sperm morphology (III, Fig.5A,B, Supplementary Figures S2 and S3A,B). The mice were fertile and their progeny showed no defects (III, Supplementary Figure S3C).

5.3.4FYCO1 is required for the integrity of the CB

Of interest, the molecular analysis of the CB by IF showed that the CB was fragmented into several small granules inside the cytoplasm of round spermatids, when compared to the single large granule in the control tissues (III, Fig.4C). MIWI and MILI, two CB components expressed during post-natal development, showed similar expression in cKO versus control tissues. MILI was localized in the IMC in spermatocytes (III, Fig.4D) and early CB (data not shown), while MIWI localized in the cytoplasmic fragments of the CB in round spermatids of FYCO1 cKO testis (III, Fig.4D).

Similar fragmentation of the CB was obtained in wild-type testis following treatment of segments of the seminiferous tubules with Nocodazol (III, Fig.4E)[384], which inhibits microtubule polymerization. This result therefore indicates that the integrity of the CB is dependent upon the microtubule cytoskeleton, in addition to the microtubule-dependent transport protein FYCO1.

5.3.5The CB and autophagocytosis

FYCO1 was first identified as a binding partner of LC3B and RAB7 in somatic cells[382]. Pankiv *et al.* described FYCO1 as connecting autophagosomes with the microtubule motor protein kinesin[382]. In subsequent studies, FYCO1 was also involved in the transport of endosomes along the axon of neurites[383]. It therefore follows the involvement of FYCO1 in the transport of cytoplasmic organelles that belong to the lysosome pathway. As such, a study into the likely involvement of FYCO1 in the interaction of the CB with the surrounding cytoplasmic vesicles was undertaken.

The entourage of the CB by electron tomography has been recently characterized (**Figure 12**). The CB is in fact surrounded by a cloud of small cytoplasmic vesicles, along with cisterns of the endoplasmic reticulum and MVBs (II). These small vesicles were investigated more in detail: 3D reconstruction revealed that these have a cup-shaped morphology with protrusions that resemble phagophores (III, Fig.6A). It is therefore plausible to conclude that these may indeed represent autophagocytic vesicles.

To verify whether FYCO1 maintains the same properties as in somatic cells, the cytoplasmic vesicle fraction from isolated round spermatids was purified. Immunoprecipitation of FYCO1 from the vesicle-enriched fraction revealed that FYCO1 interacts with LC3B in round spermatids (III Fig.6B), to indicate the involvement of FYCO1 in the transport of autophagosomes. Testis sections co-stained with LC3B and the CB marker DDX25 also revealed that LC3B stains

vesicles widely distributed in the cytoplasm, but that also concentrated in the CB area (III, Fig.6C). This finding further supports the likely interaction between the CB and the autophagy system. LC3B concentration in the CB area was not detected in the FYCO1 cKO testis (III, Fig.6C). This provides a strong indication that FYCO1 drives the localization of LC3 positive vesicles to the CB.

5.3.6 Recruitment of lysosomes to the CB is supported by FYCO1

In somatic cells, protein aggregates, such as P-bodies, stress granules and inclusion bodies, are often degraded by autophagy. The CB represents an exceptionally large RNP granule. Data presented here and from the literature[363] thus prompted the investigation into the likelihood that CB material is degraded by autophagy. Pieces of seminiferous tubules were cultured with drugs that affect the autophagic pathway, and the LAMP1-positive structures were analysed (autophagolysosomes and lysosomes). In samples cultured with vehicle (DMSO), small LAMP1 positive vesicles were detected in the cytoplasm of round spermatids and in the area which surrounds the CB (III, Fig.7; **Figure 13**), as previously described by immuno-EM[363]. Seminiferous tubule sections were then cultured with Rapamycin, which is an mTOR inhibitor and therefore induces a response similar to starvation and promotes autophagy. Rapamycin treatment induced the accumulation of LAMP1-positive vesicles onto the CB (III, Fig.7; **Figure 13**). To conclude, seminiferous tubules were also treated with Bafilomycin A1, which blocks the fusion of autophagosomes with lysosomes. Bafilomycin A1 treatment induced the accumulation of LAMP1-positive vesicles near the CB (III, Fig.7; **Figure 13**).

In seminiferous tubules from FYCO1 cKO, LAMP1 signal is similar to control tissues, when incubated with vehicle (DMSO). Conversely, no response to Rapamycin or Bafilomycin A1 treatments was detected in the FYCO1 cKO round spermatids (III, Fig.7). As such, these results strongly indicate that FYCO1 is involved in the recruitment of lysosome vesicles to the CB in post-meiotic germ cells.

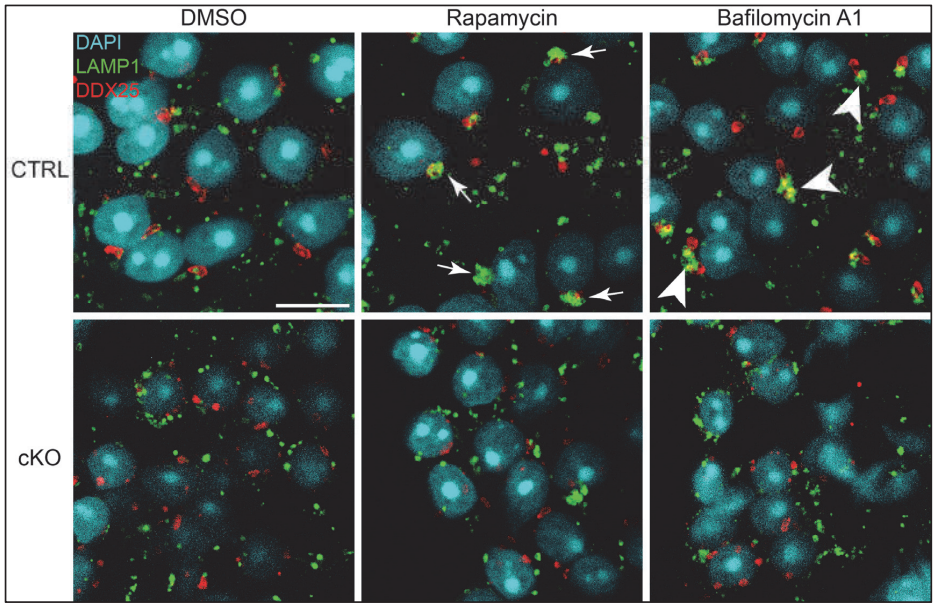

Figure 13 Lysosomal vesicles are not recruited to the CB in the absence of FYCO1. Stage-specific (II-V) pieces of seminiferous tubules were cultured in the presence of vehicle (DMSO), Rapamycin or Bafilomycin A1. After cultures, squash preparations were made and immune-stained with anti-DDX25 (red) and anti-LAMP1 (green). Nuclei were stained with DAPI (blue). Arrows point to the LAMP1-signal recruited in the CB area after Rapamycin treatment. Accumulation of LAMP1-postive vesicles next to the CB after Bafilomycin A1 treatment is indicated by arrowheads. Scale bar: 10 µm. (Reproduced from study III; FYCO1 AND AUTOPHAGY CONTROL THE INTEGRITY OF THE HAPLOID MALE GERM CELL-SPECIFIC RNP GRANULES, Da Ros *et al.* 2015 Submitted for publication).

6 Discussion

6.1 Isolation of the CB and identification of its components

The nature and function of the CB has intrigued scientists since its discovery in the late 19th century[174,214,385]. What is the function of this large agglomerate of proteins and RNAs in the cytoplasm of haploid round spermatids? And further, from where does it originate and then to where does it vanish, during elongation of the cell? In the last few decades, some of these dilemmas have now been partially answered.

A reliable and efficient protocol was developed in the present study to isolate the CB from mouse testis (I). In contrast to previous attempts, which used differential centrifugation and required an impractical number of rat testes as starting material, the protocol developed for this study required only 2 to 4 mouse testes. This relies on three major steps, *viz*: cross-link of the CB components together, concentration of the CB by centrifugation and immuno-precipitation by use of an antibody against one of the main proteins of the CB.

The CB is a huge RNP granule, measuring approximately 1 μm in diameter. Due to its size and diverse composition, it is very likely that it fragments in a standard immuno-precipitation protocol, with the loss of many of its components. To overcome this issue, this developed protocol included a mild cross-linking of the germ cells with 0.1% PFA (compared standard protocols, such as chromatin immuno-precipitation, which use 1%). With such treatment, very close molecules were expected to be covalently bound together, while excess linking of loose components is likely avoided.

MVH/DDX4 is one of the main components of the CB, and has been used as a CB marker for many years. Moreover, it has excellent antigenic properties so that antibodies raised against it show high specificity and avidity. As such, MVH/DDX4 was chosen as the target to immuno-precipitate the CB. MVH/DDX4 is highly concentrated in the CB, but is also present in the cytoplasm. To separate the CB-bound MVH/DDX4 from its cytoplasmic counterpart, the size of the CB was considered. Centrifugation of the lysed cells at 500 × *g* allowed precipitation of the CB, along with other cellular organelles of similar or larger size, while other cytoplasmic molecules remained in solution in the supernatant fraction. In the resuspended pellet, the only MVH/DDX4 present in the sample was that included in the CB.

At this stage, the CB was specifically separated from the other components in solution by immuno-precipitation through use of an antibody against MVH/DDX4. The final sample was represented by in effect purified CBs. The validity of this protocol was proved by identification of known CB components, such as MIWI and GRTH/DDX25, in the isolated CB against the control samples, along with GRTH/DDX25-bound RNAs.

By this process, the complete and precise composition of the CB in terms of its proteome and its transcriptome is now known. This data is predicted to represent the springboard for future research on the CB and post-meiotic germ cell differentiation.

From these experiments came the significant discovery of the presence of piRNAs in the CB. Indeed, this class of germ line-specific small RNAs is particularly enriched in the CB, and their presence can be detected by RNA fluorescent dyes, such as SYBR Gold, without the need for highly sensitive techniques, such as radioactivity.

Since the publication of this CB-isolation protocol, several updates were introduced and an improved protocol published, which allows any research laboratory to easily implement the technique[366]. Further, arising from the efficiency of the protocol, established for this study, to isolate pure fractions of CBs, a comprehensive list of proteins and RNAs forming the CB was also finally compiled, too[165]. This analysis revealed that the main proteins within the CB are RNA binding proteins, or at least proteins involved in RNA regulation. Further analysis of the RNAs concentrated in the CB revealed that no "localization sequence" is present which targets the RNA to the CB. Rather contrarily, it would appear that a diverse set of RNAs which form different classes (mRNAs, lncRNAs, sncRNAs, and transposable elements) could be detected in the CB. All the current data support the hypothesis that the CB may function as a screening and sorting centre for newly synthetized RNAs. The presence of proteins involved in RNA splicing and in the non-sense mediated decay, indicates that the RNA undergoes a quality control check in the CB. Members of small RNA pathways, capable of silencing and degrading RNAs, can be involved in the degradation of incorrectly spliced RNAs. For instance, the piRNA pathway is present in the CB, which provides the CB with the ability to directly control the repression and degradation of several target RNAs.

The composition of the CB is known to vary through time, to follow the turnover of its components, and the expression of some of them at different time points during spermatid maturation. Particularly during the transition from round to elongating spermatids, the CB composition is dramatically remodelled upon disappearance of all the characteristic CB proteins, including MVH, MIWI and DDX25. Other proteins, such as TSSK1, TSSK2 and TSKS, mark the CB only in elongating spermatids, when DDX25 and MIWI are absent. Our results show that FYCO1 is present in the CB during its whole existence: from the appearance of haploid round spermatids immediately after meiosis, until the CB breaks down in late elongating spermatids. Indeed, FYCO1 marks the remnants of the CB along with TSKS. So that it can be conjectured that FYCO1 may indeed be involved in the transport of these components to the CB. If this were to prove to be the case, it would explain the morphological changes in the CB in FYCO1-cKO spermatids.

The protocol developed in this study can be adjusted to the use of different antigens other than MVH to isolate the CB. Isolation of the CB through the use of target proteins that are expressed at different time points, such as MIWI and TSKS, can enable the characterisation of the CB at the different stages of spermatid

differentiation. Then, comparison of these results would provide information to how the composition of the CB changes during spermiogenesis and also would elucidate the role of the CB at these different stages. Changes in the composition of the CB, which can be observed through the marking of different proteins, are likely related to the involvement of the CB in changing processes, such as in the degradation of meiotic transcripts in early round spermatids, the storage of transcripts required for spermatid elongation in late round spermatids, and the organization of the mitochondrial sheath in late elongating spermatids.

6.2 New factors in CB-vesicles interplay

6.2.1CB components and the acrosome

The Retromer is a protein complex involved in the recycling of cargo-receptors from endosomes to the Golgi complex, in somatic cells. In this study, Retromer associated proteins in the testis and, in particular, in haploid round spermatids were characterized. VPS26A and VPS35 are conjectured to be involved in new and specific processes in differentiating germ cells. VPS proteins closely interact with the CB, as proved through CB isolation and laser scanning confocal microscopy (II). By EM, it became clear that small vesicles, which resemble phagophores, surround the CB, and MVBs are often found close by (II). Immuno-EM analysis is now required to further unravel which of these membranous organelles is VPS positive. Nevertheless, it is likely that material is acquired from the CB by either macro- or micro-autophagy into the Retromer-positive vesicles. Interaction of these vesicles with SNX proteins, possibly even germ cell specific ones, may direct them to the acrosome.

It could even be speculated that the CB provides material to the acrosome, which arises from observations in that the CB is often to be seen to establish contact with the Golgi complex and the acrosome in living cells, when observed by phase contrast microscopy[386]. As such, the Golgi complex is considered the main source of acrosomal material. However, the mechanism by which the CB is involved in the exchange and transport between the Golgi and the acrosome remains unknown, and limited data is currently available upon which to construct any hypothesis or speculation.

In this study on Retromer-positive vesicles in round spermatids, it was noticed that the cargo of several of these vesicles is marked by PNA. PNA is a lectin that marks acrosome material and has been used as an acrosome marker in several studies[156,378,387–390]. Currently, two models explain the formation of acrosomal material, *viz*: the standard model, which considers the Golgi complex as the only source of the content of the acrosome, by which material produced in the Golgi is transported by vesicles to the acrosome. These vesicles, which form the so-termed acrosomal granules, fuse together to form the acrosomal vesicle. The other model builds on the first the conjecture that some of the acrosomal content may derive from outside the haploid cell. In this case, phagocytosis acquires the material and the endocytic pathway becomes responsible to deliver it to the acrosome. In the latter case, at least some acrosomal granules would derive from endosomes.

To clarify the possible functions of the Golgi complex and the endocytic pathway with the Retromer in acrosome formation, seminiferous tubules were treated with drugs to disrupt the Golgi complex or the late lysosomal pathway. The standard role of the Retromer is to recycle proteins from endosomes back to the Golgi complex. By disruption of the Golgi complex with Brefeldin A1, either accumulation of the Retromer-positive vesicles due to the disappearance of their target organelle, or their absence, would be anticipated. However, contrary to such, no noticeable difference in the VPS35-positive vesicles was detected. Instead, they remained present and their cargo marked positively with PNA. Conversely, on disruption of the late lysosomal pathway by the use of U18666A, major effects on the system were noticed. U18666A disrupts the cholesterol flow between membranous compartments of the lysosomal pathway and blocks, as a cytological effect, the maturation and fusion of endosomes/MVBs with lysosomes. In the round spermatids treated with U18666A, the VPS35-positive vesicles became no longer visible. However, MVBs marked by the membrane protein MARCH11 remained present, along with small cytoplasmic granules positive for PNA. These observations led to the conclusion that a functional lysosomal pathway is required for the formation of such vesicles. Another response to U18666A was the disappearance of EEA1-positive vesicles. EEA1 marks early endosomes and the effects of U18666A on these have not, to our knowledge, been previously reported. This thus raises the question if it is the impairment of early endosomes - and not the maturation of lysosomes - that causes disappearance of the VPS35-positive vesicles.

It is important to keep in mind that U18666A does not represent a direct and specific disruptor of one isolated pathway, for it is also possible that the effect on early endosomes and the Retromer is indirect, and so does not implicate such a direct connection between endosomes and acrosome formation. As such, the Retromer complex may also be involved in the recycling of cargo receptors from the acrosome to the Golgi complex. Indeed, the acrosome can be considered as a highly specialised lysosome. With all this in consideration, it can be posited that the Retromer complex in haploid spermatids has no other role than that already observed in somatic cells. Further, it may also be that VPS35 vesicles retrieve material from the acrosome, which is not required in the mature sperm[358]. Several proteins derived from the Golgi or from lysosomes are indeed present in the acrosome during its formation, yet not in the acrosome of the mature sperm[339,342,358].

The VPS26A/35 complex is involved in the cargo recognition and budding of the vesicle from MVBs, and the SNX complex is involved in targeting these vesicles to their destination. In somatic cells, the Retromer coated vesicles are directed either to the Golgi apparatus or to the plasma membrane, a process likely regulated by specific SNX complexes specific for each pathway. It can be reasoned that in the spermatid – engaged in the formation of the acrosome, a structure specific to this cell type – germ line SNX proteins, or other proteins alike, direct the Retromer coated vesicles from endosomes/MVBs to the acrosome. As such, SNX proteins would thereby need to recognize the acrosome as an alternative destination, as opposite to the Golgi complex. This may account for those vesicles that also show cargo positive for acrosome material (PNA positive staining). Other Retromer-

coated vesicles that do not stain for acrosome material may be involved in "standard" Retromer-guided recycling of cargo receptors to the Golgi.

The formation of the acrosome is a lengthy process, which unfortunately cannot be followed *ex vivo* in this study's settings, as germ cells cannot survive viably for more that 1-2 days, particularly under deleterious treatments. As such, investigation of the effect of U18666A on the maturation of the acrosome could not be achieved. The results collected to date suggest different explanative scenarios. For example, the impairment of the lysosomal pathway may disrupt Retromer activity, to merely block the whole process of the recycling of cargo receptors, even in advance of the Retromer assembly onto the endosomal/lysosomal membrane. Conversely, persistency of VPS35-positive vesicles after disruption of the Golgi along with the presence of acrosomal cargo in them, strongly indicate germ cell-specific functions. In support of this hypothesis – that part of the acrosome content originates from outside the round spermatid – the disappearance of EEA1 and VPS35 associated vesicles may actually be closely correlated. EEA1 marks the early endosomes immediately after their internalization from the plasma membrane. The Retromer then marshals these vesicles and drives them toward the acrosome. It would so follow that disruption of endosome formation by U18666A, would cause the absence of subsequent VPS35 positive vesicles directed to the acrosome.

6.2.2 Retromer proteins in mouse models with disrupted CBs

The verification as to whether the CB is affecting the presence of VPS35-positive vesicles in haploid germ cells was required; as such, the presence of VPS35-positive vesicles in different mouse models with an impaired CB was investigated.

TDRD proteins are known to function as a scaffold for the formation and integrity of the CB. TDRD6, TDRD7 and MIWI knockout mice have no CB and spermiogenesis halts at early stages. In the present study, the acrosome was shown to begin to form normally in TDRD6 and TDRD7 knockout mouse models and the VPS35 and PNA positive granules were unaffected. Conversely, the MIWI-KO testis showed an impaired acrosome: acrosomal granules would not fuse together but concentrate close to the nuclear membrane. MIWI is involved in the piRNA pathway and its disruption likely has a significant effect on the regulation of both transcription and translation inside the affected cells. As such, the problems that arise in acrosome formation can be considered indirect events. Nonetheless, it is interesting to note that VPS35 positive vesicles are also absent in specific stages of the seminiferous epithelium cycle in the MIWI-KO testis.

The detection of VPS proteins by MS of the isolated CB supports the likelihood of some direct interaction between the MVB's membrane and the CB. This interaction may then give rise to two different processes, *viz*:

1. the regulation of small RNA pathways present in the CB by MVB's membrane associated proteins, as has been similarly shown in somatic cells by Gibbings *et al.*[142,171,172,360,391];
2. the autophagocytosis of CB components for their degradation or sorting to different compartments inside the cells, such as the acrosome.

Further studies shall be required to comprehend the likely functional connection between the CB-mediated processes, inclusive of the piRNA-targeted RNA regulation and the Retromer vesicles.

6.2.3 The CB and lysosomes

VPS35 positive vesicles alone cannot account for all the CB-surrounding cytoplasmic vesicles as observed by EM, but rather are likely to represent only a small group of them. Indeed, as detected by IF staining, VPS-positive structures close to the CB (II, Fig.3B) resemble in size the MVBs observed in EM pictures. These structures seen in the IF samples may therefore represent MVBs, and not a sub-group of small vesicles.

By use of LAMP1 as a marker for lysosomes, these organelles appear dispersed in the cytoplasm but also show their presence around the CB. Haraguchi *et al.* showed the presence of LAMP1 positive particles surrounding the CB by immuno-electron microscopy, precisely at the place where the small cytoplasmic vesicles were expected to localize; however, the quality of the images did not enable to distinguish whether the signal marked single vesicles[363]. When observed by electron tomography, some of the CB-surrounding vesicles did show membrane protrusions similar to phagophores. As such, it is proposed here that these vesicles are indeed involved in autophagocytosis of material from the CB. In support to these static observations, the causation of autophagocytosis by treatment of round spermatids with Rapamycin resulted in the increase of LAMP1 positive signal upon the CB. Moreover, the block of the late stages of autophagy, specifically the fusion of autophagosomes and endosomes/MVBs with lysosomes with Bafilomycin A1, resulted in the accumulation of the LAMP1 signal in one large area immediately adjacent to the CB, which is plausible on the assumption that the small autophagic vesicles, following the inclusion of material from the CB, were then prevented from fusing with lysosomes and thereby from proceeding to the next stage of the lysosomal pathway.

6.2.4 FYCO1-cKO: CB broken but functional?

The germ cell specific FYCO1-cKO was perfectly fertile and the progeny normal. Histologically no difference between the control and the cKO testes was observed. Unexpectedly, investigation of the morphology of the CB by indirect immuno-fluorescence revealed that the CB structure was severely affected. The CB appeared to be broken into several granules per cell, rather than be in a single unique body. CB core components co-localized in these granules, which demonstrated that they must thereby be the CB.

The FYCO1-cKO is likely the first example of an affected CB that rendered no detrimental effects on male fertility. In another mouse model, the TDRD7-KO, a broken apart CB was described, but whose mouse in this case proved infertile due to failure in the later stages of spermatogenesis.

In contrast to other proteins for which the KO mouse models resulted in depletion of the CB and male infertility, FYCO1 is likely not a core component of the CB. It localises to the periphery of the CB, and the data here presented (III) indicate that it is involved in the connection of the CB with the lysosome system. However, how FYCO1 is involved in the control of the assembly of the CB remains unclear. The collapse of the CB structure into smaller granules may arise from the impairment of autophagy and lysosome degradation of CB components or, conversely, alternative degradation processes, such as the proteasome pathway, may compensate for the possible absence of autophagy degradation of CB components. Such a compensation pathway may be sufficient to ensure the correct process of spermiogenesis for the formation of functional sperm, to leave a broken CB as the only visible phenotype in physiological conditions.

In-depth analysis on the composition of CB granules in the FYCO1-cKO round spermatids is expected to elucidate how the absence of FYCO1 may affect CB morphology. It is feasible that some proteins are retained in the CB for longer than in the wild type and thus be that their levels may be higher, due to an impairment of their degradation process. Since spermatogenesis proceeds as normal, no significant changes are expected to occur. However, due to the impairment of the CB-lysosomal membrane interaction in the FYCO1-cKO, it can be speculated that other pathways than protein degradation may also be affected, for example miRNA- and/or piRNA-dependent gene regulation: even though the mice were fertile and sperm appeared normal, there may still be profound effects, for example at the epigenetic level, since small RNAs are known to be involved in the regulation of gene methylation. Although these transgenerational changes may be mild in the manner that they affect neither fertility nor the development of the next generation. To discover the molecular differences, at both the protein and RNA level, between the CB of wild type and FYCO1-cKO animals will most likely unravel the mystery of the broken, yet apparently still functional, Chromatoid body.

6.2.5CB dynamics

The CB does not function in isolation in the cytoplasm. Rather it moves actively inside the cytoplasm of haploid round spermatids and these movements depend upon the microtubule cytoskeleton[392]. These movements bring the CB into contact with different organelles, such as the Golgi apparatus and the acrosome[386].

Spermatids originate from the meiotic division of spermatocytes: the cellular division at the end of meiosis does not complete and the four daughter cells remain attached to one another by cytoplasmic bridges[384,393]. These cytoplasmic bridges enable the direct connection of the cytoplasm between the four spermatids and the exchange of material. Each cell is genetically haploid but, since material can be exchanged through the cytoplasmic bridges, they behave as

diploid[384,393]. The CB has been shown to migrate to the cytoplasmic bridges and exchange material with the neighbouring cell[384,392]. Arising from this property, the CB is conjectured to be involved in the sorting of mRNAs, and possibly other signalling molecules, too, between sister spermatids[384]. As such, it would be of interest to further investigate this characteristic of the CB as a regulator of inter-cytoplasmic exchange processes between connected spermatids. Now that the components of the CB are known, it is likely possible to identify those putative players in this field. FYCO1, as a mediator of microtubule dependent transport itself, could be involved in the movement of the CB. The FYCO1-cKO described in this study (III) shows a fragmented CB, but in which spermatogenesis proceeds normally. Study of the movement, if any, of these fragments in living spermatids may elucidate the involvement of FYCO1 in CB movement.

FYCO1 is involved in the movement of cytoplasmic vesicles in the somatic cells. Despite that, its precise role in haploid spermatids still remains unclear; it is not speculative to conjecture that it may well be involved in the movement of the CB or in the shuttling of CB components around the cytoplasm and to aid their inter-cytoplasmic exchange.

6.3 The meaning of the CB-vesicle interaction

The question arises as to what is the cellular function of CB-vesicle interaction. At least two hypotheses have been advanced to explain this (**Figure 14**). The components of the CB change over time: old molecules need to be replaced by new ones as a physiological turnover to maintain their activities efficiently; during the differentiation of round spermatids into mature sperm, the composition of the CB changes to abide by the different processes that follow one another for the formation of the *spermatozoon*. In this case, specific PTMs may be involved to target proteins for autophagy and degradation by lysosomes. Bulk degradation of proteins may also occur. This autophagy-degradation hypothesis would account for the incremental lysosome localization upon the CB after induction of autophagy by Rapamycin, as well as for the clustering of lysosomes close to the CB arising from blockage of the lysosomal pathway with Bafilomycin A1. In support of this hypothesis, in both CB and FYCO1 interaction studies, several kinases and E3 ubiquitin ligases were identified. These enzymes may be involved in the generation of PTMs that direct proteins to degradation.

However, another, more intriguing hypothesis is on a functional interaction with small RNA pathways localised in the CB. It has been recently shown that the correct function of the miRNA and siRNA pathways is dependent on the correct interaction with the endosome/MVBs membrane: GW182/TNRC6 must be internalized into MVBs in order for Ago to be reloaded with a new guiding miRNA strand and unloaded Ago-GW182 complexes must be degraded, so as to not interfere with the active RISC complexes. The vicinity of lysosomes and small cytoplasmic vesicles may provide the required membrane-associated proteins and sequestration processes for the correct function of different pathways concentrated in the CB (**Figure 14**).

Meikar *et al.* have shown that RNAs concentrate in the CB before their dispersal in the cytoplasm[165]. This evidence, along with the presence of proteins that are part of different RNA-control pathways in the CB, indicate that the CB may function as a quality control and sorting hub for RNAs. Arising from these observations, along with the interaction of the CB with the Golgi and the acrosome, the likelihood that the CB provides material – whether in the form of RNA and/or proteins – to these organelles cannot be eliminate as yet.

Recently, different classes of RNA has been identified in the sperm and connected with paternal inheritance and imprinting in the embryo[394,395]. However, the localization and specific means of transport of these RNAs were not investigated. Because of the central role the CB plays during spermiogenesis as an RNA processing granule, it can be speculated that it undertakes a pivotal role in the definition of these sperm-transported RNAs. Some of these RNAs were indeed identified as miRNA, piRNAs and mRNAs, those same classes as enriched in the CB[165,184].

Retrotransposons have been shown to be degraded by autophagocytosis[172]. The presence of lysosomes near the CB, along with their increased activity upon the CB when autophagocytosis in stimulated by Rapamycin, indicates a close relationship between the CB and the lysosome pathway. As such, the lysosome pathway may likely be involved in the degradation of the retrotransposon RNA present in the CB, to cooperate in the control of gene stability.

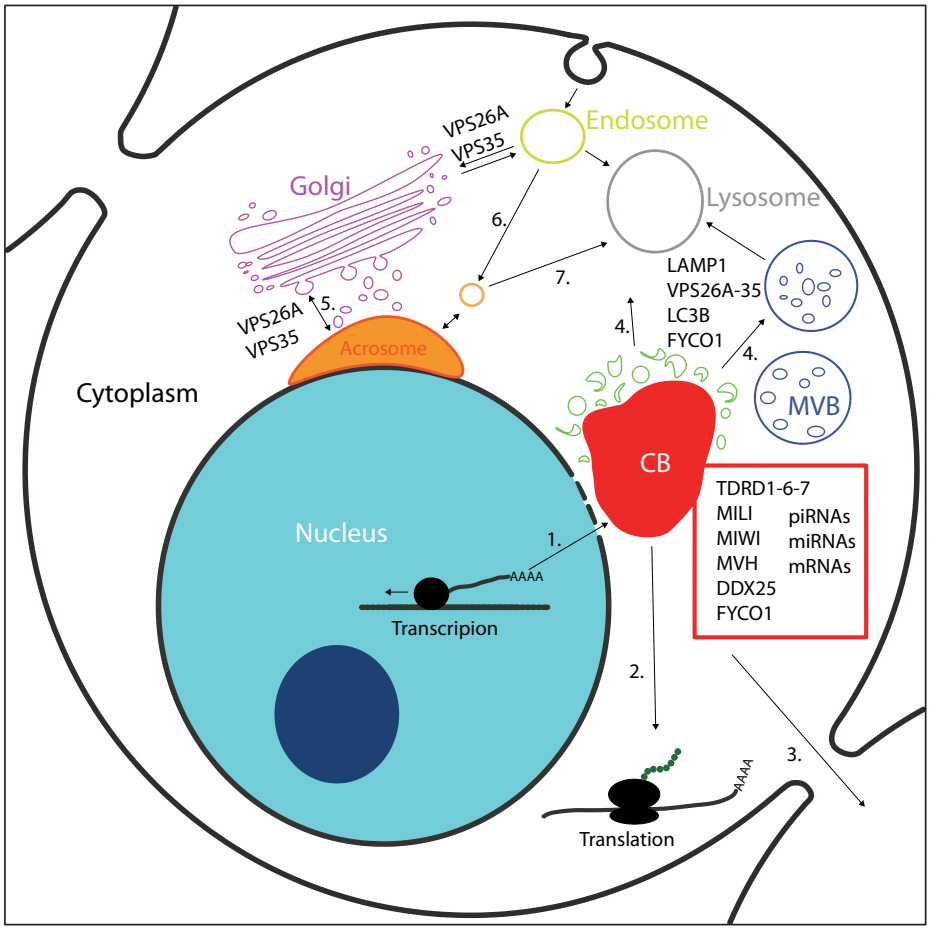

Figure 14 Summary of the CB and its interactions with the endomembrane system in haploid round spermatids. The CB is found mainly near the nuclear envelope in the cytoplasm of haploid round spermatids. There is a concentration of nuclear pores in the area near the CB as it obtains material from inside the nucleus (1). The CB is mainly formed by RNAs (such as piRNAs, miRNAs and mRNAs) and RNA-binding proteins (for instance MILI, MIWI, MVH and DDX25); due to its composition, it has also been associated with the regulation of translation (2). The CB can move around in a microtubule dependent manner and makes contacts with the Golgi apparatus and the nuclear envelope. It can also travel to inter-cytoplasmic bridges and exchange material with sister spermatids (3). A cloud of small cytoplasmic vesicles surrounds the CB; their morphology and the presence of LC3B and LAMP1 positive structures revealed by IF, support the hypothesis of to be autophagic vesicles. The interaction of these vesicles with the CB is dependent upon the function of FYCO1. At the same time, MVBs are often positioned close to the CB. This intricate vesicular system, which surrounds the CB, is speculated to be involved in the degradation of CB material and further likely in the function of small RNA pathways present in the CB (4). VPS26A and VPS35 are components of the Retromer complex, involved in the recycling of cargo receptors from endosomes to the Golgi, or to the plasma membrane. VPS26A and VPS35 have been found to interact with the CB and mark vesicles that surround it (4). Data presented in this study also indicate the involvement of Retromer proteins in the transport of acrosomal material. This transport may be involved in the recycling of molecules from the developing acrosome to the Golgi (5). Retromer positive vesicles may also be involved in a secondary pathway to provide material to the acrosome and involve the endosome as a source of acrosomal granules. To date, it remains unclear if this transport is directed from endosomes to the acrosome (6), or if it is involved in degradation of some acrosome material by the lysosome (7).

7 Summary and conclusions

The molecular biology of cellular ribonucleoprotein granules and cytoplasmic organelles has been independently studied for decades. The onset of systems biology was signified by the awareness that the different processes that occur inside the cell are not isolated from one another, but rather represent a cooperative continuum. Scientists began to investigate the relationship and interactions between different signalling and metabolic pathways to reveal their connections. For example, it was only recently discovered that RNA regulation by small RNAs occurs in discrete RNP granules that, for their function, require to interact with vesicle membranes, such as autophagosomes. In the investigations undertaken for this thesis, these principles have been applied to the male germ line.

It would not be an overstatement to advance that the development of a robust and reliable protocol for the isolation of the most prominent RNP granule in male germ cells, the Chromatoid body, represents a significant step in the studies of RNP biology and, by association, male fertility. This protocol allowed the accurate description of the proteins and RNAs that compose the CB, and therefore it set the direction for future studies that will unravel the different roles of this RNP granule in the development of functional sperm. Further, it is likely that this protocol will be applied to isolate other RNP granules, for example stress granules and inclusion bodies, both of which are involved in the development of various neurodegenerative diseases.

Moreover, this study extended the boundaries beyond the CB to also its surroundings. Through the characterization of CB proteins involved in different vesicular transport systems, the Retromer in haploid round spermatids was duly identified. Further, this study represents the first description of the involvement of components of the Retromer complex in the formation of the acrosome, this being a special structure found only in the sperm cell. On this, the data compiled hereby support the likelihood that the CB is involved in the development of the acrosome: future studies shall clarify whether the CB does provide or acquire material from it. Further, indirect evidence that some of the acrosomal material may be derived from the endocytic pathway, and thereby not exclusively from the Golgi complex, was also presented. The identification and description of two proteins, VPS26A and VPS35, involved in this pathway will allow the further detailed and specific investigation of the extracellular origin of acrosomal material.

To close, it has long been conjectured that the CB interacts with the cytoplasmic vesicles. This study proved that the lysosomal system does indeed interact directly with the CB and that one of the CB's main components, FYCO1, is essential for this interaction. The FYCO1-cKO mouse model hereby produced now provides a useful tool for the study of the various transcription regulation pathways that are present in the CB, along with their interaction with the autophagosome/lysosome system.

8 Acknowledgements

This current study was carried out at the Department of Physiology, Institute of Biomedicine, University of Turku, during the years 2009-2015.

My deepest gratitude goes to my supervisors, Assistant Professor Noora Kotaja, PhD, and Professor Jorma Toppari, MD, PhD. Thank you Jorma for always providing useful critical comments on my research projects and experiments: you really contributed to making my final work better; your near to infinite and yet extremely precise knowledge is inspirational. All the work presented in this thesis would not have been possible without the guidance and support of Noora: I cannot describe what a great supervisor you are! I am proud and privileged to have been your student. You allowed me the freedom to explore different paths in my scientific quest and were always there to bring me back on track whenever I was lost. I will always enjoy the love we both share for molecular biology.

A special thank goes to Professor Emeritus Martti Parvinen, MD, PhD, for his support and encouragement from the beginning to the close of my PhD. I cannot but be impressed by your excitement about the still mysterious Chromatoid body.

A sincere thank you also goes to Professor Emeritus Lauri Pelliniemi, MD, PhD, who introduced me to professional microscopy in the early days of my PhD. Ever since, microscopy has been my greatest passion.

I am very grateful to the reviewers of this thesis, Dr. Timo Tuuri, PhD, and Dr. Varpu Marjomäki, PhD, for their careful and critical review. You greatly contributed to the improvement of this thesis and helped me to keep time with those tight schedules.

I would also like to thank Professor Klaus Elenius, PhD, and Dr. Cecilia Sahlgren, PhD, for being the members of my thesis committee: you helped me with thorough comments and contributed to improving the quality of my scientific work.

All my co-authors are kindly acknowledged for their contribution to this work.

During these years, I have had the privilege to be a member of the Turku Doctoral Programme of Biomedical Sciences (TuBS), and lately of the Turku Doctoral Programme of Molecular Medicine (TuDMM). As such, my most joyful thanks are for Professor Olli Lassila, MD, PhD, and Nina Widberg as Director and Secretary of TuBS, respectively. I am deeply grateful to TuBS for so kindly sponsoring my numerous trips to conferences and courses abroad and in Finland. A nostalgic thought goes also to all the other TuBS and TuDMM students with whom I had such an enjoyable time during our social events and meetings.

A privileged thank goes to Henriette Undeutsch, MSc, Milena Doroszko, MSc, and Tiina Lehtiniemi, MSc, for so much support and “motivation” to, among many other things, make me actually set down this thesis! They know what I mean…

Further, Adolfo Rivero-Müller, PhD, deserves my deepest gratitude for all his spontaneous help and guidance given in everyday laboratory work and in experiment design and planning. You have been my mentor in all these years, sharing both everyday frustrations as well as triumphs. I will miss the endless discussions we had about Science and Reason over good food and even better drinks.

I cannot find words to describe the bond with my dearest friends and colleagues Oliver Meikar, PhD, and Juho-Antti Mäkelä, PhD. except to express that you both have been and are like older brothers to me.

My immense gratitude goes to the other present and past members of the Kotaja's group for all the help and collaboration provided. My sincere thanks to all the members of the Department of Physiology for bearing with me all through these years and providing all the equipment, support, help and expertise that enabled me to reach the finish line. A special consideration must go to Tuula Hämäläinen, PhD, since I am aware I may not have always behaved exemplarily, my apologies for that.

I could not have survived the long winters in Finland without the warm company of my capoeira group: thank you Erika Halonen, Peter Sundell, Rosa Rantanen, Tuomas Kaukoranta, Laura Kauppi and the other capoeira friends for bearing with me not speaking Finnish all this time.

I am most grateful to my parents, Remo and Elena, for always being supportive and motivating, for providing me a worry-free childhood and for letting me choose my path in life. You taught me to always aim for excellence and made me the person I am today. A big hug goes also to my little brother Marco: I wish you the same happiness in life. A big thank goes also to my grandparents, who nurtured and educated me during my childhood, I hope this would make them proud. My close relatives, too, deserve my gratitude for being an extension of my family.

And last but most certainly never the least, my beloved wife, Megha, I cannot express the gratitude for making every day, since we first met, a special one. You supported me during the hardship of my work, giving up so much for me and offering a warm embrace whenever felt down. You are always present when I need you and you never spare any energy to make me happy.

Advancement in Science is made by the single small contribution of every unimportant person working in the lab, from the undergraduate student learning how to design an experiment, to the major professor striving for grants and putting everything together for the improvement of our society. Thank you to everyone for your dedication and your love for Science.

This study was financially supported by the Academy of Finland, Sigrid Jusélius Foundation, Emil Aaltonen Foundation, the Finnish Cultural Foundation, Centre for Reproductive and Developmental Medicine, Novo Nordisk Foundation, Turku University Foundation, Turku Doctoral Programme of Biomedical Sciences (TuBS) and Turku Doctoral Programme of Molecular Medicine (TuDMM).

Matteo Da Ros, Turku, November 2015

9 References

1. Russell, L. D., Ettlin, R. A., Hikim, A. P. S. & Clegg, E. D. Histological and Histopathological Evaluation of the Testis. *Int. J. Androl.* **16,** 83–83 (1993).
2. Clermont, Y. Kinetics of spermatogenesis in mammals: seminiferous epithelium cycle and spermatogonial renewal. *Physiol. Rev.* **52,** 198–236 (1972).
3. Heller, C. G. & Clermont, Y. Spermatogenesis in man: an estimate of its duration. *Science* **140,** 184–6 (1963).
4. Orth, J. M., Gunsalus, G. L. & Lamperti, A. A. Evidence from Sertoli cell-depleted rats indicates that spermatid number in adults depends on numbers of Sertoli cells produced during perinatal development. *Endocrinology* **122,** 787–94 (1988).
5. Oatley, M. J., Racicot, K. E. & Oatley, J. M. Sertoli cells dictate spermatogonial stem cell niches in the mouse testis. *Biol. Reprod.* **84,** 639–45 (2011).
6. Mruk, D. D. & Cheng, C. Y. Sertoli-Sertoli and Sertoli-germ cell interactions and their significance in germ cell movement in the seminiferous epithelium during spermatogenesis. *Endocr. Rev.* **25,** 747–806 (2004).
7. Dym, M. & Fawcett, D. W. The blood-testis barrier in the rat and the physiological compartmentation of the seminiferous epithelium. *Biol. Reprod.* **3,** 308–26 (1970).
8. Lebond, C. P. & Clermont, Y. Definition of the stages of the cycle of the seminiferous epithelium in the rat. *Ann. N. Y. Acad. Sci.* **55,** 548–73 (1952).
9. Parvinen, M. Regulation of the seminiferous epithelium. *Endocr. Rev.* **3,** 404–17 (1982).
10. Toppari, J. & Parvinen, M. In vitro differentiation of rat seminiferous tubular segments from defined stages of the epithelial cycle morphologic and immunolocalization analysis. *J. Androl.* **6,** 334–43 (1985).
11. Kotaja, N. *et al.* Preparation, isolation and characterization of stage-specific spermatogenic cells for cellular and molecular analysis. *Nat. Methods* **1,** 249–54 (2004).
12. Alberts, B. *et al.* Molecular Biology of the Cell. (2002). at <http://www.ncbi.nlm.nih.gov/books/NBK21054/>
13. Smith, Z. D. & Meissner, A. DNA methylation: roles in mammalian development. *Nat. Rev. Genet.* **14,** 204–20 (2013).
14. Deaton, A. M. & Bird, A. CpG islands and the regulation of transcription. *Genes Dev.* **25,** 1010–22 (2011).
15. Bannister, A. J. & Kouzarides, T. Regulation of chromatin by histone modifications. *Cell Res.* **21,** 381–95 (2011).
16. Shandilya, J. & Roberts, S. G. E. The transcription cycle in eukaryotes: from productive initiation to RNA polymerase II recycling. *Biochim. Biophys. Acta* **1819,** 391–400 (2012).
17. Brennicke, A., Marchfelder, A. & Binder, S. RNA editing. *FEMS Microbiol. Rev.* **23,** 297–316 (1999).
18. Tang, W., Fei, Y. & Page, M. Biological significance of RNA editing in cells. *Mol. Biotechnol.* **52,** 91–100 (2012).
19. Hocine, S., Singer, R. H. & Grünwald, D. RNA processing and export. *Cold Spring Harb. Perspect. Biol.* **2,** a000752 (2010).
20. Martin, K. C. & Ephrussi, A. mRNA localization: gene expression in the spatial dimension. *Cell* **136,** 719–30 (2009).
21. Martin, K. C. & Zukin, R. S. RNA trafficking and local protein synthesis in dendrites: an overview. *J. Neurosci.* **26,** 7131–4 (2006).
22. Lécuyer, E. *et al.* Global analysis of mRNA localization reveals a prominent role in organizing cellular architecture and function. *Cell* **131,** 174–87 (2007).
23. Sonenberg, N. & Hinnebusch, A. G. Regulation of translation initiation in eukaryotes: mechanisms and biological targets. *Cell* **136,** 731–45 (2009).
24. Birney, E. *et al.* Identification and analysis of functional elements in 1% of the human genome by the ENCODE pilot project. *Nature* **447,** 799–816 (2007).
25. Pennisi, E. Genetics. Working the (gene count) numbers: finally, a firm answer? *Science* **316,** 1113 (2007).
26. Lander, E. S. *et al.* Initial sequencing and analysis of the human genome. *Nature* **409,** 860–921 (2001).
27. Taft, R. J., Pheasant, M. & Mattick, J. S. The relationship between non-protein-coding DNA and eukaryotic complexity. *Bioessays* **29,** 288–99 (2007).
28. Bird, A. P. Gene number, noise reduction and biological complexity. *Trends Genet.* **11,** 94–100 (1995).
29. Djebali, S. *et al.* Landscape of transcription in human cells. *Nature* **489,** 101–8 (2012).

30. Carninci, P. *et al.* The transcriptional landscape of the mammalian genome. *Science* **309,** 1559–63 (2005).

31. Mattick, J. S. & Makunin, I. V. Non-coding RNA. *Hum. Mol. Genet.* **15 Spec No,** R17–29 (2006).

32. Derrien, T. *et al.* The GENCODE v7 catalog of human long noncoding RNAs: analysis of their gene structure, evolution, and expression. *Genome Res.* **22,** 1775–89 (2012).

33. Tsai, M.-C. *et al.* Long noncoding RNA as modular scaffold of histone modification complexes. *Science* **329,** 689–93 (2010).

34. Zappulla, D. C. & Cech, T. R. RNA as a flexible scaffold for proteins: yeast telomerase and beyond. *Cold Spring Harb. Symp. Quant. Biol.* **71,** 217–24 (2006).

35. Huarte, M. *et al.* A large intergenic noncoding RNA induced by p53 mediates global gene repression in the p53 response. *Cell* **142,** 409–19 (2010).

36. Kino, T., Hurt, D. E., Ichijo, T., Nader, N. & Chrousos, G. P. Noncoding RNA gas5 is a growth arrest- and starvation-associated repressor of the glucocorticoid receptor. *Sci. Signal.* **3,** ra8 (2010).

37. Penny, G. D., Kay, G. F., Sheardown, S. A., Rastan, S. & Brockdorff, N. Requirement for Xist in X chromosome inactivation. *Nature* **379,** 131–7 (1996).

38. Krol, J., Loedige, I. & Filipowicz, W. The widespread regulation of microRNA biogenesis, function and decay. *Nat. Rev. Genet.* **11,** 597–610 (2010).

39. Ghildiyal, M. & Zamore, P. D. Small silencing RNAs: an expanding universe. *Nat. Rev. Genet.* **10,** 94–108 (2009).

40. Meikar, O., Da Ros, M., Korhonen, H. & Kotaja, N. Chromatoid body and small RNAs in male germ cells. *Reproduction* **142,** 195–209 (2011).

41. Lee, R. C., Feinbaum, R. L. & Ambros, V. The C. elegans heterochronic gene lin-4 encodes small RNAs with antisense complementarity to lin-14. *Cell* **75,** 843–54 (1993).

42. Wightman, B., Ha, I. & Ruvkun, G. Posttranscriptional regulation of the heterochronic gene lin-14 by lin-4 mediates temporal pattern formation in C. elegans. *Cell* **75,** 855–62 (1993).

43. Reinhart, B. J. *et al.* The 21-nucleotide let-7 RNA regulates developmental timing in Caenorhabditis elegans. *Nature* **403,** 901–6 (2000).

44. Lee, R. C. & Ambros, V. An extensive class of small RNAs in Caenorhabditis elegans. *Science* **294,** 862–4 (2001).

45. Lee, Y., Jeon, K., Lee, J.-T., Kim, S. & Kim, V. N. MicroRNA maturation: stepwise processing and subcellular localization. *EMBO J.* **21,** 4663–70 (2002).

46. Zeng, Y. & Cullen, B. R. Sequence requirements for micro RNA processing and function in human cells. *RNA* **9,** 112–23 (2003).

47. Lee, Y. *et al.* The nuclear RNase III Drosha initiates microRNA processing. *Nature* **425,** 415–9 (2003).

48. Lund, E., Güttinger, S., Calado, A., Dahlberg, J. E. & Kutay, U. Nuclear export of microRNA precursors. *Science* **303,** 95–8 (2004).

49. Bernstein, E., Caudy, A. A., Hammond, S. M. & Hannon, G. J. Role for a bidentate ribonuclease in the initiation step of RNA interference. *Nature* **409,** 363–6 (2001).

50. Hutvágner, G. *et al.* A cellular function for the RNA-interference enzyme Dicer in the maturation of the let-7 small temporal RNA. *Science* **293,** 834–8 (2001).

51. Ketting, R. F. *et al.* Dicer functions in RNA interference and in synthesis of small RNA involved in developmental timing in C. elegans. *Genes Dev.* **15,** 2654–9 (2001).

52. Liu, Q. *et al.* R2D2, a bridge between the initiation and effector steps of the Drosophila RNAi pathway. *Science* **301,** 1921–5 (2003).

53. Pellino, J. L. & Sontheimer, E. J. R2D2 leads the silencing trigger to mRNA's death star. *Cell* **115,** 132–3 (2003).

54. Schwarz, D. S. *et al.* Asymmetry in the assembly of the RNAi enzyme complex. *Cell* **115,** 199–208 (2003).

55. Khvorova, A., Reynolds, A. & Jayasena, S. D. Functional siRNAs and miRNAs exhibit strand bias. *Cell* **115,** 209–16 (2003).

56. Hammond, S. M. Argonaute2, a Link Between Genetic and Biochemical Analyses of RNAi. *Science (80-.).* **293,** 1146–1150 (2001).

57. Stark, A., Brennecke, J., Russell, R. B. & Cohen, S. M. Identification of Drosophila MicroRNA targets. *PLoS Biol.* **1,** E60 (2003).

58. Hutvágner, G. & Zamore, P. D. A microRNA in a multiple-turnover RNAi enzyme complex. *Science* **297,** 2056–60 (2002).

59. Doench, J. G., Petersen, C. P. & Sharp, P. A. siRNAs can function as miRNAs. *Genes Dev.* **17,** 438–42 (2003).

60. Bernstein, E. *et al.* Dicer is essential for mouse development. *Nat. Genet.* **35,** 215–7 (2003).

61. Hayashi, K. *et al.* MicroRNA biogenesis is required for mouse primordial germ cell development and spermatogenesis. *PLoS One* **3,** e1738 (2008).

62. Maatouk, D. M., Loveland, K. L., McManus, M. T., Moore, K. & Harfe, B. D. Dicer1 is required for differentiation of the mouse male germline. *Biol. Reprod.* **79,** 696–703 (2008).

63. Korhonen, H. M. *et al.* Dicer is required for haploid male germ cell differentiation in mice. *PLoS One* **6,** e24821 (2011).

64. Zimmermann, C. *et al.* Germ cell-specific targeting of DICER or DGCR8 reveals a novel role for endo-siRNAs in the progression of mammalian spermatogenesis and male fertility. *PLoS One* **9,** e107023 (2014).

65. Romero, Y. *et al.* Dicer1 depletion in male germ cells leads to infertility due to cumulative meiotic and spermiogenic defects. *PLoS One* **6,** e25241 (2011).

66. Elbashir, S. M., Lendeckel, W. & Tuschl, T. RNA interference is mediated by 21- and 22-nucleotide RNAs. *Genes Dev.* **15,** 188–200 (2001).

67. Hammond, S. M., Bernstein, E., Beach, D. & Hannon, G. J. An RNA-directed nuclease mediates post-transcriptional gene silencing in Drosophila cells. *Nature* **404,** 293–6 (2000).

68. Zamore, P. D., Tuschl, T., Sharp, P. A. & Bartel, D. P. RNAi: double-stranded RNA directs the ATP-dependent cleavage of mRNA at 21 to 23 nucleotide intervals. *Cell* **101,** 25–33 (2000).

69. Grishok, A. *et al.* Genes and mechanisms related to RNA interference regulate expression of the small temporal RNAs that control C. elegans developmental timing. *Cell* **106,** 23–34 (2001).

70. Knight, S. W. & Bass, B. L. A role for the RNase III enzyme DCR-1 in RNA interference and germ line development in Caenorhabditis elegans. *Science* **293,** 2269–71 (2001).

71. Hannon, G. J. RNA interference. *Nature* **418,** 244–51 (2002).

72. Fire, A. *et al.* Potent and specific genetic interference by double-stranded RNA in Caenorhabditis elegans. *Nature* **391,** 806–11 (1998).

73. Ding, S.-W. & Voinnet, O. Antiviral immunity directed by small RNAs. *Cell* **130,** 413–26 (2007).

74. Lecellier, C.-H. *et al.* A cellular microRNA mediates antiviral defense in human cells. *Science* **308,** 557–60 (2005).

75. Waterhouse, P. M., Wang, M. B. & Lough, T. Gene silencing as an adaptive defence against viruses. *Nature* **411,** 834–42 (2001).

76. van Rij, R. P. & Andino, R. The silent treatment: RNAi as a defense against virus infection in mammals. *Trends Biotechnol.* **24,** 186–93 (2006).

77. Hamilton, A., Voinnet, O., Chappell, L. & Baulcombe, D. Two classes of short interfering RNA in RNA silencing. *EMBO J.* **21,** 4671–9 (2002).

78. Ambros, V., Lee, R. C., Lavanway, A., Williams, P. T. & Jewell, D. MicroRNAs and other tiny endogenous RNAs in C. elegans. *Curr. Biol.* **13,** 807–18 (2003).

79. Zilberman, D., Cao, X. & Jacobsen, S. E. ARGONAUTE4 control of locus-specific siRNA accumulation and DNA and histone methylation. *Science* **299,** 716–9 (2003).

80. Yang, N. & Kazazian, H. H. L1 retrotransposition is suppressed by endogenously encoded small interfering RNAs in human cultured cells. *Nat. Struct. Mol. Biol.* **13,** 763–71 (2006).

81. Tam, O. H. *et al.* Pseudogene-derived small interfering RNAs regulate gene expression in mouse oocytes. *Nature* **453,** 534–8 (2008).

82. Watanabe, T. *et al.* Endogenous siRNAs from naturally formed dsRNAs regulate transcripts in mouse oocytes. *Nature* **453,** 539–43 (2008).

83. Song, R. *et al.* Male germ cells express abundant endogenous siRNAs. *Proc. Natl. Acad. Sci. U. S. A.* **108,** 13159–64 (2011).

84. Lin, H. & Spradling, A. C. A novel group of pumilio mutations affects the asymmetric division of germline stem cells in the Drosophila ovary. *Development* **124,** 2463–76 (1997).

85. Cox, D. N. *et al.* A novel class of evolutionarily conserved genes defined by piwi are essential for stem cell self-renewal. *Genes Dev.* **12,** 3715–27 (1998).

86. Aravin, A. *et al.* A novel class of small RNAs bind to MILI protein in mouse testes. *Nature* **442,** 203–7 (2006).

87. Girard, A., Sachidanandam, R., Hannon, G. J. & Carmell, M. A. A germline-specific class of small RNAs binds mammalian Piwi proteins. *Nature* **442,** 199–202 (2006).

88. Grivna, S. T., Beyret, E., Wang, Z. & Lin, H. A novel class of small RNAs in mouse spermatogenic cells. *Genes Dev.* **20,** 1709–14 (2006).

89. Lau, N. C. *et al.* Characterization of the piRNA complex from rat testes. *Science* **313,** 363–7 (2006).

90. Watanabe, T. *et al.* Identification and characterization of two novel classes of small RNAs in the mouse germline: retrotransposon-derived siRNAs in oocytes and germline small RNAs in testes. *Genes Dev.* **20,** 1732–43 (2006).

91. Kirino, Y. & Mourelatos, Z. Mouse Piwi-interacting RNAs are 2′-O-methylated at their

3' termini. *Nat. Struct. Mol. Biol.* **14,** 347–8 (2007).

92. Saito, K. *et al.* Pimet, the Drosophila homolog of HEN1, mediates 2'-O-methylation of Piwi-interacting RNAs at their 3' ends. *Genes Dev.* **21,** 1603–8 (2007).

93. Vagin, V. V *et al.* A distinct small RNA pathway silences selfish genetic elements in the germline. *Science* **313,** 320–4 (2006).

94. Aravin, A. A., Hannon, G. J. & Brennecke, J. The Piwi-piRNA pathway provides an adaptive defense in the transposon arms race. *Science* **318,** 761–4 (2007).

95. Das, P. P. *et al.* Piwi and piRNAs act upstream of an endogenous siRNA pathway to suppress Tc3 transposon mobility in the Caenorhabditis elegans germline. *Mol. Cell* **31,** 79–90 (2008).

96. Houwing, S. *et al.* A role for Piwi and piRNAs in germ cell maintenance and transposon silencing in Zebrafish. *Cell* **129,** 69–82 (2007).

97. Brennecke, J. *et al.* An epigenetic role for maternally inherited piRNAs in transposon silencing. *Science* **322,** 1387–92 (2008).

98. Gunawardane, L. S. *et al.* A slicer-mediated mechanism for repeat-associated siRNA 5′ end formation in Drosophila. *Science* **315,** 1587–90 (2007).

99. Malone, C. D. *et al.* Specialized piRNA pathways act in germline and somatic tissues of the Drosophila ovary. *Cell* **137,** 522–35 (2009).

100. Mohn, F., Sienski, G., Handler, D. & Brennecke, J. The rhino-deadlock-cutoff complex licenses noncanonical transcription of dual-strand piRNA clusters in Drosophila. *Cell* **157,** 1364–79 (2014).

101. Homolka, D. *et al.* PIWI Slicing and RNA Elements in Precursors Instruct Directional Primary piRNA Biogenesis. *Cell Rep.* **12,** 418–28 (2015).

102. Xiol, J. *et al.* RNA clamping by Vasa assembles a piRNA amplifier complex on transposon transcripts. *Cell* **157,** 1698–711 (2014).

103. Aravin, A. A., Sachidanandam, R., Girard, A., Fejes-Toth, K. & Hannon, G. J. Developmentally regulated piRNA clusters implicate MILI in transposon control. *Science* **316,** 744–7 (2007).

104. Pane, A., Wehr, K. & Schüpbach, T. zucchini and squash encode two putative nucleases required for rasiRNA production in the Drosophila germline. *Dev. Cell* **12,** 851–62 (2007).

105. Czech, B., Preall, J. B., McGinn, J. & Hannon, G. J. A transcriptome-wide RNAi screen in the Drosophila ovary reveals factors of the germline piRNA pathway. *Mol. Cell* **50,** 749–61 (2013).

106. Handler, D. *et al.* The genetic makeup of the Drosophila piRNA pathway. *Mol. Cell* **50,** 762–77 (2013).

107. Huang, H. *et al.* piRNA-associated germline nuage formation and spermatogenesis require MitoPLD profusogenic mitochondrial-surface lipid signaling. *Dev. Cell* **20,** 376–87 (2011).

108. Watanabe, T. *et al.* MITOPLD is a mitochondrial protein essential for nuage formation and piRNA biogenesis in the mouse germline. *Dev. Cell* **20,** 364–75 (2011).

109. Shiromoto, Y. *et al.* GPAT2, a mitochondrial outer membrane protein, in piRNA biogenesis in germline stem cells. *RNA* **19,** 803–10 (2013).

110. Saxe, J. P., Chen, M., Zhao, H. & Lin, H. Tdrkh is essential for spermatogenesis and participates in primary piRNA biogenesis in the germline. *EMBO J.* **32,** 1869–85 (2013).

111. Ma, L. *et al.* GASZ is essential for male meiosis and suppression of retrotransposon expression in the male germline. *PLoS Genet.* **5,** e1000635 (2009).

112. Zheng, K. *et al.* Mouse MOV10L1 associates with Piwi proteins and is an essential component of the Piwi-interacting RNA (piRNA) pathway. *Proc. Natl. Acad. Sci. U. S. A.* **107,** 11841–6 (2010).

113. Kota, S. K. & Feil, R. Epigenetic transitions in germ cell development and meiosis. *Dev. Cell* **19,** 675–86 (2010).

114. Ewen, K. A. & Koopman, P. Mouse germ cell development: from specification to sex determination. *Mol. Cell. Endocrinol.* **323,** 76–93 (2010).

115. Carmell, M. A. *et al.* MIWI2 is essential for spermatogenesis and repression of transposons in the mouse male germline. *Dev. Cell* **12,** 503–14 (2007).

116. Deng, W. & Lin, H. miwi, a Murine Homolog of piwi, Encodes a Cytoplasmic Protein Essential for Spermatogenesis. *Dev. Cell* **2,** 819–30 (2002).

117. Kuramochi-Miyagawa, S. *et al.* Mili, a mammalian member of piwi family gene, is essential for spermatogenesis. *Development* **131,** 839–49 (2004).

118. Aravin, A. A. A. *et al.* A piRNA pathway primed by individual transposons is linked to de novo DNA methylation in mice. *Mol. Cell* **31,** 785–99 (2008).

119. Li, X. Z. *et al.* An ancient transcription factor initiates the burst of piRNA production during early meiosis in mouse testes. *Mol. Cell* **50,** 67–81 (2013).

120. Dönertas, D., Sienski, G. & Brennecke, J. Drosophila Gtsf1 is an essential component of

the Piwi-mediated transcriptional silencing complex. *Genes Dev.* **27,** 1693–705 (2013).

121. Muerdter, F. *et al.* A genome-wide RNAi screen draws a genetic framework for transposon control and primary piRNA biogenesis in Drosophila. *Mol. Cell* **50,** 736–48 (2013).

122. Klenov, M. S. *et al.* Separation of stem cell maintenance and transposon silencing functions of Piwi protein. *Proc. Natl. Acad. Sci. U. S. A.* **108,** 18760–5 (2011).

123. Saito, K. *et al.* Roles for the Yb body components Armitage and Yb in primary piRNA biogenesis in Drosophila. *Genes Dev.* **24,** 2493–8 (2010).

124. Kuramochi-Miyagawa, S. *et al.* DNA methylation of retrotransposon genes is regulated by Piwi family members MILI and MIWI2 in murine fetal testes. *Genes Dev.* **22,** 908–17 (2008).

125. Gou, L.-T. *et al.* Pachytene piRNAs instruct massive mRNA elimination during late spermiogenesis. *Cell Res.* **24,** 680–700 (2014).

126. Rouget, C. *et al.* Maternal mRNA deadenylation and decay by the piRNA pathway in the early Drosophila embryo. *Nature* **467,** 1128–32 (2010).

127. Goh, W. S. S. *et al.* piRNA-directed cleavage of meiotic transcripts regulates spermatogenesis. *Genes Dev.* **29,** 1032–1044 (2015).

128. Watanabe, T., Cheng, E., Zhong, M. & Lin, H. Retrotransposons and pseudogenes regulate mRNAs and lncRNAs via the piRNA pathway in the germline. *Genome Res.* **25,** 368–380 (2015).

129. Ashe, A. *et al.* piRNAs can trigger a multigenerational epigenetic memory in the germline of C. elegans. *Cell* **150,** 88–99 (2012).

130. Buckley, B. A. *et al.* A nuclear Argonaute promotes multigenerational epigenetic inheritance and germline immortality. *Nature* **489,** 447–51 (2012).

131. Luteijn, M. J. *et al.* Extremely stable Piwi-induced gene silencing in Caenorhabditis elegans. *EMBO J.* **31,** 3422–30 (2012).

132. Shirayama, M. *et al.* piRNAs initiate an epigenetic memory of nonself RNA in the C. elegans germline. *Cell* **150,** 65–77 (2012).

133. Erickson, S. L. & Lykke-Andersen, J. Cytoplasmic mRNP granules at a glance. *J. Cell Sci.* **124,** 293–7 (2011).

134. Anderson, P. & Kedersha, N. RNA granules: post-transcriptional and epigenetic modulators of gene expression. *Nat. Rev. Mol. Cell Biol.* **10,** 430–6 (2009).

135. Parker, R. & Sheth, U. P bodies and the control of mRNA translation and degradation. *Mol. Cell* **25,** 635–46 (2007).

136. Kulkarni, M., Ozgur, S. & Stoecklin, G. On track with P-bodies. *Biochem. Soc. Trans.* **38,** 242 (2010).

137. Zeitelhofer, M. *et al.* Dynamic interaction between P-bodies and transport ribonucleoprotein particles in dendrites of mature hippocampal neurons. *J. Neurosci.* **28,** 7555–7562 (2008).

138. Decker, C. J. & Parker, R. P-bodies and stress granules: possible roles in the control of translation and mRNA degradation. *Cold Spring Harb. Perspect. Biol.* **4,** a012286 (2012).

139. Moser, J. J. & Fritzler, M. J. Cytoplasmic ribonucleoprotein (RNP) bodies and their relationship to GW/P bodies. *Int. J. Biochem. Cell Biol.* **42,** 828–843 (2010).

140. Fabian, M. R. *et al.* Mammalian miRNA RISC recruits CAF1 and PABP to affect PABP-dependent deadenylation. *Mol. Cell* **35,** 868–80 (2009).

141. Lee, Y. S. *et al.* Silencing by small RNAs is linked to endosomal trafficking. *Nat. Cell Biol.* **11,** 1150–6 (2009).

142. Gibbings, D. J., Ciaudo, C., Erhardt, M. & Voinnet, O. Multivesicular bodies associate with components of miRNA effector complexes and modulate miRNA activity. *Nat. Cell Biol.* **11,** 1143–9 (2009).

143. Anderson, P. & Kedersha, N. Stress granules: the Tao of RNA triage. *Trends Biochem. Sci.* **33,** 141–50 (2008).

144. Voronina, E., Seydoux, G., Sassone-Corsi, P. & Nagamori, I. RNA granules in germ cells. *Cold Spring Harb. Perspect. Biol.* **3,** (2011).

145. Brengues, M., Teixeira, D. & Parker, R. Movement of eukaryotic mRNAs between polysomes and cytoplasmic processing bodies. *Science* **310,** 486–9 (2005).

146. Bhattacharyya, S. N., Habermacher, R., Martine, U., Closs, E. I. & Filipowicz, W. Stress-induced reversal of microRNA repression and mRNA P-body localization in human cells. *Cold Spring Harb. Symp. Quant. Biol.* **71,** 513–21 (2006).

147. Nagamori, I., Cruickshank, V. A. & Sassone-Corsi, P. Regulation of an RNA granule during spermatogenesis: acetylation of MVH in the chromatoid body of germ cells. *J. Cell Sci.* **124,** 4346–55 (2011).

148. Hüttelmaier, S. *et al.* Spatial regulation of beta-actin translation by Src-dependent phosphorylation of ZBP1. *Nature* **438,** 512–5 (2005).

149. Buchan, J. R. & Parker, R. Eukaryotic stress granules: the ins and outs of translation. *Mol. Cell* **36,** 932–41 (2009).

150. Kedersha, N. *et al.* Stress granules and processing bodies are dynamically linked sites of mRNP remodeling. *J. Cell Biol.* **169,** 871–84 (2005).

151. Buchan, J. R., Muhlrad, D. & Parker, R. P bodies promote stress granule assembly in Saccharomyces cerevisiae. *J. Cell Biol.* **183,** 441–55 (2008).

152. Mollet, S. *et al.* Translationally repressed mRNA transiently cycles through stress granules during stress. *Mol. Biol. Cell* **19,** 4469–79 (2008).

153. Gilks, N. *et al.* Stress granule assembly is mediated by prion-like aggregation of TIA-1. *Mol. Biol. Cell* **15,** 5383–98 (2004).

154. Liu-Yesucevitz, L. *et al.* Tar DNA binding protein-43 (TDP-43) associates with stress granules: analysis of cultured cells and pathological brain tissue. *PLoS One* **5,** e13250 (2010).

155. Bosco, D. A. *et al.* Mutant FUS proteins that cause amyotrophic lateral sclerosis incorporate into stress granules. *Hum. Mol. Genet.* **19,** 4160–75 (2010).

156. Tanaka, T. *et al.* Tudor domain containing 7 (Tdrd7) is essential for dynamic ribonucleoprotein (RNP) remodeling of chromatoid bodies during spermatogenesis. *Proc. Natl. Acad. Sci. U. S. A.* **108,** 10579–84 (2011).

157. Kirino, Y. *et al.* Arginine methylation of Piwi proteins catalysed by dPRMT5 is required for Ago3 and Aub stability. *Nat. Cell Biol.* **11,** 652–8 (2009).

158. Kirino, Y. *et al.* Arginine methylation of Aubergine mediates Tudor binding and germ plasm localization. *RNA* **16,** 70–8 (2010).

159. Côté, J. & Richard, S. Tudor domains bind symmetrical dimethylated arginines. *J. Biol. Chem.* **280,** 28476–83 (2005).

160. Goulet, I., Boisvenue, S., Mokas, S., Mazroui, R. & Côté, J. TDRD3, a novel Tudor domain-containing protein, localizes to cytoplasmic stress granules. *Hum. Mol. Genet.* **17,** 3055–74 (2008).

161. Rzeczkowski, K. *et al.* c-Jun N-terminal kinase phosphorylates DCP1a to control formation of P bodies. *J. Cell Biol.* **194,** 581–96 (2011).

162. Kwon, S., Zhang, Y. & Matthias, P. The deacetylase HDAC6 is a novel critical component of stress granules involved in the stress response. *Genes Dev.* **21,** 3381–94 (2007).

163. Loschi, M., Leishman, C. C., Berardone, N. & Boccaccio, G. L. Dynein and kinesin regulate stress-granule and P-body dynamics. *J. Cell Sci.* **122,** 3973–82 (2009).

164. Clemson, C. M. *et al.* An architectural role for a nuclear noncoding RNA: NEAT1 RNA is essential for the structure of paraspeckles. *Mol. Cell* **33,** 717–26 (2009).

165. Meikar, O. *et al.* An atlas of chromatoid body components. *RNA* **20,** 483–95 (2014).

166. Wilczynska, A., Aigueperse, C., Kress, M., Dautry, F. & Weil, D. The translational regulator CPEB1 provides a link between dcp1 bodies and stress granules. *J. Cell Sci.* **118,** 981–92 (2005).

167. Aizer, A., Kafri, P., Kalo, A. & Shav-Tal, Y. The P body protein Dcp1a is hyper-phosphorylated during mitosis. *PLoS One* **8,** e49783 (2013).

168. Sheth, U. & Parker, R. Decapping and decay of messenger RNA occur in cytoplasmic processing bodies. *Science* **300,** 805–8 (2003).

169. Tsai, N.-P., Ho, P.-C. & Wei, L.-N. Regulation of stress granule dynamics by Grb7 and FAK signalling pathway. *EMBO J.* **27,** 715–26 (2008).

170. Buchan, J. R., Kolaitis, R.-M., Taylor, J. P. & Parker, R. Eukaryotic stress granules are cleared by autophagy and Cdc48/VCP function. *Cell* **153,** 1461–74 (2013).

171. Gibbings, D. *et al.* Selective autophagy degrades DICER and AGO2 and regulates miRNA activity. *Nat. Cell Biol.* **14,** 1314–21 (2012).

172. Guo, H. *et al.* Autophagy supports genomic stability by degrading retrotransposon RNA. *Nat. Commun.* **5,** 5276 (2014).

173. Hermann, F. Beiträge zur Histologie des Hodens. *Arch mikr Anat* 58–105 (1889).

174. Benda, C. Neue Mittheilungen über die Entwickelung der Genitadrüsen und über die Metamorphose der Samenzellen (Histogenese der Spermatozoen). *Arch. Anat. Physiol. Physiol. Abt.* 549–552 (1891).

175. Hegner, R. The Germ-Cell Cycle in Animals. *Macmillan* (1914).

176. Fawcett, D. W., Eddy, E. M. & Phillips, D. M. Observations on the fine structure and relationships of the chromatoid body in mammalian spermatogenesis. *Biol. Reprod.* **2,** 129–153 (1970).

177. Russell, L. & Frank, B. Ultrastructural characterization of nuage in spermatocytes of the rat testis. *Anat. Rec.* **190,** 79–97 (1978).

178. SUD, B. N. Morphological and Histochemical Studies of the Chromatoid Body and Related Elements in the Spermatogenesis of the Rat. *Q. J. Microsc. Sci.* **s3-102,** 495–506 (1961).

179. Eddy, E. M. & Ito, S. Fine structural and radioautographic observations on dense

perinuclear cytoplasmic material in tadpole oocytes. *J. Cell Biol.* **49,** 90–108 (1971).

180. Eddy, E. M. Cytochemical observations on the chromatoid body of the male germ cells. *Biol. Reprod.* **2,** 114–128 (1970).

181. Conway, C. M. Evidence for RNA in the heavy bodies of sea urchin eggs. *J. Cell Biol.* **51,** 889–93 (1971).

182. Söderström, K. O. & Parvinen, M. Incorporation of (3H)uridine by the chromatoid body during rat spermatogenesis. *J. Cell Biol.* **70,** 239–46 (1976).

183. Kotaja, N., Lin, H., Parvinen, M. & Sassone-Corsi, P. Interplay of PIWI/Argonaute protein MIWI and kinesin KIF17b in chromatoid bodies of male germ cells. *J. Cell Sci.* **119,** 2819–25 (2006).

184. Meikar, O., Da Ros, M., Liljenbäck, H., Toppari, J. & Kotaja, N. Accumulation of piRNAs in the chromatoid bodies purified by a novel isolation protocol. *Exp. Cell Res.* **316,** 1567–75 (2010).

185. André, J. & Rouiller, C. L'ultrastructure de la membrane nucléaire des ovocytes del l'araignée (Tegenaria domestica Clark). *Proc. Eur. Conf. Electron Microsc.* 162–164 (1956).

186. Sengupta, M. S. & Boag, P. R. Germ granules and the control of mRNA translation. *IUBMB Life* **64,** 586–94 (2012).

187. Gao, M. & Arkov, A. L. Next generation organelles: Structure and role of germ granules in the germline. *Mol. Reprod. Dev.* **80,** 610–623 (2013).

188. Leatherman, J. L. & Jongens, T. A. Transcriptional silencing and translational control: key features of early germline development. *Bioessays* **25,** 326–335 (2003).

189. McLaren, A. Primordial germ cells in the mouse. *Dev. Biol.* **262,** 1–15 (2003).

190. Dufau, M. L. & Tsai-Morris, C.-H. Gonadotropin-regulated testicular helicase (GRTH/DDX25): an essential regulator of spermatogenesis. *Trends Endocrinol. Metab.* **18,** 314–20 (2007).

191. Onohara, Y., Fujiwara, T., Yasukochi, T., Himeno, M. & Yokota, S. Localization of mouse vasa homolog protein in chromatoid body and related nuage structures of mammalian spermatogenic cells during spermatogenesis. *Histochem. Cell Biol.* **133,** 627–639 (2010).

192. Hay, B., Jan, L. Y. & Jan, Y. N. A protein component of Drosophila polar granules is encoded by vasa and has extensive sequence similarity to ATP-dependent helicases. *Cell* **55,** 577–87 (1988).

193. Hosokawa, M. *et al.* Tudor-related proteins TDRD1/MTR-1, TDRD6 and TDRD7/TRAP: domain composition, intracellular localization, and function in male germ cells in mice. *Dev. Biol.* **301,** 38–52 (2007).

194. Vasileva, A. *et al.* Tdrd6 is required for spermiogenesis, chromatoid body architecture, and regulation of miRNA expression. *Curr. Biol.* **19,** 630–9 (2009).

195. Yabuta, Y. *et al.* TDRD5 is required for retrotransposon silencing, chromatoid body assembly, and spermiogenesis in mice. *J. Cell Biol.* **192,** 781–95 (2011).

196. Nishida, K. M. *et al.* Functional involvement of Tudor and dPRMT5 in the piRNA processing pathway in Drosophila germlines. *EMBO J.* **28,** 3820–31 (2009).

197. Linder, P. & Lasko, P. Bent out of shape: RNA unwinding by the DEAD-box helicase Vasa. *Cell* **125,** 219–21 (2006).

198. Sengoku, T., Nureki, O., Nakamura, A., Kobayashi, S. & Yokoyama, S. Structural basis for RNA unwinding by the DEAD-box protein Drosophila Vasa. *Cell* **125,** 287–300 (2006).

199. Styhler, S., Nakamura, A., Swan, A., Suter, B. & Lasko, P. vasa is required for GURKEN accumulation in the oocyte, and is involved in oocyte differentiation and germline cyst development. *Development* **125,** 1569–1578 (1998).

200. Tomancak, P., Guichet, A., Zavorszky, P. & Ephrussi, A. Oocyte polarity depends on regulation of gurken by Vasa. *Development* **125,** 1723–1732 (1998).

201. Tanaka, S. S. *et al.* The mouse homolog of Drosophila Vasa is required for the development of male germ cells. *Genes Dev.* **14,** 841–53 (2000).

202. Vagin, V. V *et al.* Proteomic analysis of murine Piwi proteins reveals a role for arginine methylation in specifying interaction with Tudor family members. *Genes Dev.* **23,** 1749–62 (2009).

203. Mathioudakis, N. *et al.* The multiple Tudor domain-containing protein TDRD1 is a molecular scaffold for mouse Piwi proteins and piRNA biogenesis factors. *RNA* **18,** 2056–72 (2012).

204. Frankel, A. & Clarke, S. PRMT3 is a distinct member of the protein arginine N-methyltransferase family. Conferral of substrate specificity by a zinc-finger domain. *J. Biol. Chem.* **275,** 32974–82 (2000).

205. Kirino, Y. *et al.* Arginine methylation of vasa protein is conserved across phyla. *J. Biol. Chem.* **285,** 8148–54 (2010).

206. Chen, C. *et al.* Mouse Piwi interactome identifies binding mechanism of Tdrkh Tudor domain to arginine methylated Miwi. *Proc. Natl. Acad. Sci. U. S. A.* **106,** 20336–41 (2009).

207. Creed, T. M., Loganathan, S. N., Varonin, D., Jackson, C. A. & Arkov, A. L. Novel role of specific Tudor domains in Tudor-Aubergine protein complex assembly and distribution during Drosophila oogenesis. *Biochem. Biophys. Res. Commun.* **402,** 384–9 (2010).

208. Klenov, M. S. *et al.* Repeat-associated siRNAs cause chromatin silencing of retrotransposons in the Drosophila melanogaster germline. *Nucleic Acids Res.* **35,** 5430–8 (2007).

209. Li, C. *et al.* Collapse of germline piRNAs in the absence of Argonaute3 reveals somatic piRNAs in flies. *Cell* **137,** 509–21 (2009).

210. Saunders, P. T., Millar, M. R., Maguire, S. M. & Sharpe, R. M. Stage-specific expression of rat transition protein 2 mRNA and possible localization to the chromatoid body of step 7 spermatids by in situ hybridization using a nonradioactive riboprobe. *Mol. Reprod. Dev.* **33,** 385–91 (1992).

211. Wu, S.-M. *et al.* Analysis of mouse germ-cell transcriptome at different stages of spermatogenesis by SAGE: biological significance. *Genomics* **84,** 971–81 (2004).

212. Shima, J. E., McLean, D. J., McCarrey, J. R. & Griswold, M. D. The murine testicular transcriptome: characterizing gene expression in the testis during the progression of spermatogenesis. *Biol. Reprod.* **71,** 319–30 (2004).

213. Soumillon, M. *et al.* Cellular source and mechanisms of high transcriptome complexity in the mammalian testis. *Cell Rep.* **3,** 2179–90 (2013).

214. von Brunn, A. Beiträge zur Entwicklungsgeschichte der Samenkörper. *Arch. Mikr. Anat.* **12,** 528–536 (1876).

215. Shang, P. *et al.* Functional transformation of the chromatoid body in mouse spermatids requires testis-specific serine/threonine kinases. *J. Cell Sci.* **123,** 331–339 (2010).

216. Kotaja, N. *et al.* The chromatoid body of male germ cells: similarity with processing bodies and presence of Dicer and microRNA pathway components. *Proc. Natl. Acad. Sci. U. S. A.* **103,** 2647–52 (2006).

217. Nguyen Chi, M. *et al.* Temporally regulated traffic of HuR and its associated ARE-containing mRNAs from the chromatoid body to polysomes during mouse spermatogenesis. *PLoS One* **4,** e4900 (2009).

218. Kuramochi-Miyagawa, S. *et al.* Two mouse piwi-related genes: miwi and mili. *Mech. Dev.* **108,** 121–33 (2001).

219. Tsai-Morris, C.-H., Sheng, Y., Lee, E., Lei, K.-J. & Dufau, M. L. Gonadotropin-regulated testicular RNA helicase (GRTH/Ddx25) is essential for spermatid development and completion of spermatogenesis. *Proc. Natl. Acad. Sci. U. S. A.* **101,** 6373–8 (2004).

220. Meikar, O., Da Ros, M. & Kotaja, N. Epigenetic regulation of male germ cell differentiation. *Subcell. Biochem.* **61,** 119–38 (2013).

221. Scita, G. & Di Fiore, P. P. The endocytic matrix. *Nature* **463,** 464–73 (2010).

222. Doherty, G. J. & McMahon, H. T. Mechanisms of endocytosis. *Annu. Rev. Biochem.* **78,** 857–902 (2009).

223. Jackson, C. L. Mechanisms of transport through the Golgi complex. *J. Cell Sci.* **122,** 443–52 (2009).

224. Brighouse, A., Dacks, J. B. & Field, M. C. Rab protein evolution and the history of the eukaryotic endomembrane system. *Cell. Mol. Life Sci.* **67,** 3449–65 (2010).

225. Deshaies, R. J. & Schekman, R. A yeast mutant defective at an early stage in import of secretory protein precursors into the endoplasmic reticulum. *J. Cell Biol.* **105,** 633–45 (1987).

226. Hierro, A. *et al.* Functional architecture of the retromer cargo-recognition complex. *Nature* **449,** 1063–7 (2007).

227. Rojas, R., Kametaka, S., Haft, C. R. & Bonifacino, J. S. Interchangeable but essential functions of SNX1 and SNX2 in the association of retromer with endosomes and the trafficking of mannose 6-phosphate receptors. *Mol. Cell. Biol.* **27,** 1112–24 (2007).

228. Haft, C. R. *et al.* Human orthologs of yeast vacuolar protein sorting proteins Vps26, 29, and 35: assembly into multimeric complexes. *Mol. Biol. Cell* **11,** 4105–16 (2000).

229. Haft, C. R., de la Luz Sierra, M., Barr, V. A., Haft, D. H. & Taylor, S. I. Identification of a Family of Sorting Nexin Molecules and Characterization of Their Association with Receptors. *Mol. Cell. Biol.* **18,** 7278–7287 (1998).

230. Carlton, J. G. Sorting nexin-2 is associated with tubular elements of the early endosome, but is not essential for retromer-mediated endosome-to-TGN transport. *J. Cell Sci.* **118,** 4527–4539 (2005).

231. Cozier, G. E. *et al.* The phox homology (PX) domain-dependent, 3-phosphoinositide-mediated association of sorting nexin-1 with an early sorting endosomal compartment is required for its ability to regulate epidermal growth factor receptor degradation. *J. Biol. Chem.* **277,** 48730–6 (2002).

232. Zhong, Q. *et al.* Determinants of the endosomal localization of sorting nexin 1. *Mol. Biol. Cell* **16,** 2049–57 (2005).

233. Carlton, J. *et al.* Sorting nexin-1 mediates tubular endosome-to-TGN transport through coincidence sensing of high- curvature

membranes and 3-phosphoinositides. *Curr. Biol.* **14,** 1791–800 (2004).

234. Zhong, Q. *et al.* Endosomal localization and function of sorting nexin 1. *Proc. Natl. Acad. Sci. U. S. A.* **99,** 6767–72 (2002).

235. Arighi, C. N., Hartnell, L. M., Aguilar, R. C., Haft, C. R. & Bonifacino, J. S. Role of the mammalian retromer in sorting of the cation-independent mannose 6-phosphate receptor. *J. Cell Biol.* **165,** 123–33 (2004).

236. Damen, E., Krieger, E., Nielsen, J. E., Eygensteyn, J. & van Leeuwen, J. E. M. The human Vps29 retromer component is a metallo-phosphoesterase for a cation-independent mannose 6-phosphate receptor substrate peptide. *Biochem. J.* **398,** 399–409 (2006).

237. Kerr, M. C. *et al.* A Novel Mammalian Retromer Component, Vps26B. *Traffic* **6,** 991–1001 (2005).

238. Bugarcic, A. *et al.* Vps26A and Vps26B subunits define distinct retromer complexes. *Traffic* **12,** 1759–73 (2011).

239. Gullapalli, A. A Role for Sorting Nexin 2 in Epidermal Growth Factor Receptor Down-regulation: Evidence for Distinct Functions of Sorting Nexin 1 and 2 in Protein Trafficking. *Mol. Biol. Cell* **15,** 2143–2155 (2004).

240. Kurten, R. *et al.* Self-assembly and binding of a sorting nexin to sorting endosomes. *J. Cell Sci.* **114,** 1743–1756 (2001).

241. Seaman, M. N. J. Cargo-selective endosomal sorting for retrieval to the Golgi requires retromer. *J. Cell Biol.* **165,** 111–22 (2004).

242. Teasdale, R. D., Loci, D., Houghton, F., Karlsson, L. & Gleeson, P. A. A large family of endosome-localized proteins related to sorting nexin 1. *Biochem. J.* **358,** 7–16 (2001).

243. Rojas, R. *et al.* Regulation of retromer recruitment to endosomes by sequential action of Rab5 and Rab7. *J. Cell Biol.* **183,** 513–26 (2008).

244. Seaman, M. N. J., Harbour, M. E., Tattersall, D., Read, E. & Bright, N. Membrane recruitment of the cargo-selective retromer subcomplex is catalysed by the small GTPase Rab7 and inhibited by the Rab-GAP TBC1D5. *J. Cell Sci.* **122,** 2371–82 (2009).

245. Schwarz, D. G., Griffin, C. T., Schneider, E. A., Yee, D. & Magnuson, T. Genetic analysis of sorting nexins 1 and 2 reveals a redundant and essential function in mice. *Mol. Biol. Cell* **13,** 3588–600 (2002).

246. Griffin, C. T., Trejo, J. & Magnuson, T. Genetic evidence for a mammalian retromer complex containing sorting nexins 1 and 2. *Proc. Natl. Acad. Sci. U. S. A.* **102,** 15173–7 (2005).

247. Radice, G., Lee, J. J. & Costantini, F. H beta 58, an insertional mutation affecting early postimplantation development of the mouse embryo. *Development* **111,** 801–11 (1991).

248. Lee, J. J., Radice, G., Perkins, C. P. & Costantini, F. Identification and characterization of a novel, evolutionarily conserved gene disrupted by the murine H beta 58 embryonic lethal transgene insertion. *Development* **115,** 277–88 (1992).

249. Seaman, M. N. J. Identification of a novel conserved sorting motif required for retromer-mediated endosome-to-TGN retrieval. *J. Cell Sci.* **120,** 2378–89 (2007).

250. Shi, H., Rojas, R., Bonifacino, J. S. & Hurley, J. H. The retromer subunit Vps26 has an arrestin fold and binds Vps35 through its C-terminal domain. *Nat. Struct. Mol. Biol.* **13,** 540–8 (2006).

251. Fjorback, A. W. *et al.* Retromer binds the FANSHY sorting motif in SorLA to regulate amyloid precursor protein sorting and processing. *J. Neurosci.* **32,** 1467–80 (2012).

252. Nisar, S., Kelly, E., Cullen, P. J. & Mundell, S. J. Regulation of P2Y1 receptor traffic by sorting Nexin 1 is retromer independent. *Traffic* **11,** 508–19 (2010).

253. Wang, Y., Zhou, Y., Szabo, K., Haft, C. R. & Trejo, J. Down-regulation of protease-activated receptor-1 is regulated by sorting nexin 1. *Mol. Biol. Cell* **13,** 1965–76 (2002).

254. Heydorn, A. *et al.* A library of 7TM receptor C-terminal tails. Interactions with the proposed post-endocytic sorting proteins ERM-binding phosphoprotein 50 (EBP50), N-ethylmaleimide-sensitive factor (NSF), sorting nexin 1 (SNX1), and G protein-coupled receptor-associated so. *J. Biol. Chem.* **279,** 54291–303 (2004).

255. McGough, I. J. & Cullen, P. J. Recent advances in retromer biology. *Traffic* **12,** 963–71 (2011).

256. Harbour, M. E. *et al.* The cargo-selective retromer complex is a recruiting hub for protein complexes that regulate endosomal tubule dynamics. *J. Cell Sci.* **123,** 3703–17 (2010).

257. Gomez, T. S. & Billadeau, D. D. A FAM21-Containing WASH Complex Regulates Retromer-Dependent Sorting. *Dev. Cell* **17,** 699–711 (2009).

258. Derivery, E. *et al.* The Arp2/3 Activator WASH Controls the Fission of Endosomes through a Large Multiprotein Complex. *Dev. Cell* **17,** 712–723 (2009).

259. Hong, Z. *et al.* The retromer component SNX6 interacts with dynactin p150(Glued) and mediates endosome-to-TGN transport. *Cell Res.* **19,** 1334–49 (2009).

260. Wassmer, T. *et al.* The Retromer Coat Complex Coordinates Endosomal Sorting and Dynein-Mediated Transport, with Carrier Recognition by the trans-Golgi Network. *Dev. Cell* **17,** 110–122 (2009).

261. Tabuchi, M., Yanatori, I., Kawai, Y. & Kishi, F. Retromer-mediated direct sorting is required for proper endosomal recycling of the mammalian iron transporter DMT1. *J. Cell Sci.* **123,** 756–66 (2010).

262. Eaton, S. Retromer retrieves wntless. *Dev. Cell* **14,** 4–6 (2008).

263. Pocha, S. M., Wassmer, T., Niehage, C., Hoflack, B. & Knust, E. Retromer controls epithelial cell polarity by trafficking the apical determinant Crumbs. *Curr. Biol.* **21,** 1111–7 (2011).

264. Nielsen, M. S. *et al.* Sorting by the cytoplasmic domain of the amyloid precursor protein binding receptor SorLA. *Mol. Cell. Biol.* **27,** 6842–51 (2007).

265. Prosser, D. C., Tran, D., Schooley, A., Wendland, B. & Ngsee, J. K. A novel, retromer-independent role for sorting nexins 1 and 2 in RhoG-dependent membrane remodeling. *Traffic* **11,** 1347–62 (2010).

266. Puthenveedu, M. A. *et al.* Sequence-dependent sorting of recycling proteins by actin-stabilized endosomal microdomains. *Cell* **143,** 761–73 (2010).

267. Temkin, P. *et al.* SNX27 mediates retromer tubule entry and endosome-to-plasma membrane trafficking of signalling receptors. *Nat. Cell Biol.* **13,** 715–21 (2011).

268. Zech, T. *et al.* The Arp2/3 activator WASH regulates α5β1-integrin-mediated invasive migration. *J. Cell Sci.* **124,** 3753–9 (2011).

269. Andersen, O. M. *et al.* Neuronal sorting protein-related receptor sorLA/LR11 regulates processing of the amyloid precursor protein. *Proc. Natl. Acad. Sci. U. S. A.* **102,** 13461–6 (2005).

270. Andersen, O. M. *et al.* Molecular dissection of the interaction between amyloid precursor protein and its neuronal trafficking receptor SorLA/LR11. *Biochemistry* **45,** 2618–28 (2006).

271. Small, S. A. *et al.* Model-guided microarray implicates the retromer complex in Alzheimer's disease. *Ann. Neurol.* **58,** 909–19 (2005).

272. Muhammad, A. *et al.* Retromer deficiency observed in Alzheimer's disease causes hippocampal dysfunction, neurodegeneration, and Abeta accumulation. *Proc. Natl. Acad. Sci. U. S. A.* **105,** 7327–32 (2008).

273. Lane, R. F. *et al.* Diabetes-associated SorCS1 regulates Alzheimer's amyloid-beta metabolism: evidence for involvement of SorL1 and the retromer complex. *J. Neurosci.* **30,** 13110–5 (2010).

274. Wen, L. *et al.* VPS35 haploinsufficiency increases Alzheimer's disease neuropathology. *J. Cell Biol.* **195,** 765–79 (2011).

275. Zimprich, A. *et al.* A mutation in VPS35, encoding a subunit of the retromer complex, causes late-onset Parkinson disease. *Am. J. Hum. Genet.* **89,** 168–75 (2011).

276. Vilariño-Güell, C. *et al.* VPS35 mutations in Parkinson disease. *Am. J. Hum. Genet.* **89,** 162–7 (2011).

277. Zavodszky, E. *et al.* Mutation in VPS35 associated with Parkinson's disease impairs WASH complex association and inhibits autophagy. *Nat. Commun.* **5,** 3828 (2014).

278. Tsukada, M. & Ohsumi, Y. Isolation and characterization of autophagy-defective mutants of Saccharomyces cerevisiae. *FEBS Lett.* **333,** 169–174 (1993).

279. Thumm, M. *et al.* Isolation of autophagocytosis mutants of Saccharomyces cerevisiae. *FEBS Lett.* **349,** 275–280 (1994).

280. Harding, T. M. Isolation and characterization of yeast mutants in the cytoplasm to vacuole protein targeting pathway. *J. Cell Biol.* **131,** 591–602 (1995).

281. Harding, T. M., Hefner-Gravink, A., Thumm, M. & Klionsky, D. J. Genetic and Phenotypic Overlap between Autophagy and the Cytoplasm to Vacuole Protein Targeting Pathway. *J. Biol. Chem.* **271,** 17621–17624 (1996).

282. Mizushima, N. & Komatsu, M. Autophagy: renovation of cells and tissues. *Cell* **147,** 728–41 (2011).

283. Axe, E. L. *et al.* Autophagosome formation from membrane compartments enriched in phosphatidylinositol 3-phosphate and dynamically connected to the endoplasmic reticulum. *J. Cell Biol.* **182,** 685–701 (2008).

284. Hailey, D. W. *et al.* Mitochondria supply membranes for autophagosome biogenesis during starvation. *Cell* **141,** 656–67 (2010).

285. Ravikumar, B., Moreau, K., Jahreiss, L., Puri, C. & Rubinsztein, D. C. Plasma membrane contributes to the formation of pre-autophagosomal structures. *Nat. Cell Biol.* **12,** 747–57 (2010).

286. Puri, C., Renna, M., Bento, C. F., Moreau, K. & Rubinsztein, D. C. Diverse autophagosome membrane sources coalesce in recycling endosomes. *Cell* **154,** 1285–99 (2013).

287. Blommaart, E. F., Luiken, J. J., Blommaart, P. J., van Woerkom, G. M. & Meijer, A. J. Phosphorylation of ribosomal protein S6 is inhibitory for autophagy in isolated rat

hepatocytes. *J. Biol. Chem.* **270,** 2320–6 (1995).

288. Iwamaru, A. *et al.* Silencing mammalian target of rapamycin signaling by small interfering RNA enhances rapamycin-induced autophagy in malignant glioma cells. *Oncogene* **26,** 1840–51 (2007).

289. Noda, T. Tor, a Phosphatidylinositol Kinase Homologue, Controls Autophagy in Yeast. *J. Biol. Chem.* **273,** 3963–3966 (1998).

290. Yu, L. *et al.* Termination of autophagy and reformation of lysosomes regulated by mTOR. *Nature* **465,** 942–6 (2010).

291. Hayashi-Nishino, M. *et al.* A subdomain of the endoplasmic reticulum forms a cradle for autophagosome formation. *Nat. Cell Biol.* **11,** 1433–7 (2009).

292. Hayashi-Nishino, M. *et al.* Electron tomography reveals the endoplasmic reticulum as a membrane source for autophagosome formation. *Autophagy* **6,** 301–303 (2010).

293. Ylä-Anttila, P., Vihinen, H., Jokitalo, E. & Eskelinen, E.-L. L. 3D tomography reveals connections between the phagophore and endoplasmic reticulum. *Autophagy* **5,** 1180–1185 (2009).

294. Itoh, T. *et al.* Golgi-resident small GTPase Rab33B interacts with Atg16L and modulates autophagosome formation. *Mol. Biol. Cell* **19,** 2916–25 (2008).

295. Young, A. R. J. *et al.* Starvation and ULK1-dependent cycling of mammalian Atg9 between the TGN and endosomes. *J. Cell Sci.* **119,** 3888–900 (2006).

296. Sou, Y. *et al.* The Atg8 conjugation system is indispensable for proper development of autophagic isolation membranes in mice. *Mol. Biol. Cell* **19,** 4762–75 (2008).

297. Kuma, A. *et al.* The role of autophagy during the early neonatal starvation period. *Nature* **432,** 1032–6 (2004).

298. Komatsu, M. *et al.* Impairment of starvation-induced and constitutive autophagy in Atg7-deficient mice. *J. Cell Biol.* **169,** 425–34 (2005).

299. Onodera, J. & Ohsumi, Y. Autophagy is required for maintenance of amino acid levels and protein synthesis under nitrogen starvation. *J. Biol. Chem.* **280,** 31582–6 (2005).

300. Suzuki, S. W., Onodera, J. & Ohsumi, Y. Starvation induced cell death in autophagy-defective yeast mutants is caused by mitochondria dysfunction. *PLoS One* **6,** e17412 (2011).

301. Guo, J. Y. *et al.* Activated Ras requires autophagy to maintain oxidative metabolism and tumorigenesis. *Genes Dev.* **25,** 460–70 (2011).

302. Singh, R. *et al.* Autophagy regulates lipid metabolism. *Nature* **458,** 1131–5 (2009).

303. Chen, Y. & Klionsky, D. J. The regulation of autophagy - unanswered questions. *J. Cell Sci.* **124,** 161–70 (2011).

304. Mizushima, N., Yoshimori, T. & Ohsumi, Y. The role of Atg proteins in autophagosome formation. *Annu. Rev. Cell Dev. Biol.* **27,** 107–32 (2011).

305. Nakatogawa, H., Suzuki, K., Kamada, Y. & Ohsumi, Y. Dynamics and diversity in autophagy mechanisms: lessons from yeast. *Nat. Rev. Mol. Cell Biol.* **10,** 458–67 (2009).

306. Lin, L. *et al.* The scaffold protein EPG-7 links cargo-receptor complexes with the autophagic assembly machinery. *J. Cell Biol.* **201,** 113–29 (2013).

307. Johansen, T. & Lamark, T. Selective autophagy mediated by autophagic adapter proteins. *Autophagy* **7,** 279–296 (2014).

308. Bjørkøy, G. *et al.* p62/SQSTM1 forms protein aggregates degraded by autophagy and has a protective effect on huntingtin-induced cell death. *J. Cell Biol.* **171,** 603–14 (2005).

309. Komatsu, M. *et al.* Homeostatic levels of p62 control cytoplasmic inclusion body formation in autophagy-deficient mice. *Cell* **131,** 1149–63 (2007).

310. Zatloukal, K. *et al.* p62 Is a common component of cytoplasmic inclusions in protein aggregation diseases. *Am. J. Pathol.* **160,** 255–63 (2002).

311. Osaka, M., Ito, D., Yagi, T., Nihei, Y. & Suzuki, N. Evidence of a link between ubiquilin 2 and optineurin in amyotrophic lateral sclerosis. *Hum. Mol. Genet.* **24,** 1617–29 (2015).

312. Colman, R. J. *et al.* Caloric restriction delays disease onset and mortality in rhesus monkeys. *Science* **325,** 201–4 (2009).

313. Colman, R. J. *et al.* Caloric restriction reduces age-related and all-cause mortality in rhesus monkeys. *Nat. Commun.* **5,** 3557 (2014).

314. Wu, J. J. *et al.* Increased mammalian lifespan and a segmental and tissue-specific slowing of aging after genetic reduction of mTOR expression. *Cell Rep.* **4,** 913–20 (2013).

315. Müller, O. *et al.* Autophagic Tubes: Vacuolar Invaginations Involved in Lateral Membrane Sorting and Inverse Vesicle Budding. *J. Cell Biol.* **151,** 519–528 (2000).

316. Sattler, T. & Mayer, A. Cell-free reconstitution of microautophagic vacuole invagination and vesicle formation. *J. Cell Biol.* **151,** 529–38 (2000).

317. Epple, U. D., Suriapranata, I., Eskelinen, E. L. & Thumm, M. Aut5/Cvt17p, a putative lipase essential for disintegration of autophagic

bodies inside the vacuole. *J. Bacteriol.* **183,** 5942–55 (2001).

318. Yang, Z. & Klionsky, D. J. Permeases recycle amino acids resulting from autophagy. *Autophagy* **3,** 149–50

319. Li, W., Li, J. & Bao, J. Microautophagy: lesser-known self-eating. *Cell. Mol. Life Sci.* **69,** 1125–36 (2012).

320. Bellu, A. R., Kram, A. M., Kiel, J. A., Veenhuis, M. & van der Klei, I. J. Glucose-induced and nitrogen-starvation-induced peroxisome degradation are distinct processes in Hansenula polymorpha that involve both common and unique genes. *FEMS Yeast Res.* **1,** 23–31 (2001).

321. Dawaliby, R. & Mayer, A. Microautophagy of the nucleus coincides with a vacuolar diffusion barrier at nuclear-vacuolar junctions. *Mol. Biol. Cell* **21,** 4173–83 (2010).

322. Kissová, I. *et al.* Selective and non-selective autophagic degradation of mitochondria in yeast. *Autophagy* **3,** 329–36

323. Fred Dice, J. Peptide sequences that target cytosolic proteins for lysosomal proteolysis. *Trends Biochem. Sci.* **15,** 305–309 (1990).

324. Chiang, H. L., Terlecky, S. R., Plant, C. P. & Dice, J. F. A role for a 70-kilodalton heat shock protein in lysosomal degradation of intracellular proteins. *Science* **246,** 382–5 (1989).

325. Agarraberes, F. A. & Dice, J. F. A molecular chaperone complex at the lysosomal membrane is required for protein translocation. *J. Cell Sci.* **114,** 2491–9 (2001).

326. Chiang, H. L. & Dice, J. F. Peptide sequences that target proteins for enhanced degradation during serum withdrawal. *J. Biol. Chem.* **263,** 6797–805 (1988).

327. Cuervo, A. M. & Dice, J. F. A receptor for the selective uptake and degradation of proteins by lysosomes. *Science* **273,** 501–3 (1996).

328. Bandyopadhyay, U., Kaushik, S., Varticovski, L. & Cuervo, A. M. The chaperone-mediated autophagy receptor organizes in dynamic protein complexes at the lysosomal membrane. *Mol. Cell. Biol.* **28,** 5747–63 (2008).

329. Fujiwara, Y. *et al.* Discovery of a novel type of autophagy targeting RNA. *Autophagy* **9,** 403–9 (2013).

330. Fujiwara, Y. *et al.* Direct uptake and degradation of DNA by lysosomes. *Autophagy* **9,** 1167–71 (2013).

331. Fujiwara, Y., Hase, K., Wada, K. & Kabuta, T. An RNautophagy/DNautophagy receptor, LAMP2C, possesses an arginine-rich motif that mediates RNA/DNA-binding. *Biochem. Biophys. Res. Commun.* **460,** 281–6 (2015).

332. Hase, K. *et al.* RNautophagy/DNautophagy possesses selectivity for RNA/DNA substrates. *Nucleic Acids Res.* (2015). doi:10.1093/nar/gkv579

333. Allison, A. C. & Hartree, E. F. Lysosomal enzymes in the acrosome and their possible role in fertilization. *J. Reprod. Fertil.* **21,** 501–15 (1970).

334. Miller, D. J., Gong, X. & Shur, B. D. Sperm require beta-N-acetylglucosaminidase to penetrate through the egg zona pellucida. *Development* **118,** 1279–89 (1993).

335. Saling, P. M. Involvement of trypsin-like activity in binding of mouse spermatozoa to zonae pellucidae. *Proc. Natl. Acad. Sci. U. S. A.* **78,** 6231–5 (1981).

336. Bermudez, D. *et al.* Proacrosin as a marker of meiotic and post-meiotic germ cell differentiation: quantitative assessment of human spermatogenesis with a monoclonal antibody. *Reproduction* **100,** 567–575 (1994).

337. Escalier, D. *et al.* Human acrosome biogenesis: immunodetection of proacrosin in primary spermatocytes and of its partitioning pattern during meiosis. *Development* **113,** 779–88 (1991).

338. Kremling, H. *et al.* Mouse proacrosin gene: Nucleotide sequence, diploid expression, and chromosomal localization. *Genomics* **11,** 828–834 (1991).

339. Moreno, R. D., Ramalho-Santos, J., Chan, E. K., Wessel, G. M. & Schatten, G. The Golgi apparatus segregates from the lysosomal/acrosomal vesicle during rhesus spermiogenesis: structural alterations. *Dev. Biol.* **219,** 334–49 (2000).

340. Huang, W.-P. & Ho, H.-C. Role of microtubule-dependent membrane trafficking in acrosomal biogenesis. *Cell Tissue Res.* **323,** 495–503 (2006).

341. Moreno, R. D., Palomino, J. & Schatten, G. Assembly of spermatid acrosome depends on microtubule organization during mammalian spermiogenesis. *Dev. Biol.* **293,** 218–27 (2006).

342. Moreno, R. D. Vesicular Traffic and Golgi Apparatus Dynamics During Mammalian Spermatogenesis: Implications for Acrosome Architecture. *Biol. Reprod.* **63,** 89–98 (2000).

343. Barros, C., Bedford, J. M., Franklin, L. E. & Austin, C. R. Membrane vesiculation as a feature of the mammalian acrosome reaction. *J. Cell Biol.* **34,** C1–5 (1967).

344. Barros, C., Crosby, J. A. & Moreno, R. D. Early steps of sperm-egg interactions during mammalian fertilization. *Cell Biol. Int.* **20,** 33–9 (1996).

345. Moreno, R. D. & Alvarado, C. P. The mammalian acrosome as a secretory lysosome: new and old evidence. *Mol. Reprod. Dev.* **73,** 1430–4 (2006).

346. Berruti, G., Ripolone, M. & Ceriani, M. USP8, a regulator of endosomal sorting, is involved in mouse acrosome biogenesis through interaction with the spermatid ESCRT-0 complex and microtubules. *Biol. Reprod.* **82,** 930–9 (2010).

347. West, A. P. & Willison, K. R. Brefeldin A and mannose 6-phosphate regulation of acrosomic related vesicular trafficking. *Eur. J. Cell Biol.* **70,** 315–21 (1996).

348. Li, Y.-C. *et al.* Afaf, a novel vesicle membrane protein, is related to acrosome formation in murine testis. *FEBS Lett.* **580,** 4266–73 (2006).

349. Li, S. *et al.* Interaction of SH3P13 and DYDC1 protein: a germ cell component that regulates acrosome biogenesis during spermiogenesis. *Eur. J. Cell Biol.* **88,** 509–20 (2009).

350. Zhu, G. *et al.* SPE-39 family proteins interact with the HOPS complex and function in lysosomal delivery. *Mol. Biol. Cell* **20,** 1223–40 (2009).

351. Berruti, G. & Martegani, E. The deubiquitinating enzyme mUBPy interacts with the sperm-specific molecular chaperone MSJ-1: the relation with the proteasome, acrosome, and centrosome in mouse male germ cells. *Biol. Reprod.* **72,** 14–21 (2005).

352. Takata, H., Kato, M., Denda, K. & Kitamura, N. A Hrs binding protein having a Src homology 3 domain is involved in intracellular degradation of growth factors and their receptors. *Genes to Cells* **5,** 57–69 (2000).

353. Tanaka, N., Kyuuma, M. & Sugamura, K. Endosomal sorting complex required for transport proteins in cancer pathogenesis, vesicular transport, and non-endosomal functions. *Cancer Sci.* **99,** 1293–303 (2008).

354. Row, P. E. *et al.* The MIT domain of UBPY constitutes a CHMP binding and endosomal localization signal required for efficient epidermal growth factor receptor degradation. *J. Biol. Chem.* **282,** 30929–37 (2007).

355. HARTREE, E. F. The acrosome-lysosome relationship. *Reproduction* **44,** 125–6 (1975).

356. Press, B. Mutant Rab7 Causes the Accumulation of Cathepsin D and Cation-independent Mannose 6-Phosphate Receptor in an Early Endocytic Compartment. *J. Cell Biol.* **140,** 1075–1089 (1998).

357. Bucci, C., Thomsen, P., Nicoziani, P., McCarthy, J. & van Deurs, B. Rab7: A Key to Lysosome Biogenesis. *Mol. Biol. Cell* **11,** 467–480 (2000).

358. Ramalho-Santos, J., Moreno, R. D., Wessel, G. M., Chan, E. K. & Schatten, G. Membrane trafficking machinery components associated with the mammalian acrosome during spermiogenesis. *Exp. Cell Res.* **267,** 45–60 (2001).

359. Ramalho-Santos, J. & Moreno, R. D. Targeting and fusion proteins during mammalian spermiogenesis. *Biol. Res.* **34,** 147–52 (2001).

360. Gibbings, D. & Voinnet, O. Control of RNA silencing and localization by endolysosomes. *Trends Cell Biol.* **20,** 491–501 (2010).

361. Da Ros, M., Hirvonen, N., Olotu, O., Toppari, J. & Kotaja, N. Retromer vesicles interact with RNA granules in haploid male germ cells. *Mol. Cell. Endocrinol.* **401C,** 73–83 (2014).

362. Tanaka, T. & Nakamura, A. The endocytic pathway acts downstream of Oskar in Drosophila germ plasm assembly. *Development* **135,** 1107–17 (2008).

363. Haraguchi, C. M. *et al.* Chromatoid bodies: aggresome-like characteristics and degradation sites for organelles of spermiogenic cells. *J. Histochem. Cytochem.* **53,** 455–65 (2005).

364. Liou, G. G., Jane, W. N., Cohen, S. N., Lin, N. S. & Lin-Chao, S. RNA degradosomes exist in vivo in Escherichia coli as multicomponent complexes associated with the cytoplasmic membrane via the N-terminal region of ribonuclease E. *Proc. Natl. Acad. Sci. U. S. A.* **98,** 63–8 (2001).

365. Kankaanpää, P. *et al.* BioImageXD: an open, general-purpose and high-throughput image-processing platform. *Nat. Methods* **9,** 683–9 (2012).

366. Meikar, O. & Kotaja, N. Isolation of chromatoid bodies from mouse testis as a rich source of short RNAs. *Methods Mol. Biol.* **1173,** 11–25 (2014).

367. Pall, G. S. & Hamilton, A. J. Improved northern blot method for enhanced detection of small RNA. *Nat. Protoc.* **3,** 1077–84 (2008).

368. Bustin, S. A. *et al.* The MIQE guidelines: minimum information for publication of quantitative real-time PCR experiments. *Clin. Chem.* **55,** 611–22 (2009).

369. Bryant, J. M., Meyer-Ficca, M. L., Dang, V. M., Berger, S. L. & Meyer, R. G. Separation of spermatogenic cell types using STA-PUT velocity sedimentation. *J. Vis. Exp.* (2013). doi:10.3791/50648

370. Figueroa, J. & Burzio, L. O. Polysome-like structures in the chromatoid body of rat spermatids. *Cell Tissue Res.* **291,** 575–9 (1998).

371. Tsai-Morris, C.-H., Sheng, Y., Gutti, R. K., Tang, P.-Z. & Dufau, M. L. Gonadotropin-regulated

testicular RNA helicase (GRTH/DDX25): a multifunctional protein essential for spermatogenesis. *J. Androl.* **31,** 45–52 (2010).

372. Toyooka, Y. *et al.* Expression and intracellular localization of mouse Vasa-homologue protein during germ cell development. *Mech. Dev.* **93,** 139–49 (2000).

373. Chen, C. *et al.* ERM is required for transcriptional control of the spermatogonial stem cell niche. *Nature* **436,** 1030–4 (2005).

374. Kanatsu-Shinohara, M., Toyokuni, S. & Shinohara, T. CD9 is a surface marker on mouse and rat male germline stem cells. *Biol. Reprod.* **70,** 70–5 (2004).

375. Parvinen, M. The chromatoid body in spermatogenesis. *Int. J. Androl.* **28,** 189–201 (2005).

376. Morokuma, Y. *et al.* MARCH-XI, a novel transmembrane ubiquitin ligase implicated in ubiquitin-dependent protein sorting in developing spermatids. *J. Biol. Chem.* **282,** 24806–15 (2007).

377. Yogo, K. *et al.* Identification of SAMT family proteins as substrates of MARCH11 in mouse spermatids. *Histochem. Cell Biol.* **137,** 53–65 (2012).

378. Calvo, A., Pastor, L. M., Bonet, S., Pinart, E. & Ventura, M. Characterization of the glycoconjugates of boar testis and epididymis. *J. Reprod. Fertil.* **120,** 325–35 (2000).

379. Higgins, M. & Davies, J. Niemann–Pick C1 is a late endosome-resident protein that transiently associates with lysosomes and the trans-Golgi network. *Mol. Genet. …* **68,** 1–13 (1999).

380. Kobayashi, T. *et al.* Late endosomal membranes rich in lysobisphosphatidic acid regulate cholesterol transport. *Nat. Cell Biol.* **1,** 113–8 (1999).

381. Kobayashi, T. *et al.* The tetraspanin CD63/lamp3 cycles between endocytic and secretory compartments in human endothelial cells. *… Biol. Cell* **11,** 1829–43 (2000).

382. Pankiv, S. *et al.* FYCO1 is a Rab7 effector that binds to LC3 and PI3P to mediate microtubule plus end-directed vesicle transport. *J. Cell Biol.* **188,** 253–69 (2010).

383. Raiborg, C. *et al.* Repeated ER–endosome contacts promote endosome translocation and neurite outgrowth. *Nature* **520,** 234–238 (2015).

384. Ventela, S. *et al.* Intercellular organelle traffic through cytoplasmic bridges in early spermatids of the rat: mechanisms of haploid gene product sharing. *Mol. Biol. Cell* **14,** 2768–2780 (2003).

385. Yokota, S. Historical survey on chromatoid body research. *Acta Histochem. Cytochem.* **41,** 65–82 (2008).

386. Söderström, K. O. & Parvinen, M. Transport of material between the nucleus, the chromatoid body and the golgi complex in the early spermatids of the rat. *Cell Tissue Res.* **168,** 335–342 (1976).

387. Guyonnet, B., Zabet-Moghaddam, M., SanFrancisco, S. & Cornwall, G. A. Isolation and proteomic characterization of the mouse sperm acrosomal matrix. *Mol. Cell. Proteomics* **11,** 758–74 (2012).

388. Funaki, T. *et al.* The Arf GAP SMAP2 is necessary for organized vesicle budding from the trans-Golgi network and subsequent acrosome formation in spermiogenesis. *Mol. Biol. Cell* **24,** 2633–44 (2013).

389. Kierszenbaum, A. L., Rivkin, E. & Tres, L. L. Acroplaxome, an F-actin-keratin-containing plate, anchors the acrosome to the nucleus during shaping of the spermatid head. *Mol. Biol. Cell* **14,** 4628–40 (2003).

390. Kierszenbaum, A. L. & Tres, L. L. The acrosome-acroplaxome-manchette complex and the shaping of the spermatid head. *Arch. Histol. Cytol.* **67,** 271–284 (2004).

391. Gibbings, D., Mostowy, S. & Voinnet, O. Autophagy selectively regulates miRNA homeostasis. *Autophagy* **9,** 781–3 (2013).

392. Parvinen, M. & Parvinen, L. M. Active movements of the chromatoid body. A possible transport mechanism for haploid gene products. *J. Cell Biol.* **80,** 621–628 (1979).

393. Braun, R. E., Behringer, R. R., Peschon, J. J., Brinster, R. L. & Palmiter, R. D. Genetically haploid spermatids are phenotypically diploid. *Nature* **337,** 373–376 (1989).

394. García-López, J., Hourcade, J. de D., Alonso, L., Cárdenas, D. B. & del Mazo, J. Global characterization and target identification of piRNAs and endo-siRNAs in mouse gametes and zygotes. *Biochim. Biophys. Acta* **1839,** 463–75 (2014).

395. Kawano, M., Kawaji, H., Grandjean, V., Kiani, J. & Rassoulzadegan, M. Novel small noncoding RNAs in mouse spermatozoa, zygotes and early embryos. *PLoS One* **7,** e44542 (2012).